INO NOI

[redacted]

RESTRICTIVE LEGEND

GOVERNMENT OF CANADA

GOUVERNEMENT DU CANADA

THIS DOCUMENT AND THE INFORMATION IT CONTAINS IS DISCLOSED IN CONFIDENCE TO:

FOR DEFENCE INFORMATION PURPOSES ONLY, WITH NO DISCLOSURES TO OTHERS OR ANY OTHER USE (INCLUDING ANY MANUFACTURING USE) TO BE MADE WITHOUT THE WRITTEN PERMISSION OF THE CANADIAN DEPARTMENT OF NATIONAL DEFENCE (via DRDIM 3).
THIS DOCUMENT CONTAINS PROPRIETARY INFORMATION.

REPORT

FEASIBILITY OF AN IR IMAGING PROJECTOR SYSTEM BASED ON MICRO-MIRROR TECHNOLOGY

INO #97-2908 R N/A

Presented to:

Mr. Louis Demers
Defence Research Establishment Valcartier
2459 Pie-XI Blvd. North
Val-Bélair, Québec

Prepared by:

Eugène Curatu
Francis Picard

Presented by:

Francis Picard

Francis Picard
Project Manager

Authorized by:

Hubert Jerominek
Director, Photonic Materials and Processes

INO NOI

NATIONAL OPTICS INSTITUTE
369 Franquet Street, Sainte-Foy (Québec) G1P 4N8

December 1997

Defence Research and Development Canada
Recherche et développement pour la défense Canada
Canada

Prior Top **Document:** 1 of 1 Bottom

TITLE:(U) FEASIBILITY OF AN IR IMAGING PROJECTOR SYSTEM BASED ON MICRO-MIRROR TECHNOLOGY

PERSONAL AUTHOR: Curatu, E.; Picard, F.

CORPORATE AUTHOR: Defence Research Establishment Valcartier, Valcartier QUE (CAN);National Optics Inst, Ste-Foy QUE (CAN)

ABSTRACT: (U) The application of micro-mirror technology to the problem of infrared scene project is studied. The specific challenges of modulation IR radiation are evaluated and the performance of the project system is estimated.

DESCRIPTORS: (U) Infrared radiation;Infrared detection;Simulation;Fabrication;Design;Feasibility;Light modulation;Optical correlators;Optical equipment;Optical processing;Optimization;Signal processing

IDENTIFIERS: (U) HWIL(Hardware-in-the-Loop);Hardware-in-the-loop;Infrared scene projection;Infrared projectors;Spatial light modulators;Micro-mirrors;Seekers

REPORT NUMBER: DREV-CR-976;INO-97-2908; Contractor's Report	**REPORT DATE:** 01 Dec 1997	**NUMBER OF PAGES :** 135
DRDKIM N°: 98-02414	**CANDIS N°:** 509315	**Format(s):**Hardcopy;Document Image stored on Optical Disk

---

Date modified: 2003-04-17 Important Notices

TABLE OF CONTENTS

REF TITLE **PAGE**

1. INTRODUCTION 1

2 MICRO-MIRRORS PERFORMANCES AS OPTICAL MODULATORS 2

- 2.1 TECHNOLOGICAL LIMITS OF THE FABRICATION PROCESS 2
- 2.2 DYNAMICS OF THE MICRO-MIRROR 6
  - *2.2.1. Modeling* 6
  - *2.2.2 Results* 13
- 2.3 MODULATION 15
  - *2.3.1 Operation Modes* 15
  - *2.3.2 Radiance Resolution and Frame Rate* 23

3. COMPARATIVE STUDY OF PROMISING TECHNOLOGIES FOR DYNAMIC INFRARED SCENE PROJECTION 26

- 3.1 SPECIFICATIONS FOR AN INFRARED SCENE PROJECTOR 26
- 3.2 STRENGTHS OF THE MICRO-MIRRORS TECHNOLOGY FOR DYNAMIC INFRARED SCENE PROJECTION 31
- 3.3 WEAKNESSES OF THE MICRO-MIRRORS TECHNOLOGY FOR DYNAMIC INFRARED SCENE PROJECTION 33

4. PRELIMINARY OPTICAL DESIGN STUDY 35

- 4.1 THE CONCEPTUAL CONFIGURATION 35
  - *4.1.1 Introduction* 35
  - *4.1.2 The general optical characteristics* 38
  - *4.1.3 Theoretical considerations* 40
- 4.2 POTENTIAL CONFIGURATIONS 42
  - *4.2.1 Refractive Optics – BS, bistable mode – (Lens_1)* 43
  - *4.2.2 Refractive Optics – No BS, tristable mode – (Lens_2)* 44
  - *4.2.3 Reflective Optics – 5° – (Mirror_1)* 45
  - *4.2.4 Reflective Optics – 3.5° – (Mirror_2)* 46
  - *4.2.4 Comparative Table* 47

5. RADIOMETRIC PERFORMANCES OF THE INFRARED SCENE PROJECTOR 48

6. CONCLUSION 49

7. REFERENCES 52

Appendix I - LENS_1
Appendix II - LENS_2
Appendix III - MIRROR_1
Appendix IV - MIRROR_2

1. INTRODUCTION

For many years, Hardware-in-the-Loop (HWIL) simulations have been recognized as a valuable tool for seeker development and characterization. This approach reduces the delay for seeker qualification and reduces cost by limiting the extent of field testing which is essential but costly.

One of the key building blocks of a HWIL facility is the Dynamic Infrared Scene Projector (DIRSP). The function of the DIRSP is to stimulate a unit under test (UUT) by projecting in the UUT aperture a radiation pattern which resembles as closely as possible the pattern produced by real world scenes. This way, the behavior of the UUT (typically, the seeker) can be studied in the laboratory under a wide range of controlled conditions.

Currently, two leading technologies aiming at the development of DIRSP are being developed. Those are the micro-resistors technology (developed by British Aerospace and Honeywell) and the IR laser diodes array scanner technology (developed by AEgis and Optical Sciences Corporation). For now, these two approaches of DIRSP seem to be the most promising. However, it is recognized by field experts that there is no single technology that meets all the requirements for every type of significant evaluation scenarios. Instead, it is more likely that the future's most important HWIL facilities will be based on versatile DIRSP, making use of different, complementary technologies.

In that context, it is believed that the micro-mirrors technology, mainly developed at Texas Instrument (TI), still has its place in the Dynamic Infrared Scene Projection (DIRSP) field. Historically, the first few attempts to fabricate electrostatically actuated micro-mirrors were aimed at applications like scanners and switching for optical communications. TI pursued these efforts for applications including high quality printing and projection display. Currently, TI has brought this technology to a high level of sophistication with the achievement of its Digital Light Processing projection display [1,2, 3]. Beside that main application, TI tried to apply its technology to other fields and among them, DIRSP appeared an obvious possibility. TI researchers published a few papers about the theoretical feasibility and performances of DIRSP based on the micro-mirrors technology. They also reported experimental results obtained with an infrared projector assembled with off-the-shelf components. Those quick trials did not convince the DIRSP community of the validity of the simulations based on a DIRSP making use of the micro-mirrors as infrared modulators. The conclusion at this time was that further investigations and experimental demonstrations were needed to assess the simulations validity.

Considering the present unclear status of the micro-mirrors technology within the DIRSP field, a new study has been undertaken at the National Optics Institute (NOI) under a contract given by the Defense Research Establishment Valcartier (DREV) to further investigate the possibility of using the micro-mirrors technology for DIRSP. NOI, possessing an expertise in Micro Electro Mechanical Systems (MEMS) fabrication and particularly in micro-mirrors fabrication on one hand and in optics on the other hand, was well positioned to fulfil this task. This report presents the results obtained and gives some answers to the questions raised about the validity of infrared scene simulations using the micro-mirrors technology.

2 MICRO-MIRRORS PERFORMANCES AS OPTICAL MODULATORS

2.1 Technological limits of the fabrication process

Figure 1 shows a representation of a typical micro-mirror. The NOI design of micro-mirror is quite different from the one appearing in Figure 1. However, that schematic representation is sufficient to explain how such a device operates. The micro-mirror is a highly reflective plate suspended by hinges. Four electrodes lie underneath the mirror: 2 address electrodes and 2 landing electrodes. When a voltage higher than the so-called critical voltage (see section 2.2.2 below) is applied to an address electrode, the generated electrostatic force makes the mirror rotate until it touches the substrate. The mirror rotates to + ϕ_{max} or - ϕ_{max} depending on which address electrode is activated. As the landing electrodes are kept at the same potential as the mirror, they provide areas where the mirror can touch the substrate without being discharged through a spark. It is interesting to note that the mirror (and of course the landing electrodes) can be biased in order to lower the activation voltage. The important criteria here to fully rotate the mirror is that the potential difference between the mirror and the address electrodes must be higher than the critical voltage.

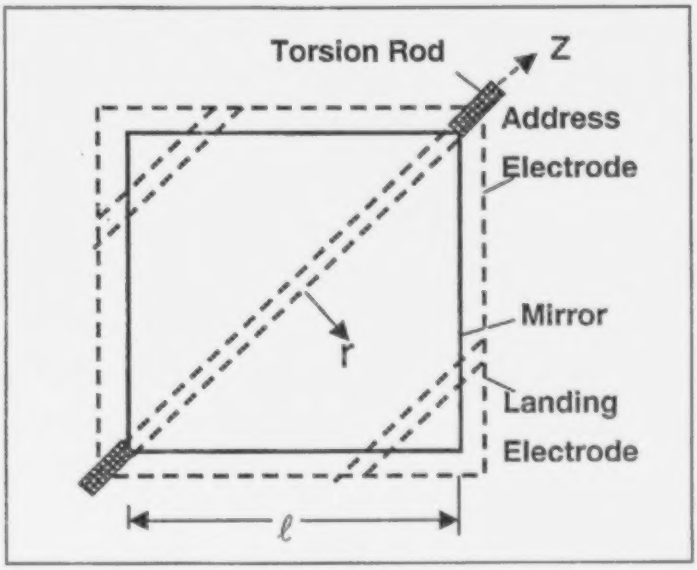
Torsion Rod
Z
Address
Electrode
r
Mirror
Landing
Electrode
ℓ

(a) Top View

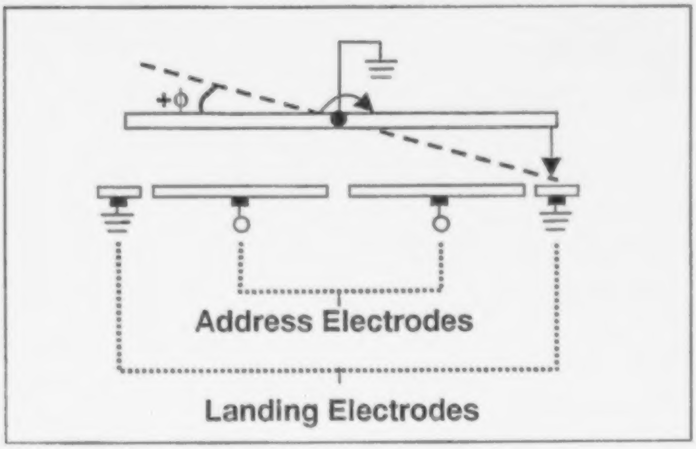
+ϕ
Address Electrodes
Landing Electrodes

(b) Cross section along beam diagonal

Figure 1. Schematic representation of a micro-mirror (adapted from reference 3).

The NOI micro-mirrors are fabricated using surface micromachining. This means that the mirrors are composed of layers of different materials. Each layer is patterned using standard photolithography process followed by an etching step. Some of those layers are structural layers whereas one layer is a sacrificial layer. At the final step, the sacrificial layer is removed by some isotropic etching process (wet or dry). That provides the gap between the mirror and the substrate necessary to rotate the mirror.

Many practical limits arise when designing micro-mirrors. The maximum size for a micro-mirror, within the NOI process context, is limited by the ability of the isotropic etching process to completely remove the sacrificial layer underneath the micro-mirror. In the NOI case, this means that the maximum size of a micro-mirror is 100 μm.

The maximum rotation angle for a micro-mirror is determined by two factors: the maximum sacrificial layer thickness achievable and the maximum internal stress generated in the hinge structure when the mirror is fully rotated. The first of these factors, the maximum sacrificial layer thickness, is limited to 5 μm. The second factor, the internal stress in the hinge, must be kept below the yield limit of the material used for the hinges. Some simulations made with an ANSYS program [4] showed that the maximum rotation angle, without exceeding the maximum stress allowed for the mirror and assuming a gap between the mirror and the substrate of 5 μm, is 10.2°. This gives, in turn, a minimum micro-mirror size of about 40 μm (the rotation axis lies along the diagonal of the mirror).

The fill factor is another important characteristic for an optical modulator. It is defined as the ratio of the active area of a pixel to the total area of a pixel. In the case of the NOI fabrication process, the fill factor is limited by the resolution of the photolithography process which is set to 2 μm (including a security factor). The fill factor F is then given by:

$$F = \frac{\ell^2}{(\ell+2)^2}$$

where ℓ is the size of the micro-mirror in μm.

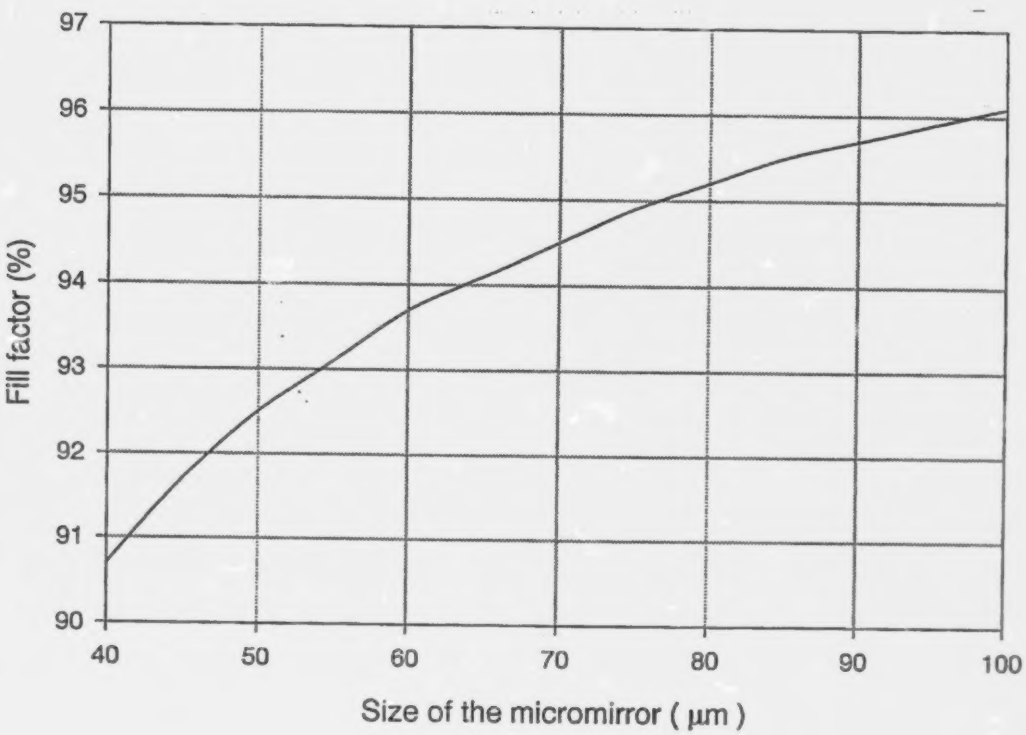

Figure 2 Fill factor of the pixels in the range of micromirror size achievable

Figure 2 gives the value of F over the range of ℓ values achievable (see above). The overall dimensions of an array of micro-mirrors are limited by the capability of the CMOS process used to fabricate the underlying addressing electronics. If possible, the size of the array should be kept below 24 mm x 24 mm. This allows the use of standard CMOS process and, consequently, a reduction in the fabrication cost. Even with this size limitation, arrays of 571 x 571 (mirrors of 40 µm) would be feasible. However, for mirrors of 100 µm, the maximum array size drops to 235 x 235.

Finally, the reflectance of the micro-mirrors is determined by the optical properties of the metallic layer deposited on top of the mirror's structure. Reflectance over 98% should be achievable in the infrared using aluminum or gold for the reflective coating. The major limiting factors, when designing micro-mirrors in the context of the NOI fabrication process, are presented in Table 1.

Table 1. Limits of the NOI fabrication process

Maximum micro-mirror size (ℓ_{max})	100 µm
Minimum micro-mirror size (ℓ_{min})	40 µm
Maximum rotation angle	10.2°
Maximum fill factor	96 %
Maximum array size	24 mm x 24 mm
Maximum micro-mirror reflectance	> 98%

2.2 Dynamics of the Micro-Mirror

2.2.1. Modeling

When assessing the performances of micro-mirrors as optical modulators, two important characteristics requiring evaluation emerge quickly: the activation voltage necessary to rotate the mirrors and the associated response time. A theoretical model was developed in order to evaluate these important parameters.

The micro-mirrors dynamics is described by the following coupled differential equations [5]:

$$I\frac{d^2\phi}{dt^2} + \eta\frac{d\phi}{dt} + K\phi\,(1+a\phi) = \Gamma_e(V,\phi) \qquad (1)$$

and,

$$R_e C(\phi)\frac{dV}{dt} + R_e\frac{dC}{d\phi}\frac{d\phi}{dt}V + V = \mathcal{E} \qquad (2)$$

where,

ϕ is the rotation angle (see Figure 1)

t	is the time
I	is the moment of inertia about the rotation axis
η	is the damping constant
K	is the linear restoring constant
Ka	is the nonlinear restoring constant
Γ_e	is the electrostatic torque, function of ϕ and V
V	is the voltage across the mirror
R_e	is the equivalent resistance of the addressing circuit
C	is the capacitance of the mirror, function of ϕ
ε	is the electromotive force of the voltage source driving the mirror

The first of these equations states that the sum of the torques acting on the mirror is zero. ϕ, in this equation, is the rotation angle as defined in Figure 1. I, the moment of inertia about the axis of rotation, is given by:

$$I = \rho e \iint_S r^2 dr\, dz \tag{3}$$

where,

r, z	are defined in Figure 1
ρ	is the mirror density
e	is the mirror thickness

and the subscript S means that the integration is performed over the entire surface of the mirror. It has been assumed here that $e \ll \ell$ (ℓ is the size of the mirror as defined in Figure 1). For the particular case illustrated in Figure 1:

$$I = \frac{\rho e \ell^4}{12} \tag{4}$$

It is difficult to achieve a good estimation of η (the damping constant) through theoretical calculations. Instead, it was assumed that for micro-mirrorlike structures, the damping force created by the air acting on a particular surface element dS was proportional to the speed of that moving element that is:

$$\frac{dF_D}{dS} = \mathrm{kr}\frac{d\phi}{dt} \qquad (5)$$

where F_D is the damping force and k is a constant.

From there, it is easy to show that:

$$\Gamma_D = \mathrm{k}\frac{d\phi}{dt}\iint_S r^2 dr\, dz$$

$$\Rightarrow \qquad \Gamma_D = \mathrm{k}\,\frac{d\phi}{dt}\,\frac{\mathrm{I}}{\rho e} \qquad (6)$$

where Γ_D is the damping torque.

Comparing with (1), we see that:

$$\eta = \frac{k\mathrm{I}}{\rho e} \qquad (7)$$

Using experimental results from references [5] and [6], it was possible to estimate k to be 87.74 kg/(m^2•s). For the particular case shown in Figure 1:

$$\eta\,[\mathrm{N{\bullet}m{\bullet}s}] = \frac{87.74\left(\ell[\mathrm{m}]\right)^4}{12}$$

$$\Rightarrow \qquad \eta\,[\mathrm{N{\bullet}m{\bullet}s}] = 7.31\left(\ell[\mathrm{m}]\right)^4 \qquad (8)$$

where the brackets give the units to be used.

K and Ka are the linear and nonlinear restoring constants. As the hinges structure of the NOI mirrors is complex, it was not possible to evaluate K and Ka using a simple model. Therefore, a finite element program, based on ANSYS, was written for the estimation of these constants [4]. Roughly, this ANSYS program calculates the restoring torque provided by the NOI hinges for various rotation angles. These data are then fed into the core program used to solve the differential equations (1) and (2). Within this program, the data are fitted to the equation:

$$\Gamma_r = \mathrm{K}\phi + \mathrm{Ka}\phi^2 \qquad (9)$$

where Γ_r is the restoring torque.

The best fit provides the values of K and Ka.

Γ_e is the electrostatic torque acting on the mirror when some voltage is applied to one of the address electrodes. The force generated by surface unit on a conductor immersed in an electrostatic field is given by [7]:

$$\left|\frac{dF}{dS}\right| = \frac{1}{2}\,\frac{\sigma^2}{\varepsilon_0} \qquad (10)$$

where σ is the charge density created by the electrostatic field at the conductor surface and ε_0 is the permittivity of the vacuum (and ,approximately, of the air). (Note that the direction of **F** depends on the signs of the electric charges accumulated on the mirror and on the address electrodes).

Therefore, the electrostatic torque is given by:

$$\Gamma_e = \frac{1}{2\varepsilon_0}\iint_S r\sigma^2 dr\, dz \qquad (11)$$

It is well known, by application of the Gauss Theorem, that σ, for a good conductor, is given by:

$$\sigma = \varepsilon_0\,|\mathbf{E}| \qquad (12)$$

$$= \varepsilon_0\,|-\nabla\Phi| \qquad (13)$$

In those equations, **E** is the electrostatic field at the point where σ is to be evaluated and Φ is the electrostatic potential. Formula (13) is obtained using the familiar expression $\mathbf{E} = -\nabla\Phi$. Solving the Laplace equation:

$$\nabla^2\Phi = 0$$

for Φ in cylindrical coordinates for the situation depicted in Figure 3a), it is easy to show that [8]:

$$\Phi = (V_1 - V_2)\,\frac{\theta}{\phi} + V_2 \qquad (14)$$

where V_1, V_2 and θ are defined in Figure 3a).

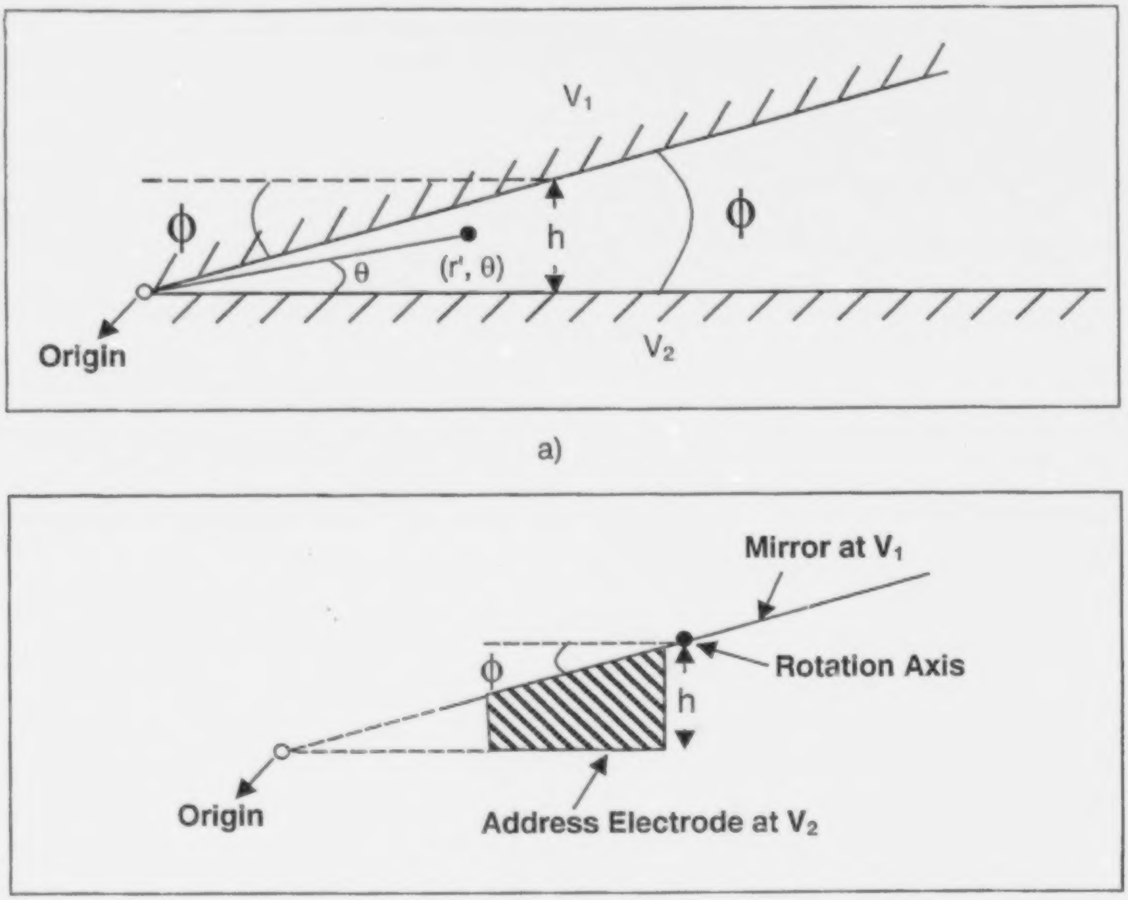
V₁
φ
φ
h
θ
(r', θ)
Origin
V₂
Mirror at V₁
Rotation Axis
φ
h
Origin
Address Electrode at V₂

a)

b)

Figure 3 a) Idealized situation used to evaluate Φ
b) Real situation approximated by the idealized situation

Now, assuming that the potential in the hatched area of Figure 3b) can be approximated by the one calculated from Figure 3a), the electrostatic field at the surface of the mirror can be evaluated:

$$\mathbf{E} = \frac{(V_1 - V_2)\mathbf{e}_\theta}{r'\phi} \qquad (15)$$

where $\mathbf{e}_\theta$ is the unitary vector in the θ direction (perpendicular to the mirror surface). Using equation (12), σ is given by:

$$\sigma = \frac{\varepsilon_0 V}{r'\phi} \qquad (16)$$

where, V_1-V_2 has been rewritten as the potential difference across the mirror, V and r' is defined in Figure 3a).

Finally, an expression for Γ_e is obtained using (11) and taking into account that the coordinate system has been changed from the one illustrated in Figure 1 to the one given in Figure 3a).

$$\Gamma_e = \frac{\varepsilon_0 V^2}{2\phi^2} \iint_A \frac{h/\phi - r'}{r'^2}\, dr'\, dz \qquad (17)$$

where h is defined in Figure 3b) and the subscript A indicates that the integration is performed on the mirror surface facing the address electrode. It should be noted that, in equation (17), it was assumed that ϕ is always small enough to use the approximation $\sin \phi \cong \phi$.

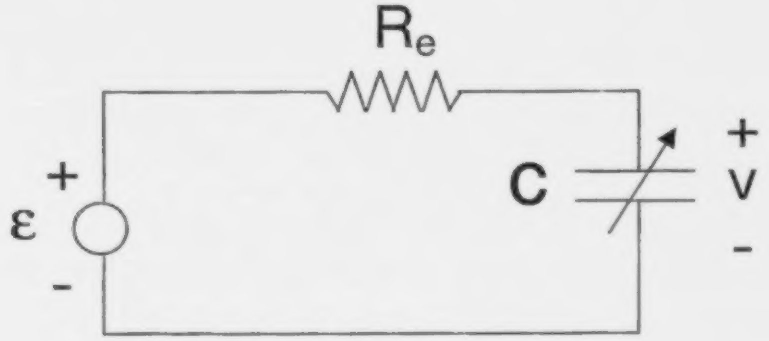

Figure 4. Simple model of the addressing circuit.

Figure 4 presents a simplified version of the addressing circuit. As it was mentioned above, in that circuit, ε is the electromotive force of the voltage source and R_e is the equivalent resistance of the addressing circuit. The micro-mirror is represented by a variable capacitance, C. As previously defined (see equation (16)), V is the voltage across that capacitance. The differential equation (2) simply states that the voltage sum in that circuit is zero and takes into account that:

$$i = \frac{dQ}{dt} = \frac{d(C(\phi(t))V)}{dt} \qquad (18)$$

where i is the current flowing in the circuit and Q is the capacitance charge.

C(ϕ) is obtained using the definition:

$$C(\phi) = \frac{Q}{V}$$

$$\Rightarrow \qquad C(\phi) = \frac{1}{V}\iint_S \sigma \, dr' \, dz \qquad (19)$$

For the micro-mirror case, (19) is approximated by:

$$C(\phi) = \frac{\varepsilon_0}{\phi}\iint_A \frac{dr'}{r'} dz \qquad (20)$$

using (16). r' and the subscript A are defined as above (see Figure 3a) and (17)).

At that point, all the functions and parameters required to solve the differential equations (1) and (2) and to obtain the functions $\phi(t)$ and V(t) are known (or, at least, approximated). This information was integrated in a MATHCAD PLUS 6.0 program [4] in order to solve the system of coupled differential equations. However, it soon appeared that this approach was very time-consuming and that the memory required to run the program exceeded the MATHCAD capabilities. Assuming that the change in capacitance with ϕ would be small (less than one order of magnitude), the time needed to charge the micro-mirror was evaluated using $C = 10\,C(0)$ and $dC/d\phi = 0$ in (2). This calculation gave an upper limit for the time required to charge the micro-mirror in the real situation. The results obtained showed that the micro-mirrors capacitance is so small that the time required to charge them is much smaller than the typical time required to rotate micro-mirrors (~10 μs). Therefore, the assumptions that the micro-mirror is quickly charged with respect to the time required to fully rotate the mirror ($\Rightarrow$ $dV/dt \cong 0$ during almost all the rotation) and that the current i induced by the small changes of C with ϕ is negligible ($\Rightarrow dC/d\phi \ll \left(R_e \frac{d\phi}{dt}\right)^{-1}$) were used in (2). This leads to the simplified form:

$$V = \mathcal{E} \qquad (21)$$

where V is now a constant.

Introducing (21) in (1), it was possible to obtain $\phi(t)$ by solving just one differential equation. This approach was used to produce the results presented in section 2.2.2.

2.2.2 Results

Table 2 shows the results obtained from the modeling of the NOI micro-mirrors. In this table, the micro-mirror size ℓ is defined in Figure 1. V_c, the critical voltage, is the minimum voltage under which the mirrors will rotate spontaneously to the maximum angle allowed by the micro-mirrors' geometry. This phenomenon can be explained by observing Figure 5. This figure gives a general representation of the steady-state angular position of the mirror, as a function of the actuation voltage.

Table 2. Results of the modeling of the micro-mirrors' dynamics

Size, ℓ (μm)	V_c (V)	Response Time (μs)			
		V = 5V	V = 10V	V = 15V	V = 20V
40	5.5	-	264	109	63
44	3.2	621	130	60	37
50	2.0	343	86	42	26
60	1.0	226	61	31	20

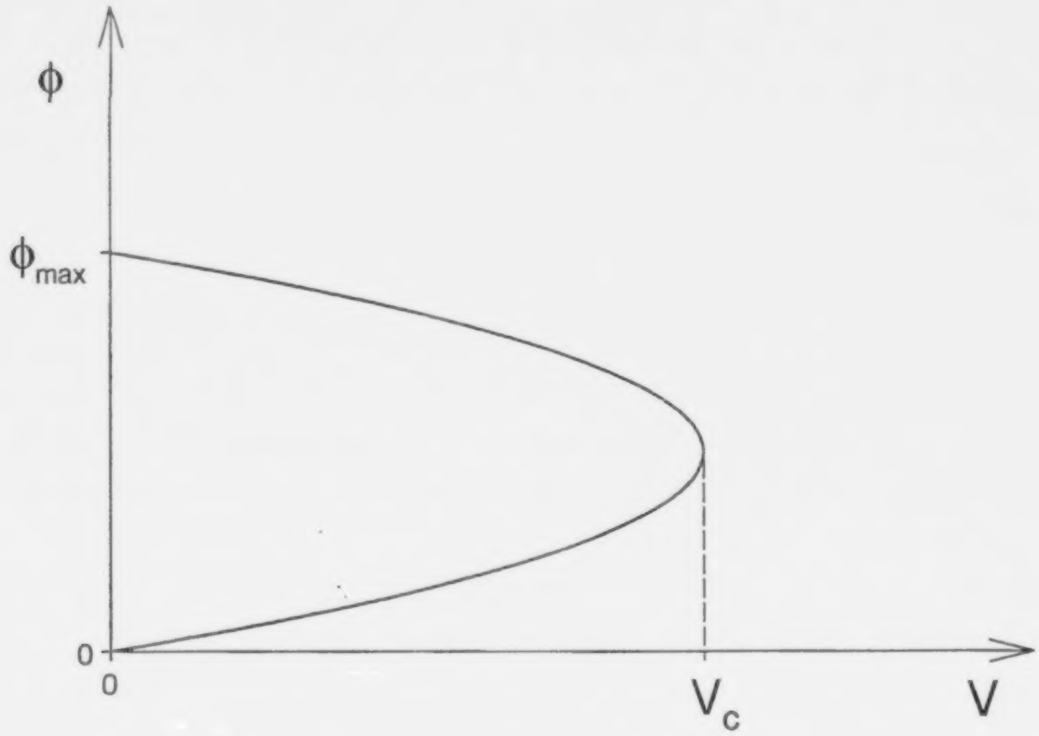

Figure 5 General representation of the steady-state ϕ vs V curve.

It can be seen that there are two equilibrium points for each V value comprised in the range $0 \leq V < V_c$. The points on the lower branch are stable equilibrium points while the points on the upper branch are unstable equilibrium points. Furthermore, it can be seen that when $V > V_c$, there is no equilibrium point and the mirror will then rotate until it touches the landing electrode.

The response time given in Table 2 is defined as the time required by the mirror to rotate from $\phi = 0$ to the maximum angle allowed by the micro-mirrors' geometry (ϕ_{max}). This response time is a function of the actuation voltage. It has been evaluated for actuation voltages of 5, 10, 15 and 20 V.

The main result to be retained from the data presented in Table 2 is that, according to the simulations, the NOI micro-mirrors can be actuated in a few tens of microseconds with reasonable activation voltages.

Other simulations were performed in order to evaluate the time required by the mirror to return to the $\phi = 0$ position when the actuation voltage is turned off. The results obtained show that about 3 to 9 ms (depending on the mirror size) would be necessary. It is then clear that if the state $\phi=0$ is to be used for light modulation and if the advantage given by the quick response time of the mirrors is to be retained, counting just on the restoring torque to bring back the mirror to $\phi = 0$ is not sufficient. For instance, some active reset on the mirror would have to be performed through the generation of a repulsive force between the address electrode and the mirror. Many different reset schemes of various complexity levels can be imagined. They can involve some voltage change on just one or two address electrodes, combined or not with variations of the bias applied to the mirror. This type of addressing strategy is also applicable in situations where the mirror must be rotated directly from $+\phi_{max}$ to $-\phi_{max}$ (i.e. the state $\phi = 0$ is not used). That would allow to decrease the switching time.

2.3 Modulation

2.3.1 Operation Modes

Figure 6 shows a simple projection system using micro-mirrors as optical modulators. The modulation of the radiation intensity passing through the optical system is obtained by varying the angular position of the micro-mirrors. Typically, the micro-mirrors are used in the so-called digital mode where they are either fully rotated or unrotated. There are many reasons why not to use the micro-mirrors in the analog mode. One of the main reasons is that it would be very difficult to reliably adjust the precise angular position of a micro-mirror just using the applied voltage as a control parameter. A second important reason to avoid the analog mode is that for some critical value of the applied voltage, the micro-mirrors will spontaneously rotate to their maximum angular position, determined by the device geometry (this was already discussed in section 2.2.2). So, the angular range available for analog control is generally small.

In the digital mode, the radiation falling on a micro-mirror will be reflected either in a direction where it will be collected by the objective (the "ON" state, see figure 6) or in a direction where it will not, ideally, be collected (the "OFF" state). Figure 7 shows the three possible positions of the mirrors when using them in the digital mode that is $-\phi_{max}$, 0 or $+\phi_{max}$.

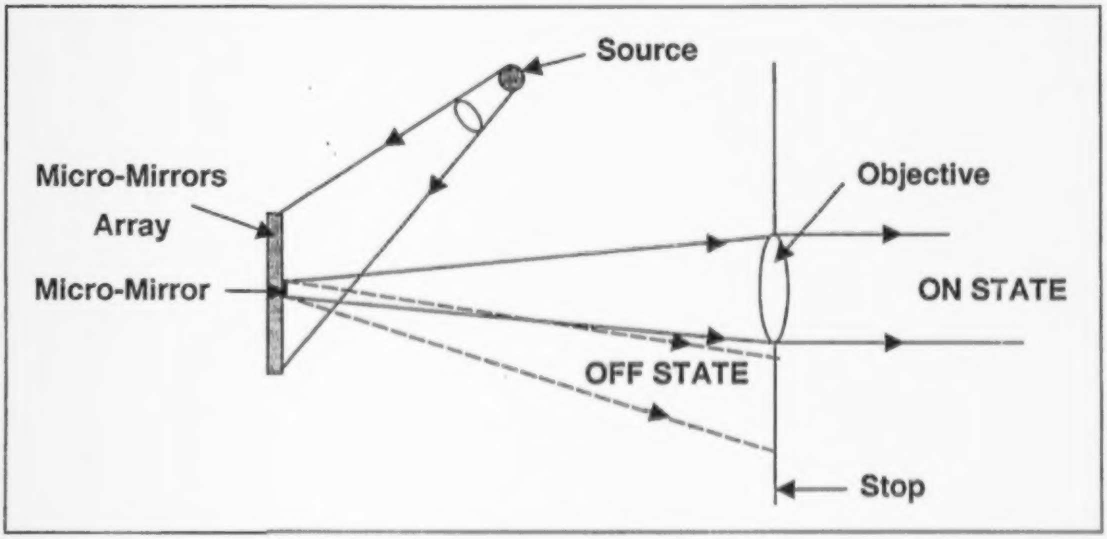
Source
Micro-Mirrors
Array
Objective
Micro-Mirror
ON STATE
OFF STATE
Stop

Figure 6. Schematic representation of a projection system using micro-mirrors as optical modulators (Digital mode shown).

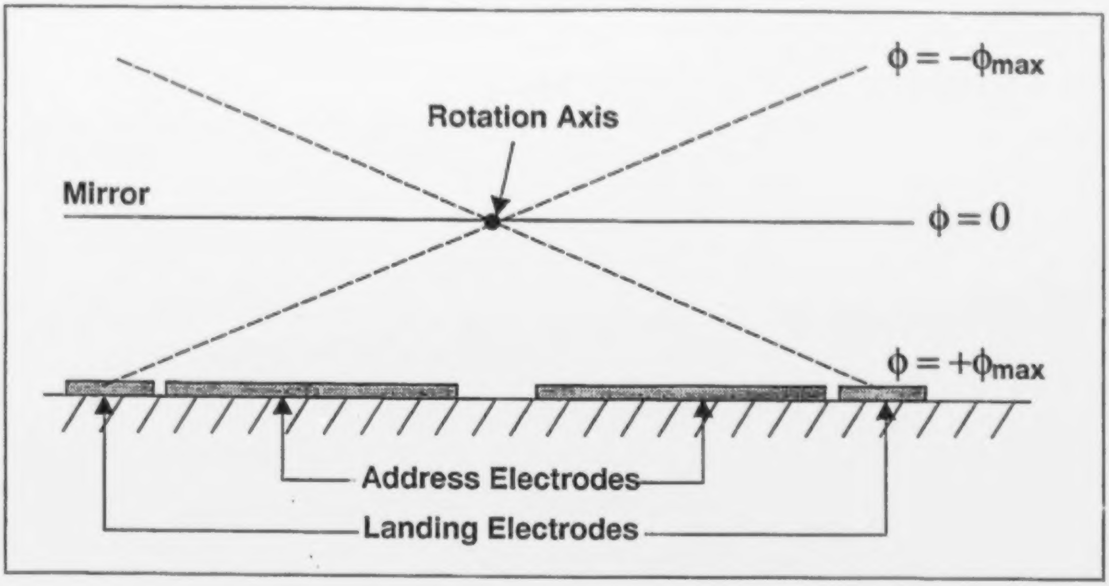

Figure 7. The three stable states when using the micro-mirrors in the digital mode.

Two different digital modes exist. One, called bistable, makes used of only two of the three stable positions. In this case, for example, $+\phi_{max}$ is used as the "ON" state and $-\phi_{max}$ as the "OFF" state. The other digital mode, called tristable, takes advantage of the three states available. $+\phi_{max}$ and $-\phi_{max}$ are used as "ON" states and $\phi = 0$ is the "OFF" state. There are advantages and drawbacks in the use of either modes. This will be discussed later.

At first sight, it could seem that only two radiance levels are achievable in the projection system i.e. the ON level (when the radiation reflected by the mirror is collected by the objective) and the OFF level (determined by parasitic reflections and the background radiation). However, intermediate intensity levels can be obtained through the use of pulse width modulation (PWM). In that case, the signal level perceived by the stimulated optical detector is proportional to the duration of the ON state. Of course, for that approach to work, the duration of the radiation pulses reflected by the mirrors must be smaller than the integration time used by the detector. If this criterion is fulfilled, the UUT will not "see" any flicker caused by the switching of the mirrors from the "ON" to the "OFF" state in the projected image.

Different types of PWM can be imagined. For example, the scheme used by Texas Instrument is the so-called Binary Pulse Width Modulation (BPWM) [2]. This is illustrated in Figure 8 for the case where 4 addressing bits are used (i.e. 16 radiance levels available). It can be seen on this figure that, generally, the mirrors will have to be switched from the ON to the OFF state many times during one image frame when using BPWM. This can be a disadvantage in some cases.

An alternative to the BPWM is the "Single Pulse Width Modulation" (SPWM), shown in Figure 9 (an example with 26 radiance levels is given). In this case, the mirrors are switched ON only once during one frame period. However, the drawback here is that the number of points along the time axis where it must be possible to switch OFF the mirrors is much larger. For SPWM, this number is equal to N-1 where N is the number of radiance levels achievable. For BPWM, the number of "OFF points" is reduced to $\log_2 N$ (i.e. to the number of addressing bits). The consequences of this difference will be discussed later on in this section.

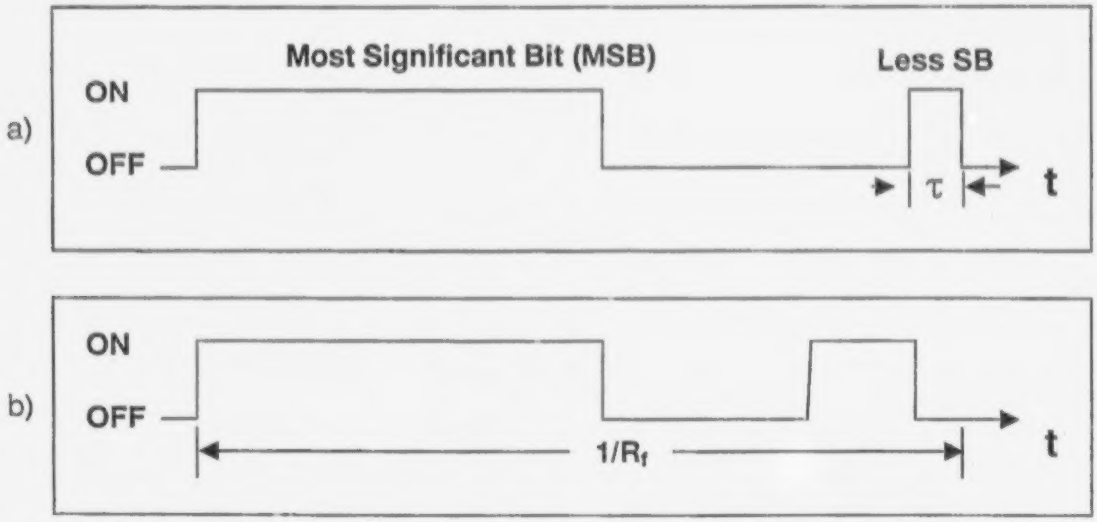

Figure 8. Binary Pulse Width Modulation with 4 bits. (t: time, R_f: frame rate, τ: minimum pulse duration achievable).
a) Radiance level 9 (1001)
b) Radiance level 10 (1010)
Radiance level 0 is (0000)

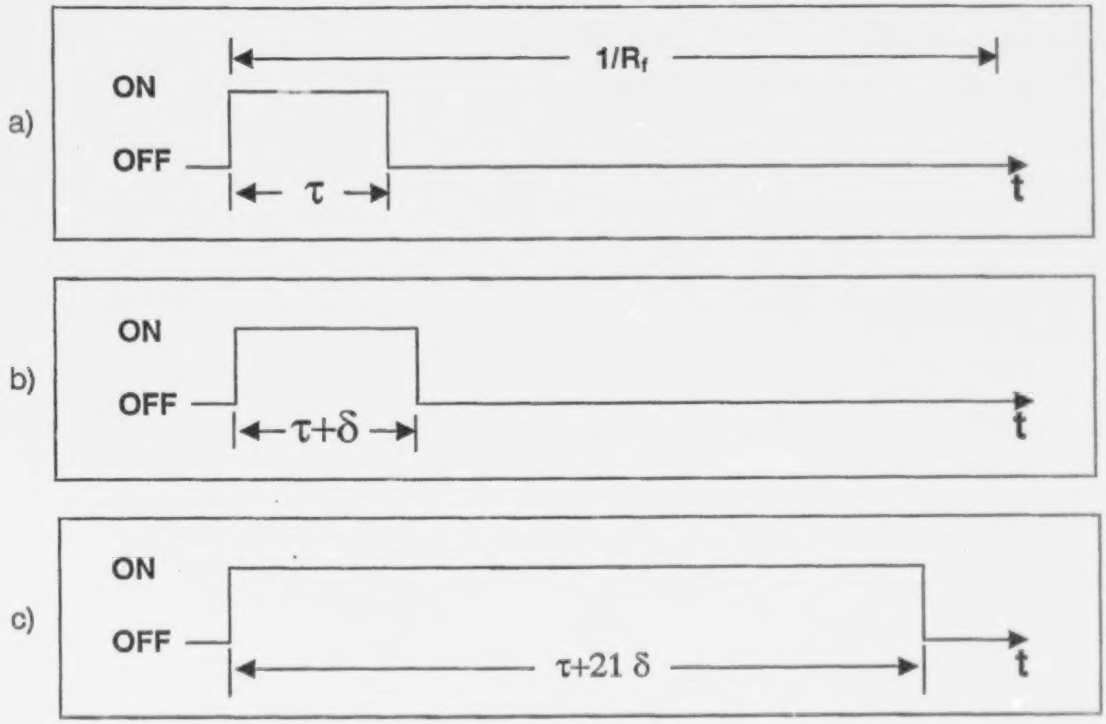

Figure 9. Single Pulse Width Modulation. (t: time, R_f: frame rate, τ: minimum pulse duration achievable, δ: resolution of the pulse duration achievable).

a) Radiance level 1

b) Radiance level 2

C) Radiance level 23

Another drawback of the SPWM is that the signal difference between radiance level 0 and radiance level 1 is typically higher than between any other two consecutive radiance levels. It should be possible to solve that problem through direct modulation of the radiation source used in the projection system during a time τ starting at the beginning of a frame. That is illustrated in Figure 10. If the condition $\tau P_m = \delta P_{on}$ is fulfilled (P_m and P_{on} are defined in Figure 10), then the signal difference between two consecutive radiance levels will always be the same (the small radiance associated with the radiance level 0 is neglected here). Of course, the time required to modulate the radiation source must be much smaller than δ in order to avoid important errors in the signal generated for the low radiance levels. Lasers, for example, would be good candidates as radiation sources in projection systems using the "Equalized Single Pulse Width Modulation" (ESPWM) approach.

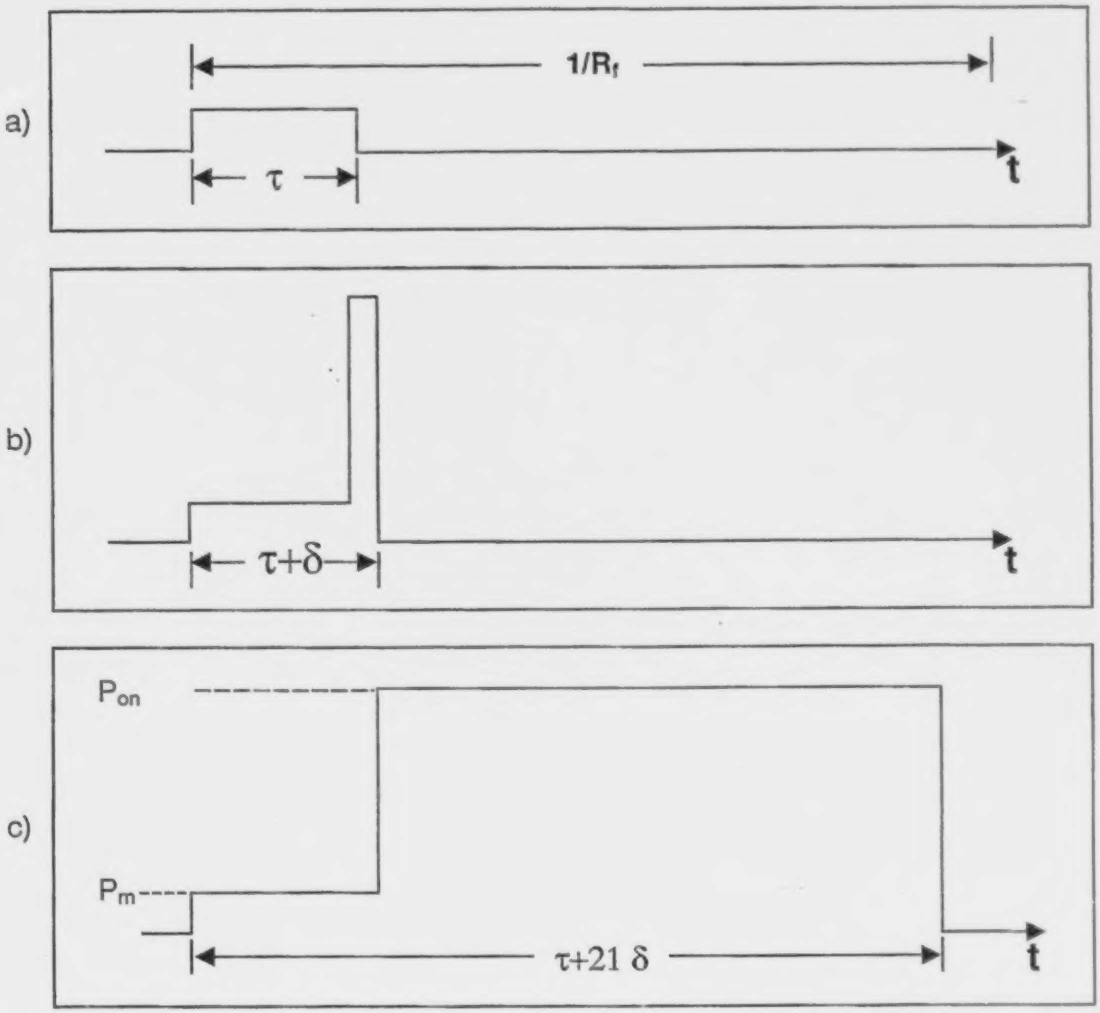

Figure 10. Equalized Single Pulse Width Modulation (P_m: modulated power, P_{on}: power for the ON state).

a) Radiance level 1
b) Radiance level 2
c) Radiance level 23

The implementation of the different modulation schemes described above can be a complex task in practice. For example, Table 3 gives the sequence of operations performed by the addressing electronics in the case of the BPWM developed by Texas Instrument (TI). It should be noted here that TI uses the micro-mirrors in the bistable mode, i.e. $+\phi_{max}$ is the ON state and $-\phi_{max}$ is the OFF state. The reset pulse (step 1, applied to the mirror and to the landing electrodes) is used to facilitate the rotation of the mirrors which have to change state. This would not be necessary for the mirrors which remain in the same state. The reset pulse is nevertheless applied to every mirror. The reason for that will be given below.

Table 3. Operations Performed by the Addressing Electronics for BPWM.

1	Reset pulse is applied to the mirrors.
2	Bias on the mirrors is turned off. This allows the mirrors to begin to rotate toward $\phi = 0^\circ$.
3	Bias on the mirrors is turned on. The mirrors rotate towards their assigned ON or OFF states.
4	Voltage on the address electrodes is updated.
5	Mirrors are still in their previous ON or OFF states, latched by the bias voltage applied to them.
6	See 1.

Previously, TI used the so-called unipolar pulse reset which stored elastic energy in the mirrors hinges to facilitate their rotation in the other state. Now, TI is moving towards the bipolar pulse reset where a repulsive electrostatic torque is used to facilitate the mirrors rotation into another state. In step 2, the bias (applied on the mirrors and the landing electrodes) is turned off on all mirrors. At that point, every mirror begins to rotate towards $\phi = 0^\circ$. Before they reach that position, the bias is turned on once again.

Whatever was the previous mirror's angular position, they will then rotate towards the state determined by the voltage on the address electrodes. Once the micro-mirrors are fully rotated, the bias latches them in that angular position and the voltage on the address electrodes can be updated without changing the mirrors state. After a specified time, the sequence begins again with a new reset pulse being applied to the micro-mirrors.

This particular way of addressing the mirrors for BPWM has the advantage that the bias variations in time are the same on all the mirrors. This allows to separate the electronics generating bias voltages from the control electronics on the micro-mirror chip (just a metallic routing is required to bring the bias to the mirrors). That, in turn, makes it possible to use a conventional 5 V CMOS for the micro-mirrors electronic chip fabrication. This is why it can be advantageous to apply reset pulses and bias changes even on micro-mirrors which do not require a state change. The major drawback here is that this can somewhat increase the lowest radiance level achievable (i.e. the small angular displacement of the mirrors after the bias is turned off could let some radiation pass through the projection system, even for the mirrors in the OFF state).

The approach developed by TI would not be applicable to the SPWM if the advantage of switching the mirrors in the ON state only once by frame was to be retained. The idea behind SPWM is to keep the time necessary for state transitions within one frame to be as low as possible. Obviously, resetting every mirror for each possible transition to the OFF state (see Figures 9 or 10) would make the situation even worst than in the case of BPWM (except if the time required for the reset would be much smaller than δ, which is very unlikely (see Figure 9)). Therefore, it seems that the control electronics for SPWM (including the bias control) would be entirely located on the micro-mirrors chip. This would imply that it would probably not be possible to use standard 5 V CMOS for the chip fabrication. Moreover, each mirror would have its own and complete control electronics and this electronics would have to be updated once every time interval δ. This should lead to very demanding requirements for the data transfer rate on the chip.

However, if this modulation mode (SPWM) can be implemented, it would give many more radiance levels than the BPWM for the same frame rate.

Considering the examples described above, it is clear that the micro-mirrors control can be quite complex. The choice of a particular PWM scheme must be based on a thorough experimental characterization of the micro-mirrors. In particular, the time required to switch the mirrors from $\phi = 0$ to $\phi = \phi_{max}$, from $\phi = -\phi_{max}$ to $\phi = +\phi_{max}$ and from $\phi = \phi_{max}$ to $\phi = 0$ must be measured under various addressing sequences. The parameters distinguishing an addressing sequence include the voltage waveform applied to the mirrors and the landing electrodes (with or without reset pulses) and the two different voltage waveforms applied simultaneously to both address electrodes. Once the experimental characterization is completed, it becomes possible to choose an adequate PWM scheme and to design the associated addressing electronic circuit.

The situation is even more complex since external electronics are needed to transform some, let say, "digitized" version of the scene to be projected into signals compatible with the micro-mirrors electronic chip. This transformation can include sophisticated signal processing like spatial and temporal filtering, format changes, non-linear scaling, etc [9, 10, 11]. So, the main conclusion here is that addressing the micro-mirrors is not an obvious task. It should be noted, however, that this conclusion can be generalized and applied to every technology used for Dynamic Infrared Scene Projection.

2.3.2 Radiance Resolution and Frame Rate.

Observing Figure 8, 9 and 10, it can be seen that a relation exists between the radiance resolution (or the number of simulated radiance levels achievable) and the frame rate. Roughly, using Figure 8, this relation for BPWM is given by:

$$R_f = \frac{1}{N\tau} \qquad (22)$$

where, R_f is the frame rate

τ is the minimum pulse duration achievable with the micro-mirrors
and N is the number of radiance levels achievable.

In that particular case, N will only have values equal to 2^B where B is an integer corresponding to the number of bits used to address the mirrors. For SPWM, the relation between R_f and N is given by:

$$R_f = [\delta(N-2)+\tau]^{-1} \qquad (23)$$

where δ is the pulse duration resolution achievable.

The expressions (22) and (23) have been plotted in Figure 11 using 40 μs for τ (see Table 2) and 1 or 2 μs for δ. Moreover, it has been assumed that the mirrors are operated in the bistable mode. For tristable operation, the frame rate would be roughly divided by two. Two major facts can be noted from Figure 11. First, it is clear that there is a trade-off between the maximum frame rate and the achievable number of simulated radiance levels. This is particularly true for the BPWM. Second, the SPWM allows much higher frame rates than BPWM for the same number of radiance levels. However, the drawback here is that the addressing electronics for SPWM would probably be more complex than the one required for BPWM. This should also be considered when selecting an adequate PWM scheme.

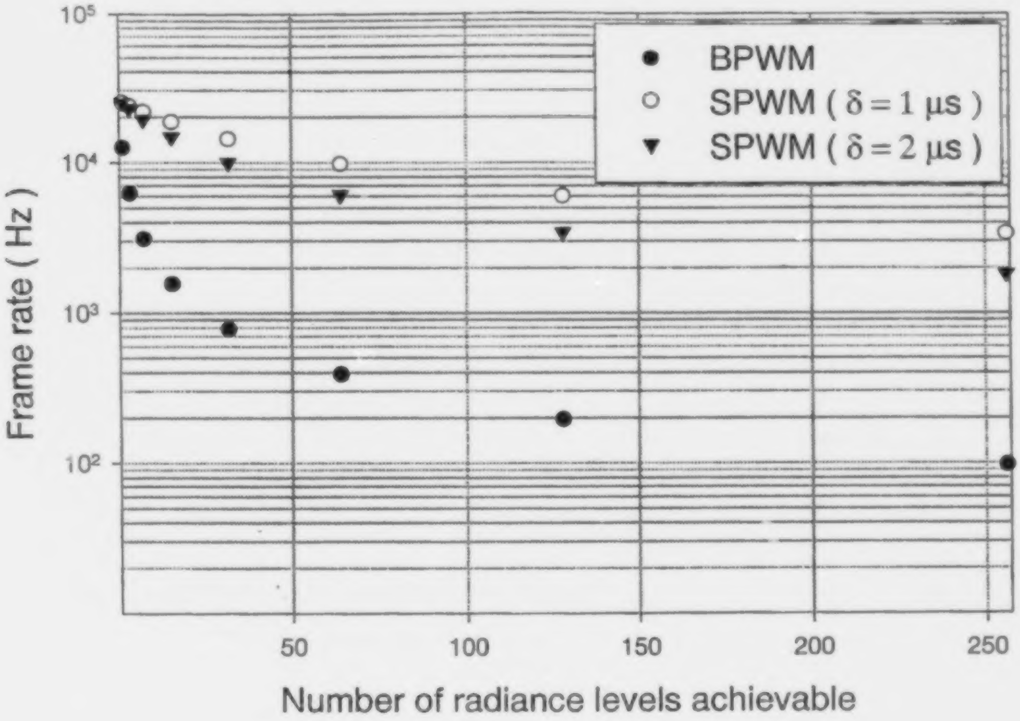

Figure 11 Plot of the frame rate vs the number of radiance levels achievable for various PWM shemes.

It should be noted that the frame rates shown in Figure 11 are achievable if the addressing electronics can keep up with such high data transfer rates. As the micro-mirrors arrays dimensions increase, the data transfer rate to and within the micro-mirrors chip quickly becomes the limiting factor for the frame rate. For example, in the Texas Instrument case, SRAM (Static Random Access Memory) cells, fabricated with a conventional CMOS process, are used to address the mirrors. (This particular choice of SRAM was made because this type of circuit is insensitive to visible light. This is obviously important for projection display applications. It is not clear if that criterion still holds for DIRSP applications). Using SRAMS, TI reports data transfer rates as high as 50 MHz [12]. This is sufficient to achieve a frame rate of almost 100 Hz with a 256 x 256 micro-mirrors array and 256 radiance levels. However, this is far from enough to reach the 2 to 3 kHz shown in Figure 11 in the SPWM case or to address larger arrays even at frame rate as low as 100 Hz. It is possible to reduce the limitations imposed by the data transfer rate. This can be obtained by partitioning the micro-mirrors array and using a massively parallel electronics architecture for the pixels addressing. Of course, this can be done at the expense of an increased complexity of the control electronics.

Finally, it must be kept in mind that whatever the scheme retained for the micro-mirrors addressing, some provisions should be made to allow the synchronization of the Dynamic Infrared Scene Projector (DIRSP) with the Unit Under Test (UUT). If this is not done, it could happen that parts of different scene frames would stimulate the UUT during one of its integration time. This, clearly, would not be acceptable from the projection validity point of view. Hence, it is of utmost importance that a synchronization signal from the UUT is provided. It should be noted that this requirement applies as well to the other promising technologies (micro-resistors and IR laser diodes array) involved in DIRSP development.

3. COMPARATIVE STUDY OF PROMISING TECHNOLOGIES FOR DYNAMIC INFRARED SCENE PROJECTION

3.1 Specifications for an Infrared Scene Projector

Part of the feasibility study reported here consisted of establishing specifications for a DIRSP. Table 4 gives two extreme sets of specifications for such a system. One of these sets lists the minimum requirements for a "down-market" DIRSP still useful for simple Hardware-in-the-Loop simulations. The second one would apply to a "top-of-the-line" DIRSP. In fact, there is no DIRSP in operation in the world showing such exceptional performances. Moreover, the current status of the different technologies involved in DIRSP development does not permit to predict that a single DIRSP will, someday, encompass all those desired features. So, that second specification set should be seen as the ideal case, probably not achievable before a distant future.

Table 4 was constructed by consulting three separate specification sets coming from different sources. One of these sources was a document provided to NOI by DREV in

1995 [13]. A second source was the specification obtained through a contract given to an external consultant (Beaulieu Consultant Inc.) [14]. In this contract, general models of different seekers types (reticle, rosette, imaging seekers, etc.) were elaborated and the desired performances of an infrared projector designed to stimulate such sekers were extracted from these models. Finally, the third set of specifications used to produce Table 4 came from the TTCP report "Imaging Infrared Projector Design" [15].

Table 4. Range of Specifications for a Dynamic Infrared Scene Projector

	Down-Market Specs.	**Top-of-the-line Specs.**
Instantaneous field of view (°)	5	7
Total field of view (°)	± 20	± 20
Diameter of the input aperture of the UUT (mm)	102	102
Angular resolution (mrad)	0.17	0.05
Array size (# pixels)	512	≥ 1024
Spectral range	3 to 5 μm	UV to 12 μm
Maximum radiance (W/sr m^2)	2500	9000 (1 to 3 μm) 6500 (3 to 5 μm)
Frame rate (Hz)	60	7000 to 10000
IR signal resolution (bits)	7	16
Maximum scene (°/s) angular speed	30	30
Maximum scene (°/s^2) angular acceleration	300	300
Flicker/frame	< 1%	< 0.1%
Spatial coherence	none	none
Temporal coherence	acceptable	acceptable
Polarization	acceptable	none, if possible
Intensity uniformity across the image plane	3%	3%
Countermeasures simulation	no	yes
Flight table mountable	desired	desired

As already mentioned above, some of the "top-of-the-line" specifications are quite difficult to achieve in practice. For example, an angular resolution of 0.05 mrad with an instantaneous field of view of 7° means that the size of the infrared modulator array should be at least 2444 pixels x 2444 pixels. There are a lot of practical problems related to the fabrication and the addressing at high frame rate of such a huge chip. The spectral range listed in the "top-of-the-line" specifications is also all but easy to obtain. First, such a large spectral range leads inevitably to a reflective design for the DIRSP. This, in turn, implies that expensive aspherical optical components must be used. Even then, the image quality at the UV end of the spectral range would not be very good due to the poor surface finish obtained with the diamond turning technique required to fabricate the off-axis aspherical components needed. Finally, the desired frame rate for the "top-of-the-line" DIRSP (7-10 kHz) is mainly based on the modelization of seekers working with just one or a few detectors with very short integration time. This is typical of reticle or rosette seekers. It is obvious that such a high frame rate in conjunction with the large size of the pixels array will be very demanding in terms of addressing scheme and addressing electronics. However, the frame rate could be significantly reduced without loosing the simulation validity for many seekers based on imaging focal plane array.

The few examples just presented illustrate the fact that the "top-of-the-line" specifications of Table 4 are really difficult to achieve simultaneously. Considering that fact, it seems that a more realistic and more useful approach would be to specify a DIRSP with performances lying within the extremes of Table 4. Table 5 shows such a revised specifications set. A DIRSP exhibiting these specifications would still be a very high quality system and would be more feasible than the futuristic "top-of-the-line" DIRSP presented in Table 4.

Table 5. Specifications for a First Generation Dynamic Infrared Scene Projector

Instantaneous field of view (°)	5
Total field of view (°)	± 20
Diameter of the input aperture of the UUT (mm)	102
Angular resolution (mrad)	0.17
Array size (# pixels)	512
Spectral range	2 to 5 μm
Maximum radiance (W/sr m^2)	9000 (2 to 3 μm) 3000 (3 to 5 μm)
Frame rate (Hz)	200 to 500
IR signal resolution (bits)	7
Maximum scene angular speed (°/s)	30
Maximum scene angular acceleration (°/s^2)	300
Flicker/frame	< 1%
Spatial coherence	none
Temporal coherence	acceptable
Polarization	acceptable
Intensity uniformity across the image plane	3%
Countermeasures simulation	yes
Flight table mountable	desired

3.2 Strengths of the micro-mirrors technology for Dynamic Infrared Scene Projection

In this section, the advantages of using the micro-mirrors technology for DIRSP will be outlined and compared to the corresponding performances of other promising technologies for DIRSP. In section 3.3, the same will be done but for the micro-mirrors weaknesses when used for DIRSP applications.

Micro-mirrors offer a high spatial (or angular) resolution inherent to the high level of miniaturization typical of MEMS. This is also true for the micro-resistors technology. The other most promising technology, the IR laser diodes array, do not provide such a high spatial resolution.

Fill factor is another important parameter characterizing modulator arrays. It is defined as the ratio of the active area of a pixel to the total area of a pixel. In the case of the micro-mirrors, the fill factor can be very high (above 90%, see Figure 2). This is not true for the competing technologies because of packaging issues (IR laser diodes array) or of thermal isolation issues (micro-resistors).

The micro-mirrors exhibit a very short response time on the order of tens of microseconds. This is much faster than the response time typical of the micro-resistors (1–10 ms) [15] but slower than the response time achievable with the IR laser diode array (~60 ns) [15]. However, a strong compromise exists between the frame rate and the number of grey levels (i.e. radiance levels) available when using micro-mirrors in a DIRSP. This is not true for the competing technologies. This point will be further discussed later (see Section 3.3).

One feature which is highly desirable for a DIRSP is the capability of adjusting in real time the ratio of the power injected in one spectral band to the power injected in another spectral band. Typically, for the micro-resistors and the IR laser diodes, two separate arrays would have to be used and the two images obtained would have to be combined in just one IR scene. The drawbacks of this approach are that two relatively expensive arrays have to be used and synchronized. Moreover, it could be very difficult to perfectly align the two separate images obtained. The situation for the micro-mirrors is quite different. In this case, a single micro-mirror used in the so-called tristable operation mode (see section 2.3.1) can modulate two different IR sources. This operation mode makes use of one OFF state (when the mirror is parallel to the substrate) and two ON states (when the mirror is rotated on one side or the other). Therefore, just one array is required and there is no need for synchronization or optical alignment. However, using the micro-mirrors in the tristable mode instead of the bistable mode implies a few trade-offs. First, the rotation angle available to achieve the OFF state is divided by 2, which could lead to a somewhat reduced contrast between the ON and the OFF states in the image plane. Moreover, typically, the maximum frame rate would be decreased by a factor of 2.

The requirements on DIRSP in terms of spectral range are getting more and more demanding. There is an increasing interest in systems having capabilities from the UV to the LWIR. For now, among all the promising technologies, the micro-mirrors technology is the only one providing an access to the UV spectral range. Just for this possibility, the micro-mirrors should be kept as part of the key technologies necessary to achieve the wide range of scenarios required by HWIL testing of seekers.

The power dissipation at the modulator array is also an important issue for a DIRSP. The power consumption of typical micro-resistors array can be relatively high (tens to thousands of watts) [15] and dissipation of that heat to avoid overheating of the pixels and underlying electronics is a critical design problem. In the case of the IR laser diodes arrays, the operational temperature of the laser diodes must be kept very low (cryogenics temperatures). For the micro-mirrors technology, power dissipation is generally a lesser problem. Due to the electrostatic nature of the micro-mirrors operation, the power consumption of a micro-mirrors array is very low. The main heating source here would probably be the IR source used to illuminate the micro-mirrors. It is most likely that heating would not be very significant as the mirrors can be made very reflective (over 98%). Moreover, the NOI micro-mirrors are especially designed to dissipate quickly the heat towards the underlying substrate and heat sink. This feature makes them very resistant to high incident power density. Therefore, the advantage of the micro-mirrors technology, regarding the heat dissipation, is that no complex (and possibly heavy) cooling systems are required. The side effect of that advantage is that it could facilitate the eventual integration of the micro-mirrors with a flight table.

A few years ago, the fixed pattern noise (i.e. the non-uniformity of the pixels response to a given command signal) was not considered as an important problem. However, as the technologies for DIRSP are maturing, this aspect of IR scene simulation is becoming critical for achieving high performances in IR projectors [15]. Currently, non-uniformity correction (NUC) procedures are developed for every technology involved in DIRSP development. These procedures are put into place in order to compensate the non-uniformity arising from the fabrication process of the arrays. As already mentioned, the micro-mirrors are typically used in the digital mode where the pixels are either fully rotated or unrotated (see section 2.3.1). Using the micro-mirrors in the digital mode is much less demanding in terms of precision of the driving electronics (the activation voltage should simply be set to a few times the critical voltage, V_c, see section 2.2.2) and fabrication process (only the geometry must be uniform from device to device; the material properties uniformity is not as important as in the case of the micro-resistors for example). Therefore, it is expected that the micro-mirrors arrays will be less prone to exhibit fixed pattern noise than the competing technologies. In fact, it is quite possible that the limiting factor, in that case, would be the uniformity of the infrared source.

3.3 Weaknesses of the Micro-Mirrors Technology for Dynamic Infrared Scene Projection

As mentioned above, it exists a strong compromise between the radiance resolution (number of radiance or grey levels) available and the maximum frame rate achievable when using the micro-mirrors in the digital mode. This is because the grey levels, in that case, are obtained through pulse width modulation. The idea here is to keep the mirrors "ON" for a time period proportional to the incident power to be simulated. Obviously, this time period should always be smaller or equal to the integration time of the UUT's detector stimulated in order to retain the simulation validity. Thus, the number of grey levels resolvable is a direct function of the time period available to simulate a radiance level (the longer the time period available, the higher the number of grey levels achievable). However, the maximum time period available to produce the grey levels will also determine the maximum frame rate achievable, that is, a complete frame should be simulated within one of those time periods (the longer the time period available, the lower the maximum frame rate). This feature inherent to the micro-mirror operation has been described more deeply in the previous chapter (see section 2.3.2).

For the other promising technologies involved in DIRSP development (micro-resistors and IR laser diodes), the trade-off discussed here does not exist. The grey levels, in that case, are obtained through current control and there is not a direct relationship between the number of radiance levels and the frame rate. Instead, for those two technologies, the trade-off is displaced to the maximum radiance simulated, that is the frame rate is limited by the time required by the pixels to reach the maximum radiance level achievable. For the IR laser diodes array, this limiting factor is not so important as the risetime of the laser diodes is very short (~ 90 ns) [15]. However, for the micro-resistors arrays, this trade-off is a critical design issue.

Another drawback of using the micro-mirrors for DIRSP applications is that the minimum radiance simulated could be limited by the parasitic light reflected or diffracted by the array structures in unwanted directions. It is difficult to quantify that complex aspect of the micro-mirrors operation. Some theoretical results based on simple models will be presented in chapter 5. However, experimentation seems to be the best approach for the evaluation of the minimum radiance level achievable in the micro-mirrors case.

For the competing technologies, the minimum simulated radiance is limited by the natural IR radiation emitted by the different system components. That leads to very high contrast ratios and to low minimum simulated radiances. On that particular point, the micro-resistors and the IR laser diodes arrays are expected to exhibit better performances than the micro-mirrors.

4. PRELIMINARY OPTICAL DESIGN STUDY

4.1 The conceptual configuration

4.1.1 Introduction

Figure 4-1 represents the conceptual layout of the projection system. It is formed by two optical components: an illumination system, incorporating a thermal source and a collimator, and a projection objective.

Three principal requirements for DMD based IR scene projection

They consist of two main optical simulation validity criteria followed by a particular condition concerning DMD illumination:

1. Ensuring that the UUT entrance aperture is uniformly filled with unpolarized and incoherent radiation projected from each pixel.
2. The uniform radiance distribution across the UUT image plane can only be achieved in the absence of vignetting.
3. Ensuring the telecentric illumination of DMD array, in order to direct the reflected chief rays parallel to the objective axis.

Starting from these requirements we can establish the characteristics of the optical architecture to be adopted:

1. The first condition could be accomplished if a thermal source is imaged at the UUT entrance aperture. In addition to that, any central obscuration is unwanted. It means that refractive or eccentric pupil reflective optics can only be used.
2. In order to avoid any vignetting, the entrance aperture of UUT must constitute the exit pupil of the projection objective (in this approach we consider the propagation of light from the source to the UUT focal plane). So far it is apparent that for such configuration the entrance pupil of projection system is located just in the source plane.
3. The telecentric illumination of DMD array could be accomplished if the source is located in the focal plane of the collimator.

The Figure 4-1 shows such conceptual configuration respecting all conditions stated above. The image of scene generated by DMD array and the source image travel through the projection system as described in the table below.

The image forming vs. pupil forming through the complete system

Optical component	The image forming through the system	The pupil forming through the system
Source plane		The blackbody source is placed in the focal plane of the collimator.
Collimator		The Collimator provides the source image at infinity.
DMD array	DMD array produces time-varying object-scenes.	
Projection Objective	The Projection Objective projects DMD object-scenes at infinity.	The Projection Objective images the source in the UUT entrance aperture.
UUT objective	The UUT objective images the DMD object-scenes onto its focal plane.	

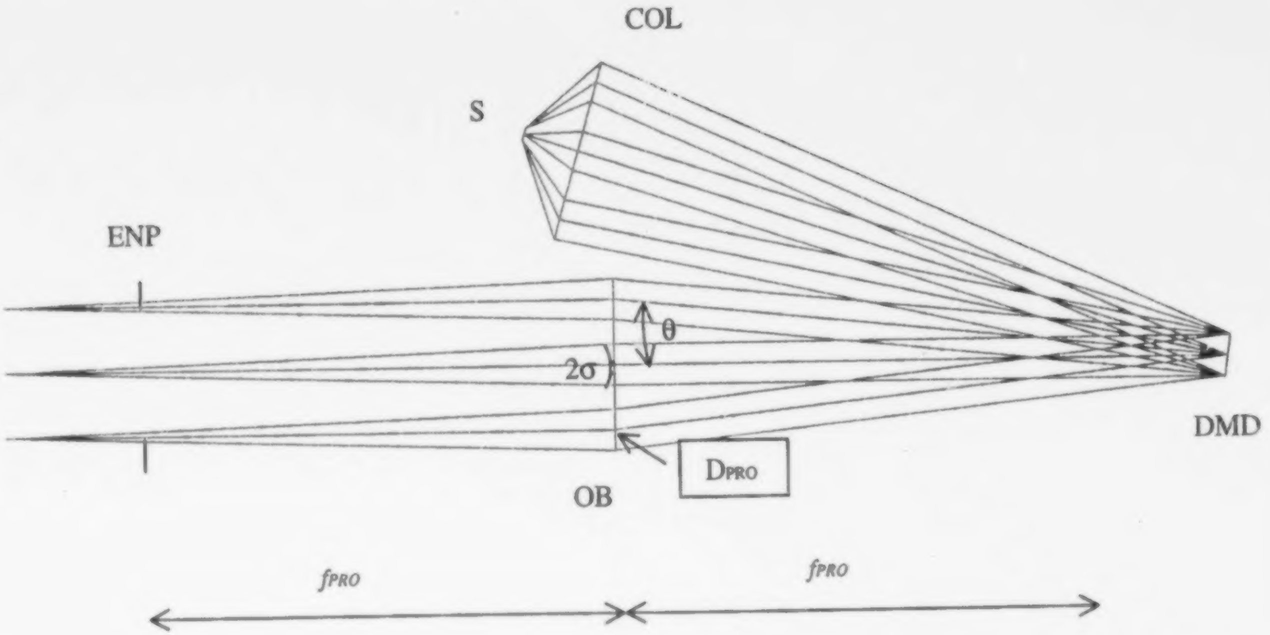
COL
S
ENP
θ
2σ
DMD
DPRO
OB
fPRO
fPRO

Figure 4-1. Conceptual Configuration

4.1.2 The general optical characteristics

The general optical characteristics refer to projection – UUT connection, spectral range, and constructive DMD parameters as follows:

Item	Target values	
Spectral Range	3..5 μm 2..5 μm 0.2..12 μm	
ENP (UUT entrance aperture)	106 mm	
Field angle (2σ)	5° 3.5°	
DMD pixel size	60 μm × 60 μm	45 μm × 45 μm
Number of pixels	256 × 256	512 × 512
DMD array size (diagonal)	22.5 mm	33.25 mm
Deflection angle (α)	± 7° ± 8.5°	
DMD operating mode	Bistable mode (ON-OFF) Tristable mode (ON-OFF-ON)	

By optical design as opposed to optical system design is generally meant the design of a single component of the system, i.e., the projection objective and collimator. When a complete optical system is designed, from light source to detector, requirements arise for the individual components, that are roughly of two kinds:

1. Gaussian optics requirements, such as focal length, magnification, numerical aperture or F/number, and field angle.
2. Aberration correction requirements.

Our task is to produce optical designs for each component that fulfill these requirements as nearly as possible. There are two parts of this task. First, It is necessary to decide on the general combination of optical elements that might be suitable, called Starting Point Configuration (SPC). Needless to say , experience and expert advice are needed in the first stage. The second stage is more mechanical in nature. The SPC must be refined to comply with the Gaussian and aberrational requirements. This can be done by means of one of optical design programs, e.g., Zeemax or CodeV. Given a good SPC and a realistic specification, it is thus possible to arrive at an optical design which can be turned into hardware by an optical manufacturer.

Using the notation of Figure 4-1 we found the Gaussian characteristics of projection system as follows.

Effective Focal Length of projection objective is given by:

$$f_{PRO} = \frac{DMD}{2\tan\sigma} \tag{4.1}$$

The semi-angle subtended by a reflected beam from each pixel is given by:

$$\tan\theta = \frac{ENP}{DMD}\tan\sigma \tag{4.2}$$

The diameter of the projection objective (a thin lens approach), is given by:

$$D_{PRO} = ENP + DMD \tag{4.3}$$

4.1.3 Theoretical considerations

A general third-order aberrations evaluation

In section 4.2. the numerical examples of different optical configurations will be given in order to determine how the optical performance varies with wavelength, field angle and F/#. This section describes how the third-order aberrations of a lens depend analytically on field and aperture parameters.

The aberrations of a general optical system can be parameterized in terms of three coordinates: r, θ, and η, where r, θ are the polar coordinates in the exit pupil, and η is a field coordinate. Taking into account the axial symmetry and monochromatic light, it is found that the wavefront aberrations (monochromatic or geometrical aberrations) depend on r^2, $r\eta\cos\theta$, η^2 and can be expressed as a power series in those variables. The terms of lowest order in r^2, $r\eta\cos\theta$, η^2 correspond to Gaussian or paraxial optics. Higher-order terms in the power series expansion represent aberrations. The next terms beyond paraxial are called primary, third-order, or Seidel aberrations; they are of fourth degree, and there are five of them as follows:

$a_s\, r^4$ represents spherical aberration
$a_c\, \eta\, r^3 \cos\theta$ represents coma
$a_a\, \eta^2\, r^2 \cos^2\theta$ represents astigmatism
$a_f\, \eta^2\, r^2$ represents field curvature
$a_d\, \eta^3\, r \cos\theta$ represents distortion

where a_s, a_c, a_a, a_f, a_d are the Seidel coefficients. They can be found from formulas involving the construction parameters of the system.

The dependence on aperture and field of the third-order aberrations can be briefly described by the following table:

	Aperture	Field
Spherical aberration	r^4	-
Coma	r^3	η
Astigmatism	r^2	η^2
Field curvature	r^2	η^2
Distortion	r	η^3

So far we assumed that the light is monochromatic. Excepting the reflective systems, all refractive lenses have chromatic aberrations. In fact what is usually meant by chromatic aberrations are variations of paraxial properties, i.e.: a shift of image-plane distance with wavelength, called longitudinal color, and a change of magnification, called transverse color. The higher-order effects are referred to chromatic variation of geometrical aberrations.

We consider now the field and aperture requirements for the optical subsystem:

> σ = 3.5° and 5°, and F/# = 544.2/106 and 258/106, respectively (see potential configurations, section 4.2).

Then, for a given optical configuration working at a given wavelength, we can estimate the order of variation of monochromatic aberrations as follows:

Spherical aberration varies 20 times
Coma varies 13.5 times
Astigmatism varies 9 times
Field Curvature varies 9 times
Distortion varies 6 times

NOTE: We assumed that the light is monochromatic.

This rough calculation gives a very first evaluation of optical design difficulty, without taking into consideration the spectral range.

4.2 Potential Configurations

Before we discuss the potential configurations we would like to present the specifications for an idealistic DMD based IR projection system and, then, their implications in optical configuration choice.

Item	Implication in optical configuration
Spectral Range 0.2..12 μm	Reflective Optics.
No Beam Splitter	A quite large DMD deflection angle.
Tristable operating mode (ON-OFF-ON)	Symmetry of optical configuration and a large deflection angle.
Unpolarized and incoherent radiation	Thermal source.
Source imaged at the UUT entrance aperture	A conceppt configuration as shown in Figure 4-1.
Telecentric illumination	
No vignetting	
No diffuser in optical layout	Thermal source and a fill factor of 100% at the UUT entrance aperture.

We will show that there are limitations involving materials and manufacturing. But also there are limitations involving the kind of optical systems that can actually be designed, as opposed to those that are theoretically possible.

4.2.1 Refractive Optics – BS, bistable mode – (Lens_1)

Item	Characteristics
Spectral range	3..5 µm
Configuration	Thermal source in the focal plane of Collimator Beam Splitter Bistable operating mode (ON-OFF) Telecentric illumination Source imaged at the UUT entrance aperture No vignetting No diffuser in optical layout
ENP	106 mm
Field angle (2σ)	5°
DMD (array diagonal)	22.5 mm
Deflection angle (α)	±7°
Objective focal length (f_{PRO})	258 mm
Angle of reflected beam from each pixel	23.2°
Collimator focal length (f_{COL})	50 mm
Source diameter	20.54 mm

In the Appendix I we give the layout, prescription data, spot diagram, distortion, and MTF graphics of the projection objective, followed by the layout and prescription data of the collimator. Finally, three layouts showing the bistable operating mode of this configuration are given.

4.2.2 Refractive Optics – No BS, tristable mode – (Lens_2)

Item	Characteristics
Spectral range	2..5 μm
Configuration	Thermal source in the focal plane of Collimator No Beam Splitter Tristable operating mode (ON-OFF-ON) Telecentric illumination Source imaged at the UUT entrance aperture No vignetting No diffuser in optical layout
ENP	106 mm
Field angle (2σ)	3.5°
DMD (array diagonal)	33.25 mm
Deflection angle (α)	±8.5°
Objective focal length (f_{PRO})	544.2 mm
Angle subtended by a reflected beam from each pixel	11.12°
Collimator focal length (f_{COL})	52 mm
Source diameter	10.13 mm

In the Appendix II we give the layout, prescription data, spot diagram, distortion, and MTF graphics of two projection objectives optimized for spectral ranges of 2.5..4 μm and 2..4 μm, respectively, followed by the layout and prescription data of the collimator. Finally, three layouts showing the tristable operating mode of this configuration are given.

4.2.3 Reflective Optics – 5° – (Mirror_1)

Item	Characteristics
Spectral range	0.2..12 μm
Configuration	Thermal source in the focal plane of Collimator No Beam Splitter Bistable operating mode (ON-OFF) Telecentric illumination Source imaged at the UUT entrance aperture Vignetting No diffuser in optical layout
ENP	106 mm
Field angle (2σ)	5°
DMD (array diagonal)	22.5 mm
Deflection angle (α)	±7°
Objective focal length (f_{PRO})	258 mm
Angle subtended by a reflected beam from each pixel	28°
Collimator focal length (f_{COL})	50 mm
Source diameter	20.54 mm

In the Appendix III we give the layout, prescription data, spot diagram, distortion, and MTF graphics of the reflective projection objective, followed by three layouts showing the bistable operating mode of this configuration.

4.2.4 Reflective Optics – 3.5° – (Mirror_2)

Item	Characteristics
Spectral range	0.2..12 μm
Configuration	Thermal source in the focal plane of Collimator No Beam Splitter (BS) Tristable operating mode (ON-OFF-ON) Telecentric illumination Source imaged at the UUT entrance aperture No vignetting No diffuser in optical layout
ENP	106 mm
Field angle (2σ)	3.5°
DMD (array diagonal)	33.25 mm
Deflection angle (α)	±8.5°
Objective focal length (f_{PRO})	544.2 mm
Angle subtended by a reflected beam from each pixel	13°
Collimator focal length (f_{COL})	50 mm
Source diameter	9.74 mm

In the Appendix IV we give the layout, prescription data, spot diagram, distortion, and MTF graphics of the reflective projection objective, followed by three layouts showing the tristable operating mode of this configuration.

4.2.4 Comparative Table

Item	Lens_1	Lens_2	Mirror_1	Mirror_2
Spectral range	3..5 µm	2..5 µm	0.2..12 µm	0.2..12 µm
Configuration	▪ BS ▪ ON-OFF	★ No BS ★ON-OFF-ON	★No BS ▪ ON-OFF ▪ Vignetting	★ No BS ★ON-OFF-ON
Field angle (2σ)	★ 5°	3.5°	★ 5°	3.5°
DMD (technology)	★Low requirements	Severe requirements	★Low requirements	Severe requirements
Source diameter	20.54 mm	10.13	20.54	9.74
Compactness	★	★	★	★
Over-All-Length (OAL)	355.4 mm	590 mm	260 mm	525 mm
Axial distance UUT-Projector	27 mm	505 mm	Included in OAL	Included in OAL
Maximum transverse size	150 mm	250 mm	260	500 mm
Optical performances		★	▪	
Spot Diagram (RMS radius)	<15 µm	<18.5 µm	<36.2 µm	<8 µm
Distortion	<0.05%	<0.05%	<4.5%	<3%
MTF @ 10 lp/mm	>0.75	>0.7	>0.3	>0.25

★ Advantage

▪ Disadvantage

Recommandation

All configurations described above are outstanding because of their compactness. Three of configurations do not use beam splitter for illumination ensuring a high energy transmission through the system. In addition, the configurations Lens_2 and Mirror_2 provide tristable operating mode.

Based on the performed optical preliminary design study and taking into account the conceptual design analysis of the configurations presented in the section 4.2. we recommend that the following two optical configurations should be considered in the optical design phase: Lens_2 and Mirror_2. Both of them meet well the optical specifications, i.e., basic Gaussian requirements (however FOV is 3.5° instead of 5°), technological feasibility, compactness, as well as optical performances. Despite the weaknesses in some optical performances, as well as the difficulties in manufacturing, the reflective configuration Mirror_2 is very attractive because of its wide spectral band.

For the reflective optics, only mirrors that are useful in the UV range can be considered and very few choices are available. Aluminum mirrors over-coated with MgF_2 can be used (≤ 100 angstroms RMS), but nickel plated mirrors that are polished then over-coated with aluminum and MgF_2 are preferable (≤ 60 angstroms RMS). Metal mirrors can be diamond turned so aspherical surfaces are possible but post-polishing may modify slightly the surface shape. Intrinsically, mirrors have no dispersion.

Regarding the fabrication, it is important to notice that in the UV range scattering from rough surfaces can become important so the RMS roughness should be kept as low as possible. An rms roughness of 50-60 angstroms or less is desirable to reduce that effect. UV lenses manufacturers are more likely to be able to produce better surfaces. It should also be kept in mind that aspherical surfaces are likely to cost 2 to 5 times more than spherical surfaces. An additional cost is to be expected due to the UV requirements that asks for post-polishing after diamond turning. However, it is possible that the post polishing will affect the surface accuracy.

5. RADIOMETRIC PERFORMANCES OF THE INFRARED SCENE PROJECTOR

This chapter will be added to the report by the end of January '98.

6. CONCLUSION

As a summary of the present report, it is instructive to review the specifications given in Table 5 in the light of the data and information gathered throughout this feasibility study. According to this information, micro-mirrors arrays as large as 512 x 512 are feasible, fulfilling the specifications of Table 5. However, the mirrors size, in that case, should be kept below 45 μm in order to avoid the need for huge addressing integrated circuits.

The lower limit required for the frame rate, 200 Hz, can be achieved using Binary Pulse Width Modulation if the number of addressing bits needed is not higher than 7 bits (i.e. 128 radiance levels). Thus, BPWM just meets the basic requirements of Table 5. If the Single Pulse Width Modulation scheme would be adopted, 1024 radiance levels (10 bits) should be available at 500 Hz. If the radiance resolution specification is reduced to the value given in Table 5 (7 bits), then a frame rate of 3.5 kHz should be achievable. It is therefore obvious that the SPWM scheme easily meets the requirements for the frame rate and the signal resolution. However, it is likely that the control electronics would be more complex than in the case of BPWM. Whatever PWM scheme would be implemented, the flicker should be very close or equal to zero. Actually, when the micro-mirrors are used as modulators, the frame duration must be shorter or equal to the integration time of the detectors to be stimulated. This specific requirement aims at eliminating the flicker in the image projected and it should be sufficient to insure that any radiance variation within a particular frame, due to the switching of the mirrors from the ON to the OFF state (or vice versa), should not be detectable.

The diameter of the Unit Under Test (UUT) specified in Table 5 was taken as one of the basic geometric parameters for the optical systems design. Therefore, every design presented in chapter 4 fulfils that specification. Moreover, with the exception of the preliminary design LENS_1 optimized for 3-5 μm, they all meet or greatly exceed the spectral range specification of 2-5 μm. The preliminary designs exceeding that specification are based on reflective optical components. The drawbacks associated with this approach are that the optical components would be eventually more expensive and that a compromise exists between the size of the Instantaneous Field of View (IFOV) and the distortion level in the image projected.

The IFOV of 5° specified in Table 5 is fulfilled by two of the four designs presented in chapter 4. In two other designs, the IFOV was decreased to 3.5° in order to take advantage of the tristable operation of the micro-mirrors (see section 3.2). Moreover, reducing the IFOV allows the design of a transmissive optical system which does not include a beam splitter. This is an important advantage from the system energetic budget point of view (i.e. a beam splitter causes an intensity loss of at least 75%).

Assuming that a 512 x 512 micro-mirrors array would be used in the IR projector, the angular resolution of 0.17 mrad listed in Table 5 could be met for a IFOV of 5°. If the IFOV could be decreased to 3.5°, the angular resolution specification would be exceeded (0.12 mrad) which could be an interesting compromise in some cases. Particular attention was given to the intensity uniformity at the UUT entrance. Two particular design criteria were used to insure a good uniformity at the UUT. First, the IR source is imaged at the UUT entrance. Second, the radiation reflected by any particular micro-mirror in the ON state fills completely the UUT entrance. It should be noted that this second criteria is particularly important for the simulation validity [15]. Finally, if the uniformity would still not be good enough, it should be possible to implement a Non-Uniformity Correction procedure (NUC) with the addressing electronics in order to improve the situation.

It is clearly stated in Table 5 that the radiation projected by a Dynamic IR Scene Projector should be spatially incoherent. This requirement is necessary to insure that the UUT image plane will be free of unwanted interference effects. That simulation validity criterion [15] should be fulfilled through the use of an extended black body source, as proposed in chapter 4. However, if a laser source is to be used, a rotating diffuser should be placed in front of it in order to make the laser spatial coherence vanish.

All preliminary optical system designs presented in chapter 4 are very compact. Therefore, it should be possible to mount any of those systems on a flight table, allowing to fulfil one more requirement of Table 5. From this possibility, it follows that the total field of view (specification: ± 20°), the maximum scene angular speed (specification: 30°/s) and the maximum scene angular acceleration (specification: 300°/s) all depend on the flight table capabilities. It is likely that a flight table meeting those specifications could be found.

Discussion of the specifications related to IR projector performances characterized in chapter 5 will be added in January 1998.

In conclusion, it appears that all the specifications of Table 5 could be fulfilled by a Dynamic Infrared Scene Projector based on the micro-mirrors technology. This would lead to a high quality DIRSP characterized by outstanding capabilities. It should be noted that the specifications listed in Table 5 were used mainly as an evaluation basis. It is clear, however, that many compromises are possible to adjust the DIRSP performances to particular requirements. Hopefully, the present report allowed to point out the main decisions to be made when specifying a DIRSP based on micro-mirrors and permitted to emphasize the associated trade-offs.

Finally, satisfactory answers were given to most questions raised about the validity of simulations performed with DIRSP based on micro-mirrors. Specifically, optical designs were presented in which the radiation reflected by any particular micro-mirror in the ON state fills the UUT entrance; provisions were taken in order to avoid spatial coherence of the radiation projected and it was demonstrated that, theoretically, high frame rates should be achievable.

The main questions still remaining concern the radiance resolution at high frame rate and the minimum radiance achievable. Experimental investigation seems to be the best way to evaluate the limits of the micro-mirrors technology regarding these two particular aspects.

7. REFERENCES

1. R.L. Knipe, "Challenges of a Digital Micromirror Device: modelling and design", SPIE/EOS European Symposium on Lasers, Optics, and Vision for Productivity in Manufacturing I, Besançon, France (June 10-14, 1996).

2. L. J. Hornbeck, "Digital Light Processing and MEMS: Reflecting the digital display needs of the networked society", SPIE/EOS European Symposium on Lasers, Optics, and Vision for Productivity in Manufacturing I, Besançon, France (June 10-14, 1996).

3. L. J. Hormbeck, "Deformable-mirror Spatial Light Modulators", SPIE Critical Reviews Series, Vol. 1150, pp. 86-102.

4. R.W. Fuchs, "Novel Beam Steering Micromirror Device: Design, Fabrication and Testing", Master Thesis in Electrical and Computer Engineering, Waterloo, Ontario, Canada, 1997, 120 p.

5. G.C. Wetsel jr. and K.J. Strozewski, "Dynamical model of microscale electromechanical spatial light modulator", J. Appl. Phys. 73 (11), 1 June 1993, pp. 7120-7124.

6. K.J. Strozewski, C.-Y. Wang and G.C. Wetsel jr., "Characterization of a micromechanical spatial light modulator", J. Appl. Phys. 73 (11), 1 June 1993, pp. 7125-7128.

7. E.M. Purcell, Electricité et magnétisme, Berkeley: cours de physique, volume 2, Librairie Armand Colin, Paris, 1973, pp. 49-50.

8. E. Durand, Electrostatique, tome II: Problèmes généraux, conducteurs, Masson et Cie, Éditeurs, 1966, p. 189.

9. V. Markandey, T. Clatanoff, R. Gove and K. Ohara, "Motion Adaptive Deinterlacer for DMD (Digital Micromirror Device) Based Digital Television", IEEE Transactions on Consumer Electronics, Vol. 40, No. 3, August 1994, pp. 735-742.

10. R.J. Gove, V. Markandey, S.W. Marshall, D.B. Doherty, G. Sextro and M. DuVal, "High Definition Display System Based on Digital Micromirror Device", Signal Processing of HDTV VI, Elsevier Science, 1995, pp. 89-97.

11. V. Markandey, T. Clatanoff and G. Pettitt, "Video Processing for DLP Display Systems", SPIE Vol. 2666, pp. 21-32.

12. E.H. Chiu, C. Tran, T. Honzawa and S. Numaga, "Design and Implementation of a 525 mm^2 CMOS Digital Micromirror Device (DMD) Display Chip", Int. Symposium on VLSI Tech. Systems, and Applications, Proceeding of Technical Papers, 1995, pp. 137-139.

13. L. Demers and N. Bédard, "Imaging Infrared Projector Design", Pers. Comm., January 23, 1995, pp. 2-6.

14. A.J. Beaulieu, "Analysis of an IR imaging Projector System", Report produced by BCI Consultants, April 23, 1997, pp. 1-17.

15. O.M. Williams, "Imaging Infrared Projector Design", Final report of key technical area 18, Technical Panel WTP-5 (Guidance and Control Technology), The Technical Cooperation Program (TTCP), Subgroup W (Conventional Weapons Technology).

APPENDIX I
LENS_1

Refractive Optics – BS, bistable mode – (Lens_1)

Item	Characteristics
Spectral range	3..5 μm
Configuration	Thermal source in the focal plane of Collimator Beam Splitter Bistable operating mode (ON-OFF) Telecentric illumination Source imaged at the UUT entrance aperture No vignetting No diffuser in optical layout
ENP	106 mm
Field angle (2σ)	5°
DMD (array diagonal)	22.5 mm
Deflection angle (α)	±7°
Objective focal length (f_{PRO})	258 mm
Angle of reflected beam from each pixel	23.2°
Collimator focal length (f_{COL})	50 mm
Source diameter	20.54 mm

In the following pages we give the layout, prescription data, spot diagram, distortion, and MTF graphics of the projection objective, followed by the layout and prescription data of the collimator. Finally, three layouts showing the bistable operating mode of this configuration are given.

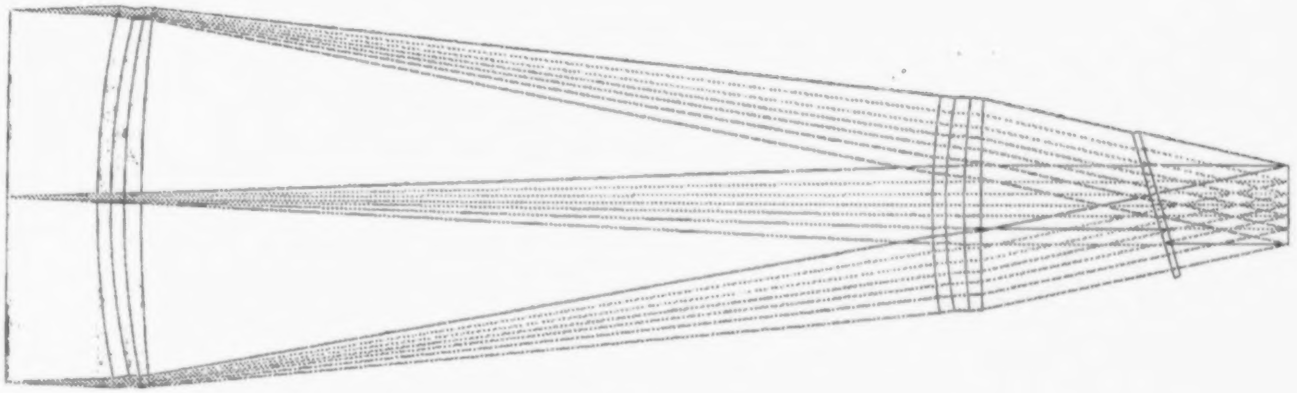

3D LAYOUT

IR_PROJECTOR_OBJ
THU NOV 6 13:25:0 1997
SCALE: 0.5000

40.00 MILLIMETERS

NATIONAL OPTICS INSTITUTE
SR. OPTICAL DESIGNER: DR. EUGENE CURATU

H:\IR_PROJECTOR\PRE_DESIGN\SEARCH_OCT18\PROBS_ESS2.ZMX

```
ystem/Prescription Data

ile : H:\IR_projector\pre_design\search_oct18\proBS_ess2.zmx
Title: IR_projector_OBJ
ate : THU NOV 6 13:25:15 1997

ENERAL LENS DATA:

Surfaces           :                  16
top                :                   1
ystem Aperture : Entrance Pupil Diameter = 106
ay aiming          : Off
Apodization        :Uniform, factor =   0.00000E+000
Eff. Focal Len. :            257.999 (in air)
ff. Focal Len. :            257.999 (in image space)
otal Track         :          382.4006
mage Space F/# :          2.433953
Para. Wrkng F/# :          2.433953
orking F/#         :          2.433837
bj. Space N.A.  :          5.3e-009
top Radius         :                53
Parax. Ima. Hgt.:          11.26448
Parax. Mag.        :                 0
ntr. Pup. Dia.  :               106
ntr. Pup. Pos.  :                 0
xit Pupil Dia.  :          163592.8
Exit Pupil Pos. :          398177.2
Field Type         : Angle in degrees
aximum Field       :               2.5
rimary Wave        :                 4
ens Units          :    Millimeters
ngular Mag.        :    -0.0006479502

ields              : 7
eld Type: Angle in degrees
          X-Value           Y-Value          Weight
1         0.000000          2.500000         0.700000
          0.000000          0.000000         1.000000
          0.000000         -2.500000         0.700000
          0.000000          1.500000         0.800000
5         0.000000         -1.500000         0.800000
6         0.000000          0.700000         1.000000
          0.000000         -0.700000         1.000000

gnetting Factors
        VDX         VDY         VCX         VCY
    0.000000   0.000000   0.000000   0.000000
    0.000000   0.000000   0.000000   0.000000
    0.000000   0.000000   0.000000   0.000000
    0.000000   0.000000   0.000000   0.000000
    0.000000   0.000000   0.000000   0.000000
    0.000000   0.000000   0.000000   0.000000
    0.000000   0.000000   0.000000   0.000000

avelengths         : 3
nits: Microns
            Value            Weight
1         3.000000         0.500000
2         4.000000         1.000000
3         5.000000         0.500000

RFACE DATA SUMMARY:

rf      Type                 Comment          Radius        Thickness          Glass          Diameter          Conic
OBJ STANDARD                                Infinity         Infinity                                0              0
STO STANDARD                                Infinity               27                              106              0
  2 STANDARD                                257.0717                4      GERMANIUM          108.8667              0
  3 STANDARD                                217.2214                4                         107.3821              0
  4 STANDARD                                256.2735                5        SILICON          108.3809              0
  5 STANDARD                                493.4031         236.3283                         107.9206              0
  6 STANDARD                                  208.25                4      GERMANIUM          62.03048              0
  7 STANDARD                                169.2766         5.499137                          60.8139              0
  8 STANDARD                                  257.05                5        SILICON          60.79495              0
  9 STANDARD                                868.1302          51.4219                         60.16524              0
 10 COORDBRK                                       -                0              -                 -              -
 11 COORDBRK                                       -                0              -                 -              -
 12 STANDARD                                Infinity                2           ZNSE          43.39654              0
 13 STANDARD                                Infinity                0                          42.5893              0
 14 COORDBRK                                       -                0              -                 -              -
 15 COORDBRK                                       -         38.15122              -                 -              -
IMA STANDARD                                Infinity                                          22.60158              0

RFACE DATA DETAIL:

urface OBJ      : STANDARD
urface STO      : STANDARD
```

```
rface   2      : STANDARD
rface   3      : STANDARD
urface   4      : STANDARD
urface   5      : STANDARD
urface   6      : STANDARD
rface   7      : STANDARD
rface   8      : STANDARD
urface   9      : STANDARD
urface  10      : COORDBRK
ecenter X      :                    0
ecenter Y      :                    0
ilt About X    :                    0
Tilt About Y    :                    0
Tilt About Z    :                    0
rder           : Decenter then tilt
rface  11      : COORDBRK
ecenter X      :                    0
Decenter Y      :                    0
Tilt About X    :                  -17
ilt About Y    :                    0
ilt About Z    :                    0
Order           : Decenter then tilt
urface  12      : STANDARD
rface  13      : STANDARD
rface  14      : COORDBRK
ecenter X      :                    0
Decenter Y      :                    0
Tilt About X    :                   17
ilt About Y    :                    0
ilt About Z    :                    0
rder           : Decenter then tilt
urface  15      : COORDBRK
Decenter X      :                    0
ecenter Y      :              -0.2315
ilt About X    :                    0
Tilt About Y    :                    0
Tilt About Z    :                    0
rder           : Decenter then tilt
rface IMA      : STANDARD

DGE THICKNESS DATA:

rf          X-Edge         Y-Edge
TO       32.522783      32.522783
 2        5.101723       5.101723
 3        2.947404       2.947404
 4        2.189944       2.189944
 5      240.481148     240.481148
 6        4.543052       4.543052
 7        4.550548       4.550548
 8        3.728689       3.728689
 9       50.900529      50.900529
10        0.000000       0.000000
11        0.000000       0.000000
12        2.000000       2.000000
13        0.000000       0.000000
14        0.000000       0.000000
15       38.151223      38.151223
MA        0.000000       0.000000

OLVE AND VARIABLE DATA:

ickness of   1       : Variable
mi Diameter   1      : Fixed
urvature of   2       : Variable
rvature of   3       : Variable
rvature of   4       : Variable
rvature of   5       : Variable
hickness of   5       : Variable
urvature of   6       : Variable
rvature of   7       : Variable
ickness of   7       : Variable
rvature of   8       : Variable
urvature of   9       : Variable
arameter  3 Surf  14  : Pickup from 11 times -1.000000
ickness of  15       : Solve, marginal ray height = 0.00000

DEX OF REFRACTION DATA:

urf     Glass       3.000000    4.000000    5.000000
 0               1.00000000  1.00000000  1.00000000
 1               1.00000000  1.00000000  1.00000000
 2  GERMANIUM    4.04478148  4.02466417  4.01552804
 3               1.00000000  1.00000000  1.00000000
 4   SILICON     3.43232207  3.42530049  3.42206716
 5               1.00000000  1.00000000  1.00000000
```

```
  6   GERMANIUM    4.04478148  4.02466417  4.01552804
  7                1.00000000  1.00000000  1.00000000
  8    SILICON     3.43232207  3.42530049  3.42206716
  9                1.00000000  1.00000000  1.00000000
 10 <CRD BRK>      1.00000000  1.00000000  1.00000000
 11 <CRD BRK>      1.00000000  1.00000000  1.00000000
 12        ZNSE    2.43757888  2.43315886  2.42952719
 13                1.00000000  1.00000000  1.00000000
 14 <CRD BRK>      1.00000000  1.00000000  1.00000000
 15 <CRD BRK>      1.00000000  1.00000000  1.00000000
 16                1.00000000  1.00000000  1.00000000

HERMAL COEFFICIENT OF EXPANSION DATA:

rf      Glass             TCE
  0                0.00000000
  1                0.00000000
  2   GERMANIUM    5.69999981
  3                0.00000000
  4    SILICON     2.61999989
  5                0.00000000
  6   GERMANIUM    5.69999981
  7                0.00000000
  8    SILICON     2.61999989
  9                0.00000000
 10 <CRD BRK>      0.00000000
 11 <CRD BRK>      0.00000000
 12        ZNSE    7.09999990
 13                0.00000000
 14 <CRD BRK>      0.00000000
 15 <CRD BRK>      0.00000000
 16                0.00000000

/# DATA:

/# calculations consider vignetting factors and ignore surface apertures.

              Wavelength:       3.000000            4.000000            5.000000
                   Field      Tan       Sag       Tan       Sag       Tan       Sag
    0.0000, 2.5000 deg:    2.4441    2.4373    2.4439    2.4372    2.4439    2.4372
2   0.0000, 0.0000 deg:    2.4339    2.4339    2.4338    2.4338    2.4338    2.4338
3  0.0000, -2.5000 deg:    2.4441    2.4373    2.4439    2.4372    2.4439    2.4372
    0.0000, 1.5000 deg:    2.4375    2.4351    2.4374    2.4351    2.4374    2.4350
   0.0000, -1.5000 deg:    2.4375    2.4351    2.4374    2.4351    2.4374    2.4350
    0.0000, 0.7000 deg:    2.4347    2.4342    2.4346    2.4341    2.4346    2.4341
7  0.0000, -0.7000 deg:    2.4347    2.4342    2.4346    2.4341    2.4346    2.4341

OBAL VERTEX COORDINATES AND DIRECTIONS:

rf        X coord        Y coord         Z coord    X direc    Y direc    Z direc
 1       0.000000       0.000000        0.000000   0.000000   0.000000   1.000000
 2       0.000000       0.000000       27.000001   0.000000   0.000000   1.000000
 3       0.000000       0.000000       31.000001   0.000000   0.000000   1.000000
 4       0.000000       0.000000       35.000001   0.000000   0.000000   1.000000
 5       0.000000       0.000000       40.000001   0.000000   0.000000   1.000000
 6       0.000000       0.000000      276.328309   0.000000   0.000000   1.000000
 7       0.000000       0.000000      280.328309   0.000000   0.000000   1.000000
 8       0.000000       0.000000      285.827446   0.000000   0.000000   1.000000
 9       0.000000       0.000000      290.827446   0.000000   0.000000   1.000000
 0       0.000000       0.000000      342.249346   0.000000   0.000000   1.000000
 1       0.000000       0.000000      342.249346   0.000000   0.292372   0.956305
 2       0.000000       0.000000      342.249346   0.000000   0.292372   0.956305
 3       0.000000       0.584743      344.161955   0.000000   0.292372   0.956305
 4       0.000000       0.584743      344.161955   0.000000   0.000000   1.000000
 5       0.000000       0.353243      344.161955   0.000000   0.000000   1.000000
 6       0.000000       0.353243      382.313178   0.000000   0.000000   1.000000

EMENT VOLUME DATA:

lues are only accurate for plane and spherical surfaces.
ement volumes are computed by assuming edges are squared up
 the larger of the front and back radial aperture.

                              Volume cc   Density g/cc          Mass g
ement surf   2 to   3         42.267058       5.327000      225.156622
ement surf   4 to   5         33.252800       2.329000       77.445772
ement surf   6 to   7         12.896374       5.327000       68.698988
ement surf   8 to   9         12.671712       2.329000       29.512418
ement surf  12 to  13          2.958217       5.264000       15.572055
tal Mass:                                                   416.385854

RDINAL POINTS:

ject space positions are measured with respect to surface 1.
age space positions are measured with respect to the image surface.
e index in both the object space and image space is considered
```

```
                                Object Space          Image Space
W = 3.000000
Principal Planes  :             258.167280           -258.003091
Nodal Planes      :             258.167280           -258.003091
Focal Planes      :               0.164381             -0.000192
Anti-Nodal Planes :            -257.838518            258.002707

W = 4.000000 (Primary)
Principal Planes  :             258.166138           -257.998968
Nodal Planes      :             258.166138           -257.998968
Focal Planes      :               0.167170             -0.000000
Anti-Nodal Planes :            -257.831797            257.998968

W = 5.000000
Principal Planes  :             258.161117           -257.994680
Nodal Planes      :             258.161117           -257.994680
Focal Planes      :               0.160364              0.006073
Anti-Nodal Planes :            -257.840390            258.006826
```

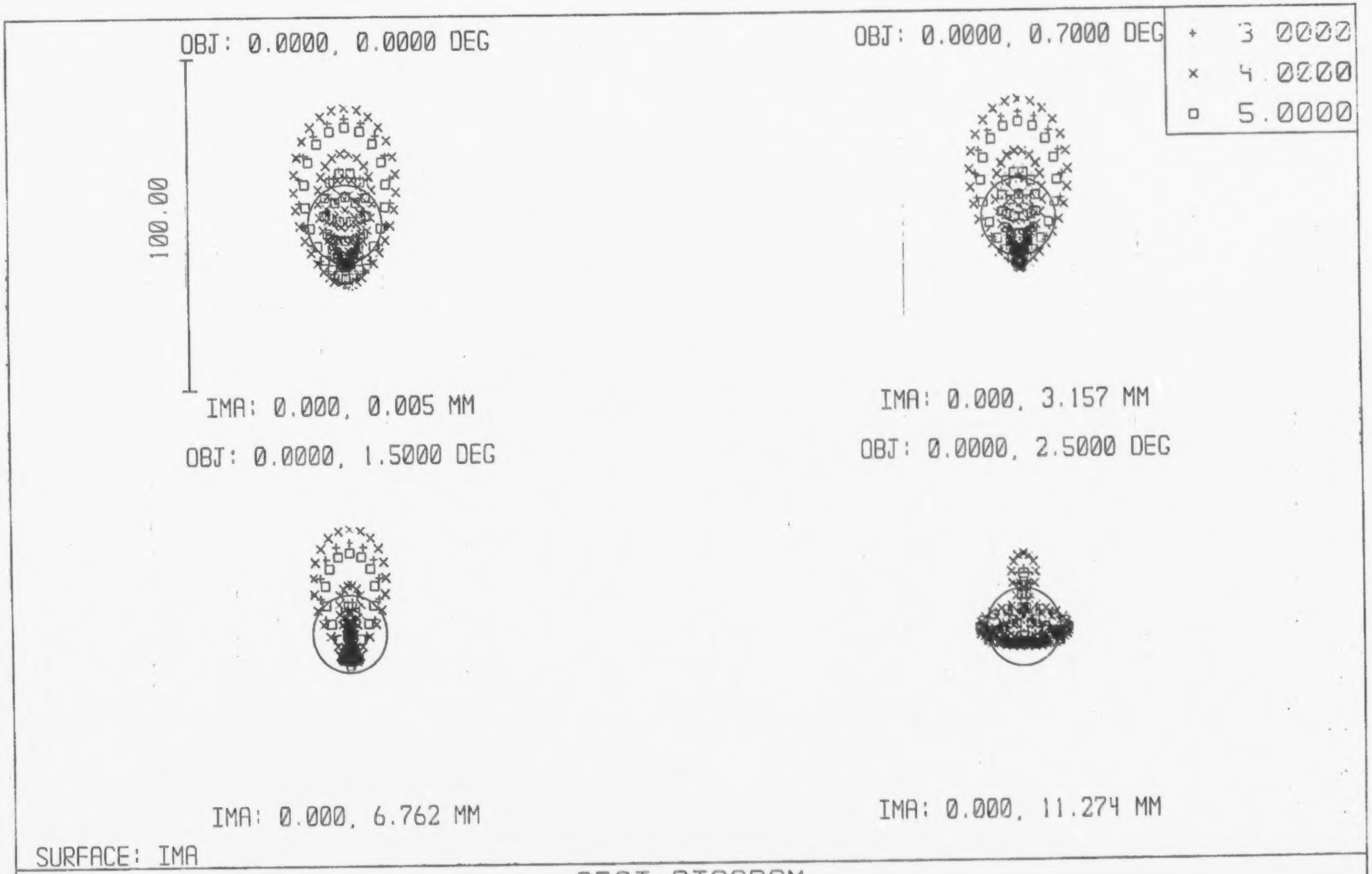

```
SPOT DIAGRAM

IR_PROJECTOR_OBJ
MON DEC 1 12:22:13 1997  UNITS ARE MICRONS.
FIELD      :        1        2        3        4
RMS RADIUS :   14.673   13.722   10.376    9.184
GEO RADIUS :   35.058   35.562   32.362   22.453
AIRY DISK  :    11.88              REFERENCE  : CENTROID

NATIONAL OPTICS INSTITUTE

H:\IR_PROJECTOR\PRE_DESIGN\SEARCH_OCT18\PROBS_ESS2.ZMX
```

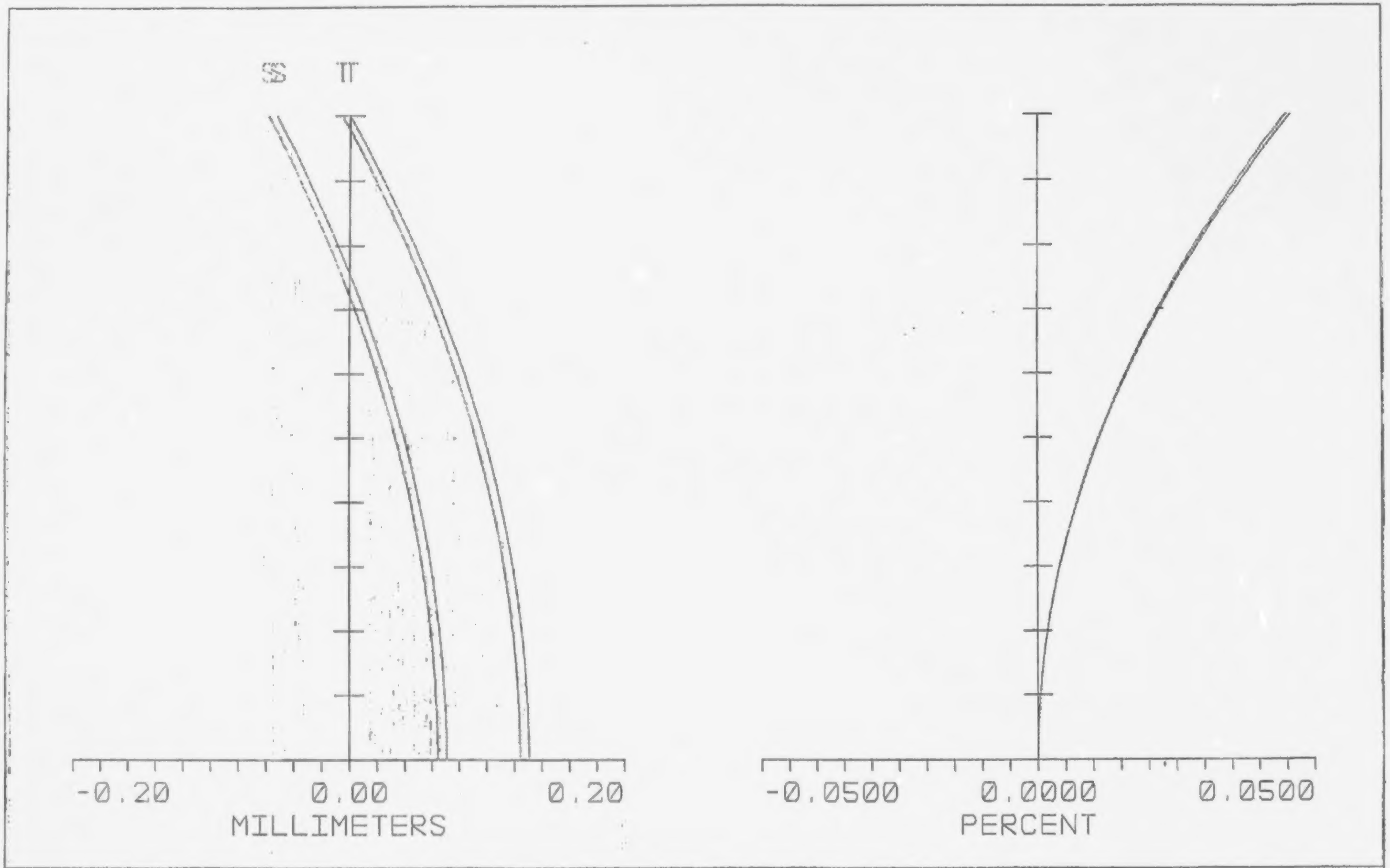

FIELD CURVATURE / DISTORTION

IR_PROJECTOR_OBJ
THU NOV 6 13:31:44 1997
MAXIMUM FIELD IS 2.500 DEGREES
WAVELENGTHS: 3.000 4.000 5.000

NATIONAL OPTICS INSTITUTE
SR. OPTICAL DESIGNER: DR. EUGENE CURATU

H:\IR_PROJECTOR\PRE_DESIGN\SEARCH_OCT18\PROBS_ESS2.ZMX

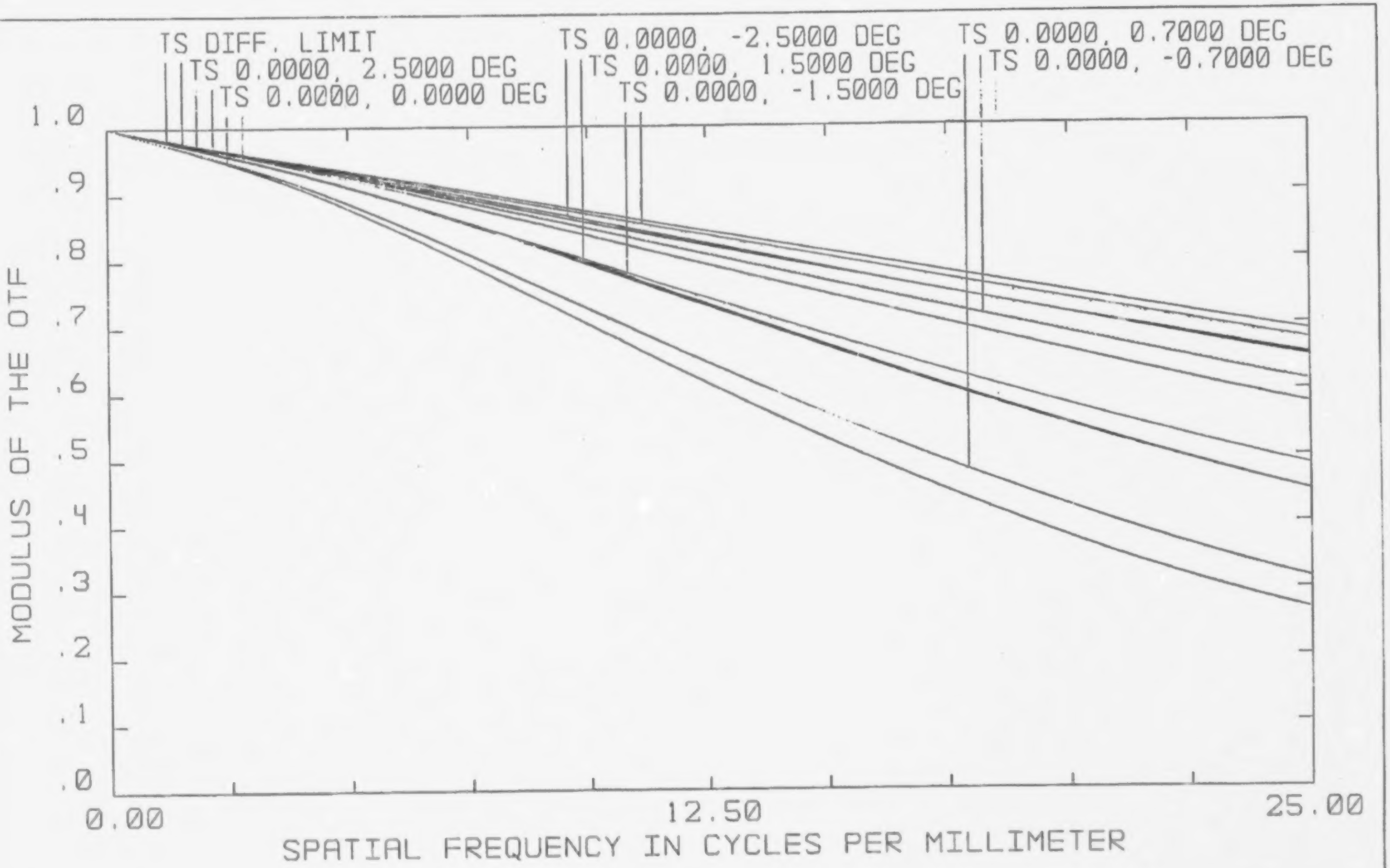

POLYCHROMATIC DIFFRACTION MODULATION TRANSFER FUNCTION

IR_PROJECTOR_OBJ
THU NOV 6 14:21:20 1997
DATA FOR 3.0000 TO 5.0000 MICRONS.

NATIONAL OPTICS INSTITUTE
SR. OPTICAL DESIGNER: DR. EUGENE CURATU

H:\IR_PROJECTOR\PRE_DESIGN\SEARCH_OCT18\PROBS_ESS2.ZMX

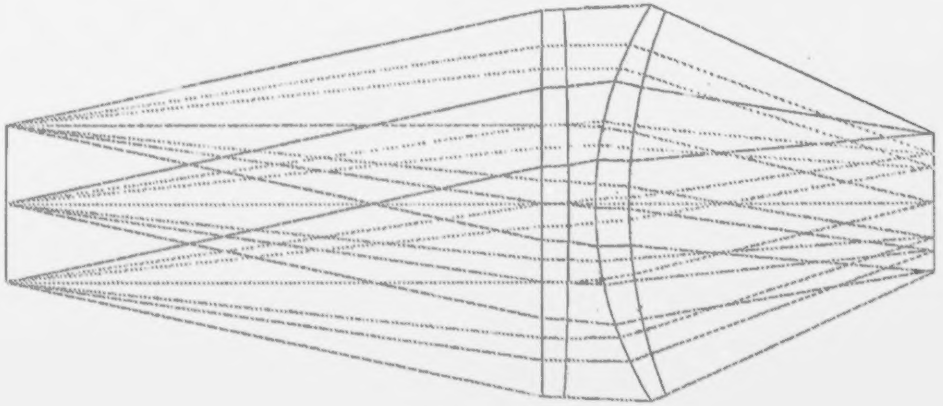

3D LAYOUT

COLLIMATOR
THU NOV 6 13:27:28 1997
SCALE: 1.0000

20.00 MILLIMETERS

NATIONAL OPTICS INSTITUTE
SR. OPTICAL DESIGNER: DR. EUGENE CURATU

H:\IR_PROJECTOR\PRE_DESIGN\SEARCH_OCT18\ILL_ESS.ZMX

```
ystem/Prescription Data

ile : H:\IR_projector\pre_design\search_oct18\ill_ess.zmx
Title: Collimator
Date : THU NOV 6 13:27:17 1997

ENERAL LENS DATA:

Surfaces           :                  6
Stop               :                  1
ystem Aperture     : Entrance Pupil Diameter = 22.5
ay aiming          : Off
Apodization        :Uniform, factor =    0.00000E+000
Eff. Focal Len.    :          50.0515 (in air)
ff. Focal Len.     :          50.0515 (in image space)
otal Track         :         138.2656
mage Space F/#     :         2.224511
Para. Wrkng F/#    :         2.224511
Working F/#        :         2.242603
bj. Space N.A.     :       1.125e-009
top Radius         :            11.25
arax. Ima. Hgt.    :             10.3
Parax. Mag.        :                0
Entr. Pup. Dia.    :             22.5
ntr. Pup. Pos.     :                0
xit Pupil Dia.     :         35.87352
Exit Pupil Pos.    :         79.80105
Field Type         : Image height in Millimeters
aximum Field       :             10.3
rimary Wave        :                4
ens Units          :   Millimeters
Angular Mag.       :       -0.6272036

ields              : 7
ield Type: Image height in Millimeters
           X-Value          Y-Value            Weight
 1        0.000000        10.300000          0.700000
 2        0.000000         0.000000          1.000000
          0.000000       -10.300000          0.700000
          0.000000         7.000000          0.800000
 5        0.000000        -7.000000          0.800000
 6        0.000000         5.000000          0.900000
          0.000000        -5.000000          0.900000

gnetting Factors
          VDX        VDY         VCX        VCY
   0.000000   0.000000   0.000000   0.000000
   0.000000   0.000000   0.000000   0.000000
   0.000000   0.000000   0.000000   0.000000
   0.000000   0.000000   0.000000   0.000000
   0.000000   0.000000   0.000000   0.000000
   0.000000   0.000000   0.000000   0.000000
   0.000000   0.000000   0.000000   0.000000

avelengths      : 3
nits: Microns
            Value            Weight
         3.000000          0.500000
         4.000000          1.000000
 3       5.000000          0.500000

RFACE DATA SUMMARY:

rf      Type              Comment           Radius       Thickness          Glass         Diameter           Conic
OBJ STANDARD                              Infinity        Infinity                               0               0
STO STANDARD                              Infinity              80                            22.5               0
  2 STANDARD                              Infinity               4      GERMANIUM         55.42608               0
  3 STANDARD                             -543.0358               4                        55.75618               0
  4 STANDARD                              53.08186               5        SILICON         56.97383               0
  5 STANDARD                              72.47935        45.26564                        55.15937               0
IMA STANDARD                              Infinity                                        20.09847               0

RFACE DATA DETAIL:

urface OBJ       : STANDARD
urface STO       : STANDARD
urface   2       : STANDARD
urface   3       : STANDARD
urface   4       : STANDARD
urface   5       : STANDARD
urface IMA       : STANDARD

GE THICKNESS DATA:

urf           Edge
TO       80.000000
```

```
  2       3.292392
  3      12.626078
  4       2.541418
  5      39.813273
IMA       0.000000

OLVE AND VARIABLE DATA:

urvature of    3          : Variable
rvature of     4          : Variable
rvature of     5          : Variable
hickness of    5          : Solve, marginal ray height = 0.00000

NDEX OF REFRACTION DATA:

rf      Glass       3.000000    4.000000    5.000000
  0               1.00000000  1.00000000  1.00000000
  1               1.00000000  1.00000000  1.00000000
  2  GERMANIUM     4.04478148  4.02466417  4.01552804
  3               1.00000000  1.00000000  1.00000000
  4   SILICON     3.43232207  3.42530049  3.42206716
  5               1.00000000  1.00000000  1.00000000
  6               1.00000000  1.00000000  1.00000000

ERMAL COEFFICIENT OF EXPANSION DATA:

urf      Glass            TCE
  0               0.00000000
  1               0.00000000
  2  GERMANIUM     5.69999981
  3               0.00000000
  4   SILICON     2.61999989
  5               0.00000000
  6               0.00000000

7# DATA:

# calculations consider vignetting factors and ignore surface apertures.

           Wavelength:        3.000000            4.000000            5.000000
#              Field       Tan       Sag       Tan       Sag       Tan       Sag
1          10.30 mm:    2.0018    2.1717    2.0073    2.1791    2.0098    2.1826
            0.00 mm:    2.2340    2.2340    2.2426    2.2426    2.2466    2.2466
          -10.30 mm:    2.0018    2.1717    2.0073    2.1791    2.0098    2.1826
            7.00 mm:    2.1272    2.2044    2.1344    2.2125    2.1377    2.2163
5          -7.00 mm:    2.1272    2.2044    2.1344    2.2125    2.1377    2.2163
6           5.00 mm:    2.1795    2.2187    2.1874    2.2271    2.1911    2.2310
           -5.00 mm:    2.1795    2.2187    2.1874    2.2271    2.1911    2.2310

OBAL VERTEX COORDINATES AND DIRECTIONS:

rf        X coord         Y coord          Z coord    X direc    Y direc    Z direc
1       0.000000        0.000000         0.000000   0.000000   0.000000   1.000000
2       0.000000        0.000000        80.000000   0.000000   0.000000   1.000000
3       0.000000        0.000000        84.000000   0.000000   0.000000   1.000000
4       0.000000        0.000000        88.000000   0.000000   0.000000   1.000000
5       0.000000        0.000000        93.000000   0.000000   0.000000   1.000000
6       0.000000        0.000000       138.265635   0.000000   0.000000   1.000000

LEMENT VOLUME DATA:

lues are only accurate for plane and spherical surfaces.
ement volumes are computed by assuming edges are squared up
 the larger of the front and back radial aperture.

                            Volume cc   Density g/cc         Mass g
ement surf    2 to    3      8.892446       5.327000      47.370059
ement surf    4 to    5      9.777287       2.329000      22.771301
tal Mass:                                                 70.141360

RDINAL POINTS:

ject space positions are measured with respect to surface 1.
nage space positions are measured with respect to the image surface.
e index in both the object space and image space is considered.

                               Object Space          Image Space
= 3.000000
incipal Planes   :               81.443928           -50.043984
dal Planes       :               81.443928           -50.043984
cal Planes       :               31.591323            -0.191379
ti-Nodal Planes  :              -18.261282            49.661226

= 4.000000 (Primary)
incipal Planes   :               81.443990           -50.051505
dal Planes       :               81.443990           -50.051505
```

```
ocal Planes       :            31.392485           0.000000
nti-Nodal Planes :           -18.659020          50.051505

 = 5.000000
rincipal Planes  :            81.443988         -50.054988
odal Planes       :            81.443988         -50.054988
ocal Planes       :            31.300937           0.088063
nti-Nodal Planes :           -18.842114          50.231114
```

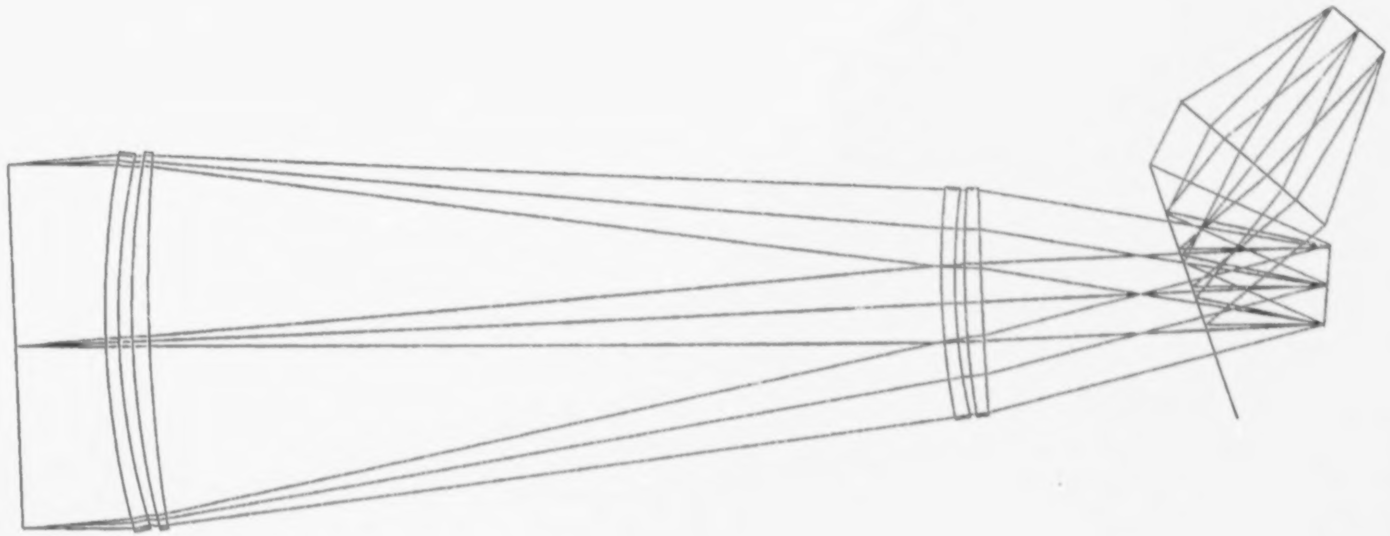

3D LAYOUT

IR_PROJECTOR
THU NOV 6 14:30:24 1997
SCALE: 0.5000
ON: +7 DEG.

40.00 MILLIMETERS

NATIONAL OPTICS INSTITUTE
SR. OPTICAL DESIGNER: DR. EUGENE CURATU

H:\IR_PROJECTOR\PRE_DESIGN\SEARCH_OCT18\PTZBS2_PUP_INV_19SEPT.ZMX

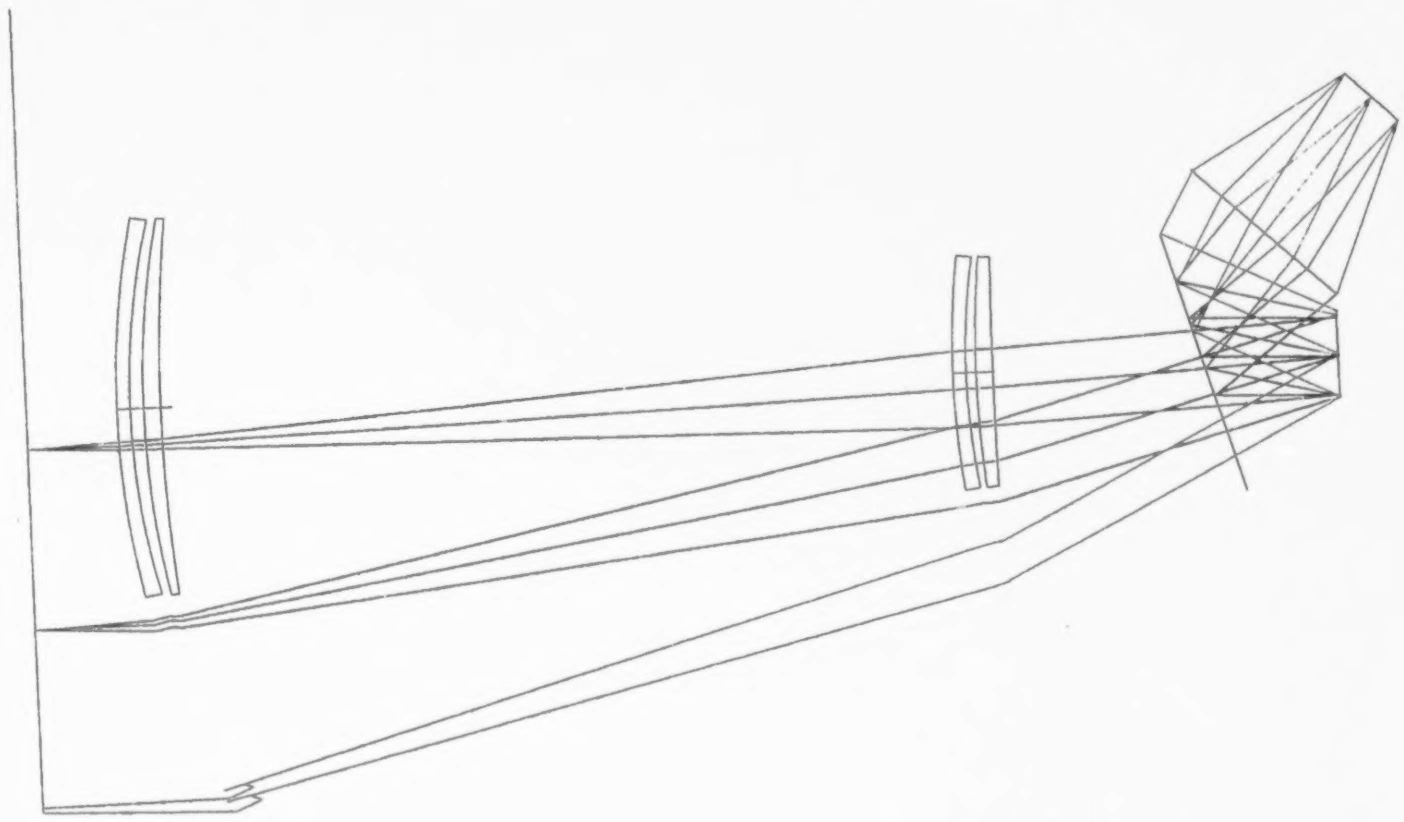

3D LAYOUT

IR_PROJECTOR
THU NOV 6 14:30:55 1997
SCALE: 0.5000
0 DEG.

40.00 MILLIMETERS

NATIONAL OPTICS INSTITUTE
SR. OPTICAL DESIGNER: DR. EUGENE CURATU

H:\IR_PROJECTOR\PRE_DESIGN\SEARCH_OCT18\PTZBS2_PUP_INV_19SEPT.ZMX

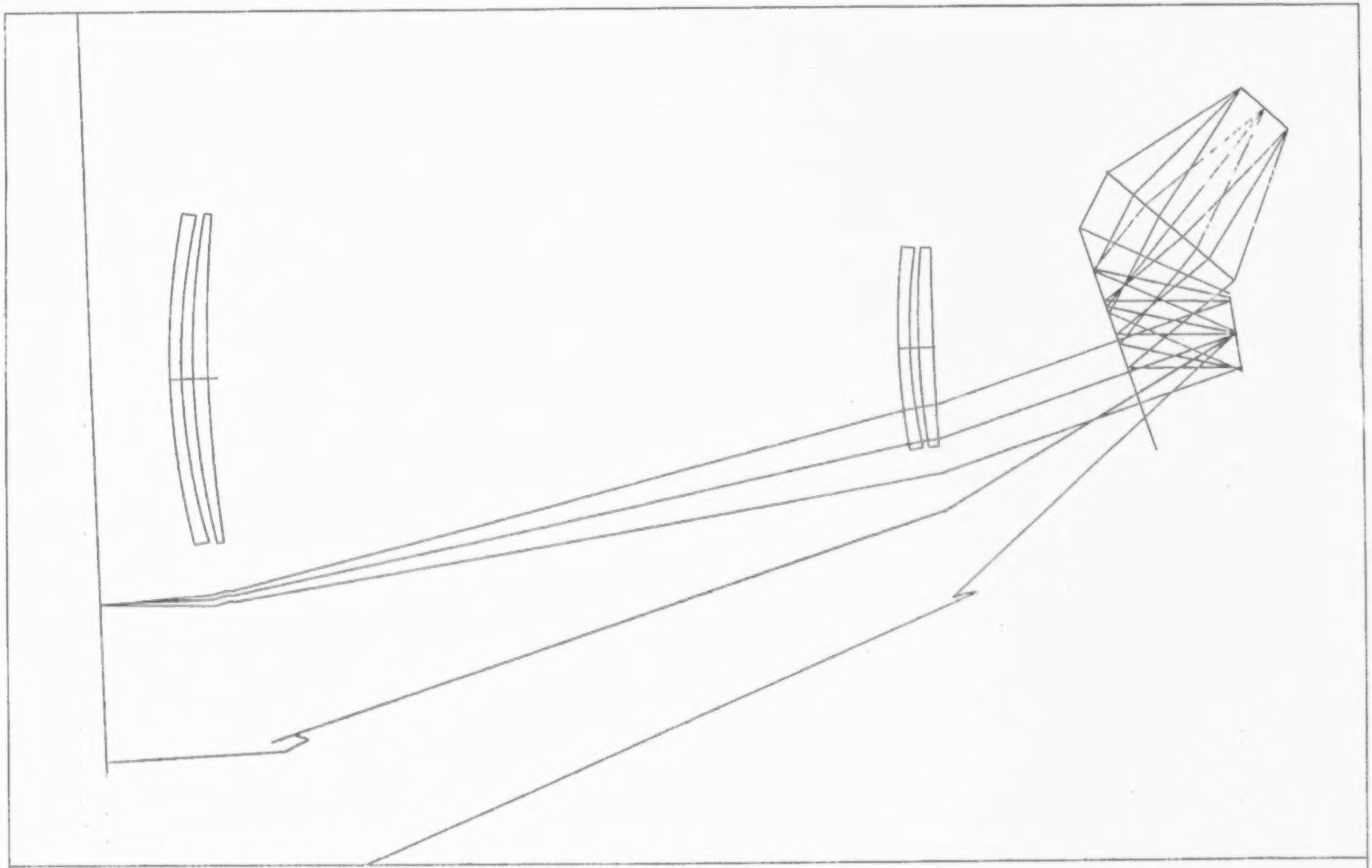

3D LAYOUT

IR_PROJECTOR
THU NOV 6 14:31:42 1997
SCALE: 0.5000
OFF: -7 DEG.

40.00 MILLIMETERS

NATIONAL OPTICS INSTITUTE
SR. OPTICAL DESIGNER: DR. EUGENE CURATU

H:\IR_PROJECTOR\PRE_DESIGN\SEARCH_OCT18\PTZBS2_PUP_INV_19SEPT.ZMX

APPENDIX II
LENS_2

Refractive Optics – No BS, tristable mode – (Lens_2)

Item	Characteristics
Spectral range	2..5 μm
Configuration	Thermal source in the focal plane of Collimator No Beam Splitter Tristable operating mode (ON-OFF-ON) Telecentric illumination Source imaged at the UUT entrance aperture No vignetting No diffuser in optical layout
ENP	106 mm
Field angle (2σ)	3.5°
DMD (array diagonal)	33.25 mm
Deflection angle (α)	±8.5°
Objective focal length (f_{PRO})	544.2 mm
Angle subtended by a reflected beam from each pixel	11.12°
Collimator focal length (f_{COL})	52 mm
Source diameter	10.13 mm

In the following pages we give the layout, prescription data, spot diagram, distortion, and MTF graphics of two projection objectives optimized for spectral ranges of 2.5..4 μm and 2..4 μm, respectively, followed by the layout and prescription data of the collimator. Finally, three layouts showing the tristable operating mode of this configuration are given.

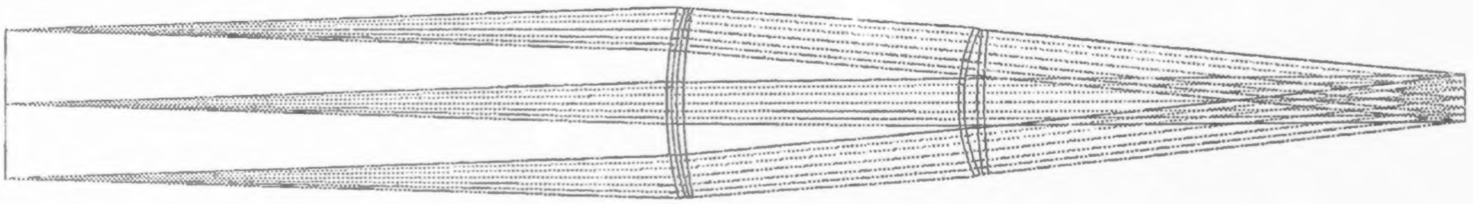

3D LAYOUT

IR_OBJ
THU NOV 6 14:48:11 1997
SCALE: 0.2000

100.00 MILLIMETERS

NATIONAL OPTICS INSTITUTE
SR. OPTICAL DESIGNER: DR. EUGENE CURATU

H:\IR_PROJECTOR\PRE_DESIGN\SEARCH_OCT18\NEWDMD\OBJ2.ZMX

```
ystem/Prescription Data

ile : H:\IR_projector\pre_design\search_oct18\newDMD\obj2.zmx
Title: IR_OBJ
Date : THU NOV 6 14:42:56 1997

ENERAL LENS DATA:

Surfaces            :               10
top                 :                1
ystem Aperture : Entrance Pupil Diameter = 106
y aiming            : Off
podization          :Uniform, factor =    0.00000E+000
Eff. Focal Len. :              544.2 (in air)
f. Focal Len. :              544.2 (in image space)
otal Track          :          1087.324
mage Space F/# :          5.133963
Para. Wrkng F/# :          5.133963
orking F/#          :           5.13506
bj. Space N.A. :           5.3e-009
top Radius          :                53
arax. Ima. Hgt.:          16.62681
Parax. Mag.         :                 0
ntr. Pup. Dia. :               106
tr. Pup. Pos. :                 0
it Pupil Dia. :          396624.3
Exit Pupil Pos. :          -2036254
ield Type           : Angle in degrees
ximum Field         :              1.75
imary Wave          :                 4
ns Units            :    Millimeters
ngular Mag.         :     0.0002672554

elds                : 7
eld Type: Angle in degrees
          X-Value            Y-Value           Weight
1         0.000000           1.750000          0.700000
          0.000000           0.000000          1.000000
          0.000000          -1.750000          0.700000
          0.000000           1.250000          0.800000
5         0.000000          -1.250000          0.800000
6         0.000000           0.700000          1.000000
          0.000000          -0.700000          1.000000

gnetting Factors
         VDX        VDY        VCX        VCY
    0.000000   0.000000   0.000000   0.000000
    0.000000   0.000000   0.000000   0.000000
    0.000000   0.000000   0.000000   0.000000
    0.000000   0.000000   0.000000   0.000000
    0.000000   0.000000   0.000000   0.000000
    0.000000   0.000000   0.000000   0.000000
    0.000000   0.000000   0.000000   0.000000

avelengths        : 3
its: Microns
          Value             Weight
        2.500000          0.500000
        4.000000          1.000000
        5.000000          0.500000

RFACE DATA SUMMARY:

rf       Type                 Comment            Radius       Thickness            Glass        Diameter           Conic
OBJ STANDARD                                   Infinity        Infinity                                0               0
TO STANDARD                                    Infinity        492.5187                              106               0
 2 STANDARD                                    251.8477               4     GERMANIUM            136.673               0
 3 STANDARD                                     225.324               4                         134.7067               0
 4 STANDARD                                    248.8228               5       SILICON            135.487               0
 5 STANDARD                                     338.336        205.8046                         134.7131               0
 6 STANDARD                                    123.6054               4     GERMANIUM            106.545               0
 7 STANDARD                                    118.2941              10                         103.6648               0
 8 STANDARD                                      351.84               5       SILICON           103.5167               0
 9 STANDARD                                    414.1206        357.0002                         102.4991               0
MA STANDARD                                    Infinity                                         33.42473               0

RFACE DATA DETAIL:

rface OBJ       : STANDARD
rface STO       : STANDARD
rface   2       : STANDARD
rface   3       : STANDARD
rface   4       : STANDARD
rface   5       : STANDARD
rface   6       : STANDARD
rface   7       : STANDARD
rface   8      : STANDARD
rface   9      : STANDARD
rface IMA      : STANDARD

DGE THICKNESS DATA:

rf          Edge
STO    498.158673
  2      5.164031
  3      2.987201
  4      2.452041
  5    218.996859
  6      4.605189
  7      1.878661
  8      4.419361
  9    353.816732
MA       0.000000

OLVE AND VARIABLE DATA:

ickness of    1        : Variable
emi Diameter   1       : Fixed
urvature of   2        : Variable
rvature of    3        : Variable
rvature of    4        : Variable
rvature of    5        : Variable
hickness of   5        : Variable
urvature of   6        : Variable
rvature of    7        : Variable
rvature of    8        : Variable
rvature of    9        : Variable
hickness of   9        : Solve, marginal ray height = 0.00000

DEX OF REFRACTION DATA:

urf      Glass        2.500000     4.000000     5.000000
  0                 1.00000000  1.00000000  1.00000000
  1                 1.00000000  1.00000000  1.00000000
  2   GERMANIUM      4.06609110  4.02466417  4.01552804
  3                 1.00000000  1.00000000  1.00000000
  4     SILICON     3.43943711  3.42530049  3.42206716
  5                 1.00000000  1.00000000  1.00000000
  6   GERMANIUM      4.06609110  4.02466417  4.01552804
  7                 1.00000000  1.00000000  1.00000000
  8     SILICON     3.43943711  3.42530049  3.42206716
  9                 1.00000000  1.00000000  1.00000000
 10                 1.00000000  1.00000000  1.00000000

ERMAL COEFFICIENT OF EXPANSION DATA:

urf      Glass           TCE
  0                 0.00000000
  1                 0.00000000
  2   GERMANIUM     5.69999981
  3                 0.00000000
  4     SILICON     2.61999989
  5                 0.00000000
  6   GERMANIUM     5.69999981
  7                 0.00000000
  8     SILICON     2.61999989
  9                 0.00000000
 10                 0.00000000

 DATA:

 calculations consider vignetting factors and ignore surface apertures.

          Wavelength:       2.500000             4.000000             5.000000
                Field     Tan       Sag        Tan       Sag        Tan       Sag
           1.7500 deg:  5.1442    5.1366     5.1442    5.1370     5.1446    5.1375
           0.0000 deg:  5.1346    5.1346     5.1351    5.1351     5.1356    5.1356
          -1.7500 deg:  5.1442    5.1366     5.1442    5.1370     5.1446    5.1375
           1.2500 deg:  5.1391    5.1355     5.1393    5.1360     5.1398    5.1365
          -1.2500 deg:  5.1391    5.1355     5.1393    5.1360     5.1398    5.1365
           0.7000 deg:  5.1359    5.1349     5.1363    5.1353     5.1368    5.1359
          -0.7000 deg:  5.1359    5.1349     5.1363    5.1353     5.1368    5.1359

EAL VERTEX COORDINATES AND DIRECTIONS:

urf      X coord        Y coord        Z coord    X direc    Y direc    Z direc
  1     0.000000       0.000000       0.000000   0.000000   0.000000   1.000000
  2     0.000000       0.000000     492.518739   0.000000   0.000000   1.000000
  3     0.000000       0.000000     496.518739   0.000000   0.000000   1.000000
  4     0.000000       0.000000     500.518739   0.000000   0.000000   1.000000
  5     0.000000       0.000000     505.518739   0.000000   0.000000   1.000000
  6     0.000000       0.000000     711.323375   0.000000   0.000000   1.000000
 7      0.000000      0.000000    715.323375  0.000000  0.000000  1.000000
 8      0.000000      0.000000    725.323375  0.000000  0.000000  1.000000
 9      0.000000      0.000000    730.323375  0.000000  0.000000  1.000000
10      0.000000      0.000000   1087.323538  0.000000  0.000000  1.000000

 LEMENT VOLUME DATA:

 alues are only accurate for plane and spherical surfaces.
 lement volumes are computed by assuming edges are squared up
 o the larger of the front and back radial aperture.

                             Volume cc    Density g/cc          Mass g
 lement surf   2 to   3      66.972841        5.327000     356.764333
 lement surf   4 to   5      53.979262        2.329000     125.717702
 lement surf   6 to   7      38.045545        5.327000     202.668624
 lement surf   8 to   9      39.643316        2.329000      92.329282
 otal Mass:                                                777.479940

 ARDINAL POINTS:

 bject space positions are measured with respect to surface 1.
 mage space positions are measured with respect to the image surface.
 he index in both the object space and image space is considered.

                           Object Space        Image Space
  = 2.500000
 rincipal Planes  :           544.229351         -544.033866
 odal Planes      :           544.229351         -544.033866
 ocal Planes      :             0.150194            0.045292
 nti-Nodal Planes :          -543.928964          544.124450

  = 4.000000 (Primary)
 rincipal Planes  :           544.054586         -544.200026
 odal Planes      :           544.054586         -544.200026
 ocal Planes      :            -0.145440            0.000000
 nti-Nodal Planes :          -544.345467          544.200026

  = 5.000000
 rincipal Planes  :           544.014128         -544.236817
 odal Planes      :           544.014128         -544.236817
 ocal Planes      :            -0.256549            0.033860
 nti-Nodal Planes :          -544.527226          544.304537
```

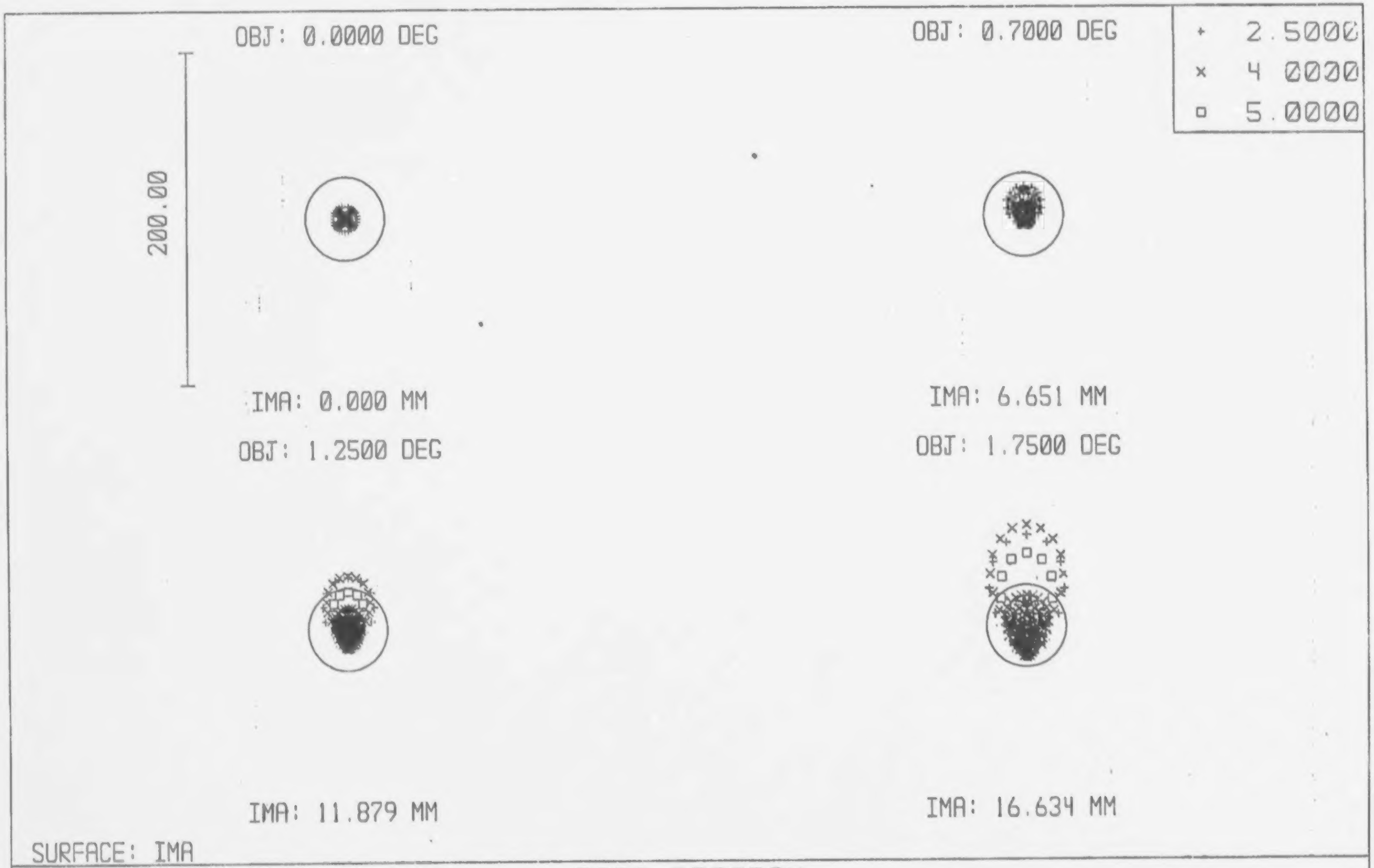

SPOT DIAGRAM

```
IR_OBJ
MON DEC 1 12:24:19 1997  UNITS ARE MICRONS.
FIELD      :        1        2        3        4
RMS RADIUS :    2.926    5.486   10.581   18.303
GEO RADIUS :    7.425   17.091   32.809   62.153
AIRY DISK  :    25.06           REFERENCE  : CENTROID
```

NATIONAL OPTICS INSTITUTE

H:\IR_PROJECTOR\PRE_DESIGN\SEARCH_OCT18\NEWDMD\OBJ2.ZMX

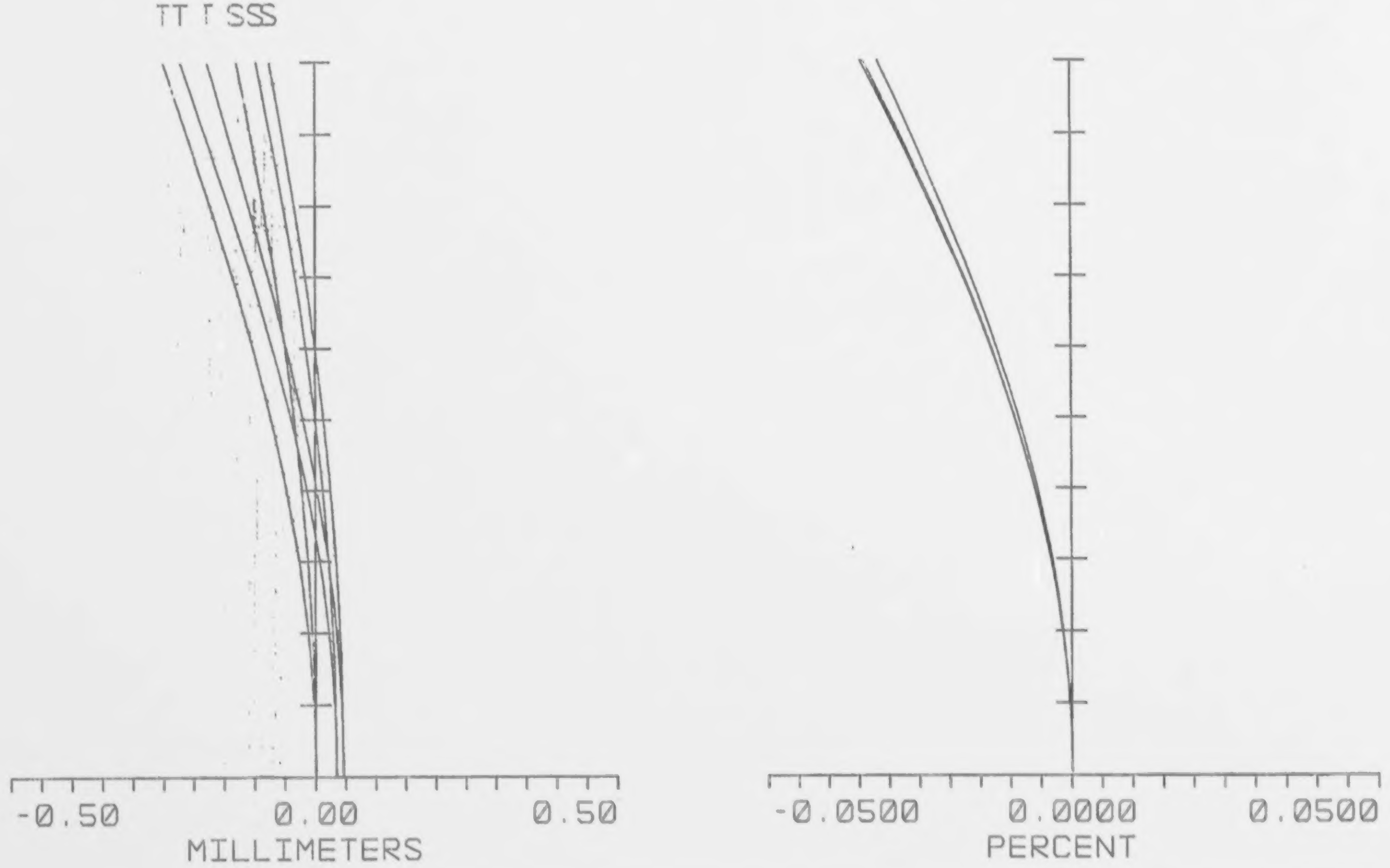

FIELD CURVATURE / DISTORTION

IR_OBJ
THU NOV 6 14:46:52 1997
MAXIMUM FIELD IS 1.750 DEGREES
WAVELENGTHS: 2.500 4.000 5.000

NATIONAL OPTICS INSTITUTE
SR. OPTICAL DESIGNER: DR. EUGENE CURATU

H:\IR_PROJECTOR\PRE_DESIGN\SEARCH_OCT18\NEWDMD\OBJ2.ZMX

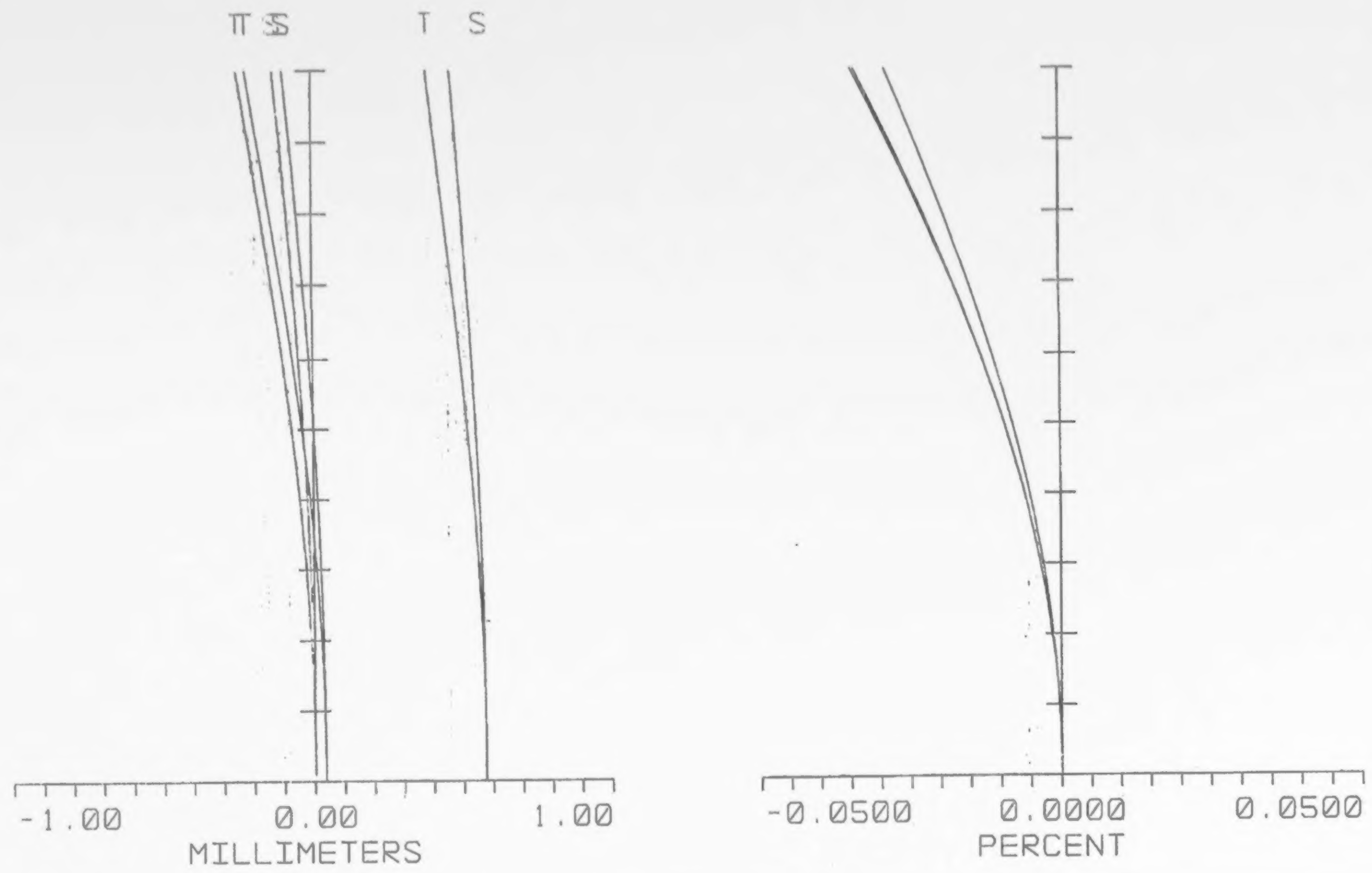

FIELD CURVATURE / DISTORTION

IR_OBJ
THU NOV 6 14:46:22 1997
MAXIMUM FIELD IS 1.750 DEGREES
WAVELENGTHS: 2.000 4.000 5.000

NATIONAL OPTICS INSTITUTE
SR. OPTICAL DESIGNER: DR. EUGENE CURATU

H:\IR_PROJECTOR\PRE_DESIGN\SEARCH_OCT18\NEWDMD\OBJ2.ZMX

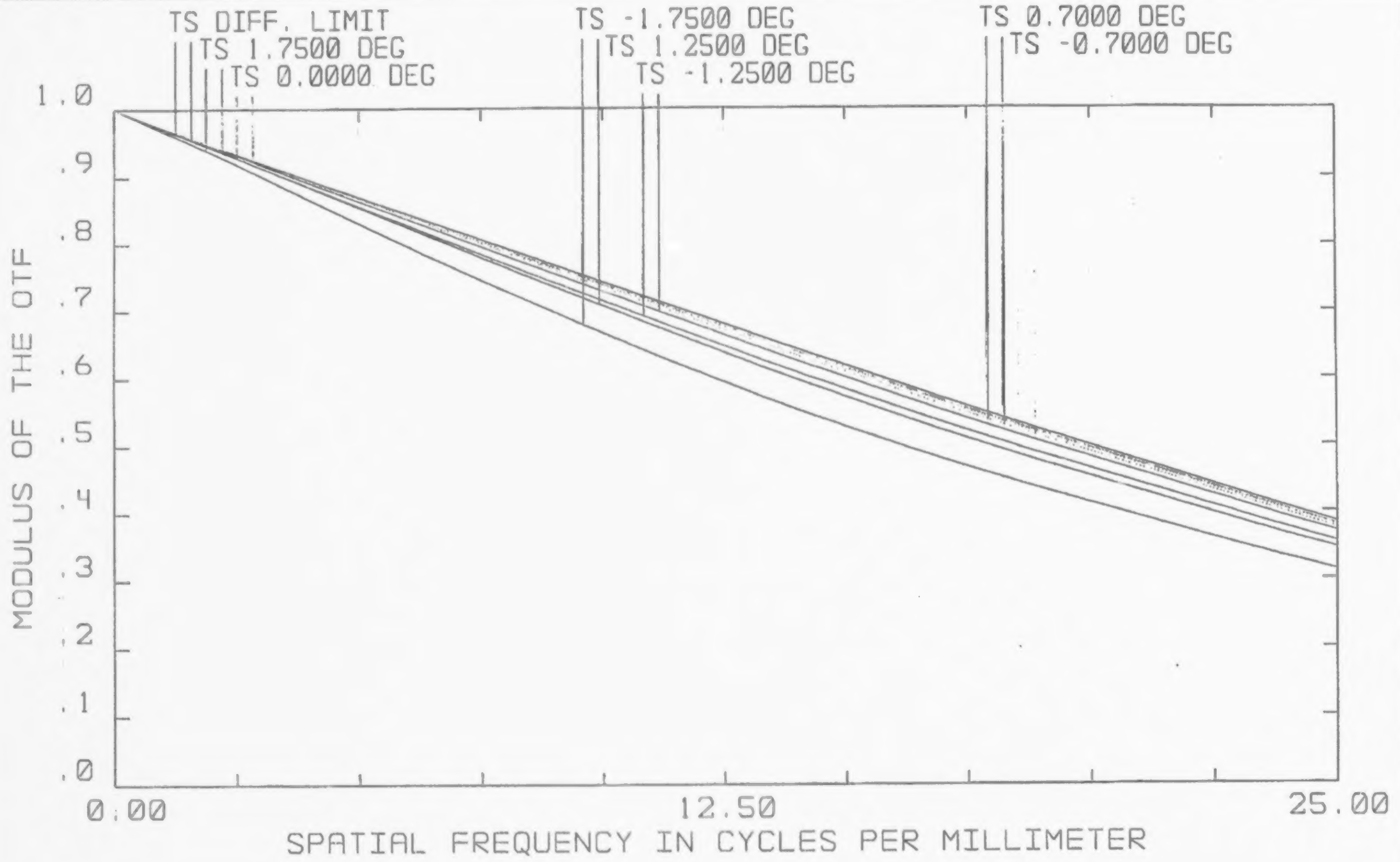

POLYCHROMATIC DIFFRACTION MODULATION TRANSFER FUNCTION

IR_OBJ
THU NOV 6 14:44:22 1997
DATA FOR 2.5000 TO 5.0000 MICRONS.

NATIONAL OPTICS INSTITUTE
SR. OPTICAL DESIGNER: DR. EUGENE CURATU

H:\IR_PROJECTOR\PRE_DESIGN\SEARCH_OCT18\NEWDMD\OBJ2.ZMX

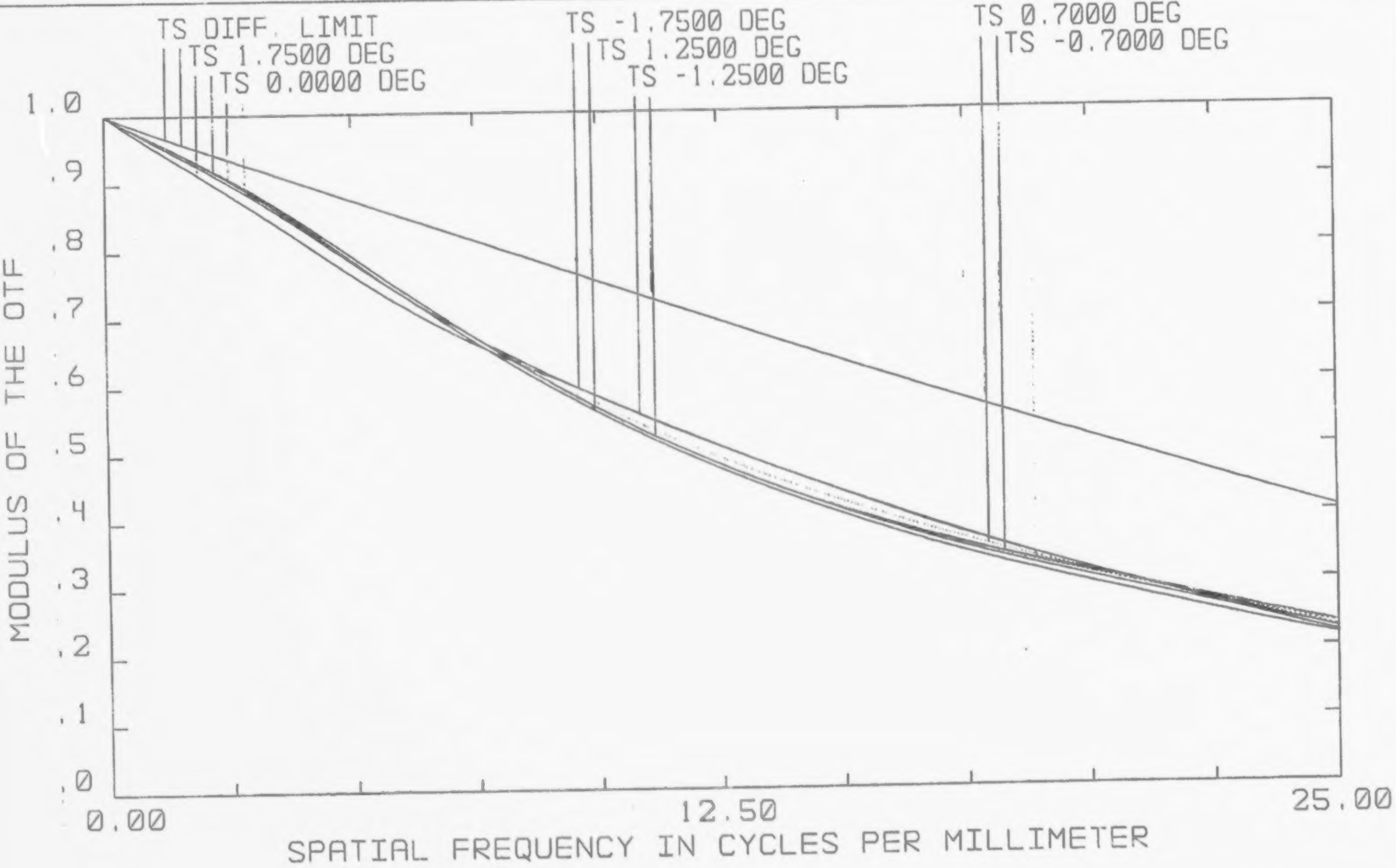

POLYCHROMATIC DIFFRACTION MODULATION TRANSFER FUNCTION

IR_OBJ
THU NOV 6 14:45:16 1997
DATA FOR 2.0000 TO 5.0000 MICRONS.

NATIONAL OPTICS INSTITUTE
SR. OPTICAL DESIGNER: DR. EUGENE CURATU

H:\IR_PROJECTOR\PRE_DESIGN\SEARCH_OCT18\NEWDMD\OBJ2.ZMX

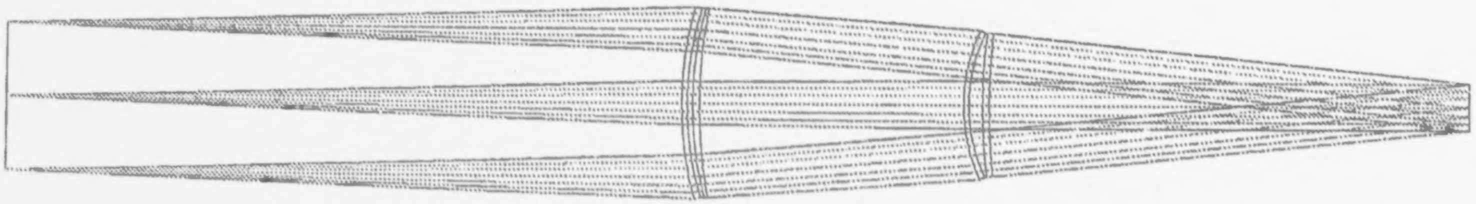

3D LAYOUT

OBJ 2-5 MICROMETERS
THU NOV 6 16:50:27 1997
SCALE: 0.2000

100.00 MILLIMETERS

NATIONAL OPTICS INSTITUTE
SR. OPTICAL DESIGNER: DR. EUGENE CURATU

H:\IR_PROJECTOR\PRE_DESIGN\SEARCH_OCT18\NEWDMD\OBJ_NOV7.ZMX

```
ystem/Prescription Data

ile : H:\IR_projector\pre_design\search_oct18\newDMD\obj_nov7.zmx
Title: OBJ 2-5 micrometers
Date : THU NOV 6 16:50:43 1997

ENERAL LENS DATA:

Surfaces           :                   10
top                :                    1
ystem Aperture     : Entrance Pupil Diameter = 106
ay aiming          : Off
Apodization        :Uniform, factor =   0.00000E+000
Eff. Focal Len.    :           544.1998 (in air)
ff. Focal Len.     :           544.1998 (in image space)
otal Track         :           1090.903
mage Space F/#     :            5.13396
Para. Wrkng F/#    :            5.13396
Working F/#        :           5.134191
bj. Space N.A.     :           5.3e-009
top Radius         :                 53
arax. Ima. Hgt.    :           16.62681
Parax. Mag.        :                  0
ntr. Pup. Dia.     :                106
ntr. Pup. Pos.     :                  0
xit Pupil Dia.     :           68523.32
Exit Pupil Pos.    :            -351796
Field Type         : Angle in degrees
aximum Field       :               1.75
rimary Wave        :                  4
ens Units          :   Millimeters
Angular Mag.       :     0.001546919

ields          : 7
ield Type: Angle in degrees
#        X-Value          Y-Value          Weight
 1       0.000000         1.750000         0.700000
 2       0.000000         0.000000         1.000000
 3       0.000000        -1.750000         0.700000
 4       0.000000         1.250000         0.800000
 5       0.000000        -1.250000         0.800000
 6       0.000000         0.700000         1.000000
 7       0.000000        -0.700000         1.000000

ignetting Factors
#      VDX        VDY        VCX        VCY
1  0.000000   0.000000   0.000000   0.000000
   0.000000   0.000000   0.000000   0.000000
   0.000000   0.000000   0.000000   0.000000
   0.000000   0.000000   0.000000   0.000000
5  0.000000   0.000000   0.000000   0.000000
6  0.000000   0.000000   0.000000   0.000000
   0.000000   0.000000   0.000000   0.000000

avelengths      : 3
nits: Microns
         Value            Weight
1       2.000000         0.500000
2       4.000000         1.000000
3       5.000000         0.500000

URFACE DATA SUMMARY:

urf      Type              Comment           Radius       Thickness         Glass         Diameter            Conic
 OBJ STANDARD                              Infinity        Infinity                               0                0
 STO STANDARD                              Infinity         504.841                             106                0
   2 STANDARD                              245.4075               4     GERMANIUM          137.4486                0
   3 STANDARD                               221.417               4                        135.4389                0
   4 STANDARD                              246.7142               5       SILICON          136.1516                0
   5 STANDARD                              332.8446         197.062                        135.3567                0
   6 STANDARD                              119.5639               4     GERMANIUM          106.5968                0
   7 STANDARD                              114.4103              10                        103.6079                0
   8 STANDARD                              366.2108               5       SILICON          103.4965                0
   9 STANDARD                              428.0705        356.9997                        102.4932                0
 IMA STANDARD                              Infinity                                        33.44047                0

URFACE DATA DETAIL:

Surface OBJ     : STANDARD
Surface STO     : STANDARD
urface   2      : STANDARD
urface   3      : STANDARD
urface   4      : STANDARD
Surface  5      : STANDARD
Surface  6      : STANDARD
urface   7      : STANDARD
urface   8      : STANDARD
urface   9      : STANDARD
urface IMA      : STANDARD

DGE THICKNESS DATA:

urf           Edge
STO     510.632520
  2       5.116232
  3       2.865918
  4       2.458053
  5     211.107090
  6       4.636197
  7       1.282427
  8       4.464725
  9     353.921165
IMA       0.000000

OLVE AND VARIABLE DATA:

hickness of   1        : Variable
emi Diameter   1       : Fixed
Curvature of  2        : Variable
urvature of   3        : Variable
urvature of   4        : Variable
urvature of   5        : Variable
Thickness of  5        : Variable
Curvature of  6        : Variable
urvature of   7        : Variable
urvature of   8        : Variable
urvature of   9        : Variable
hickness of   9        : Solve, marginal ray height = 0.00000

DEX OF REFRACTION DATA:

urf      Glass       2.000000     4.000000     5.000000
  0                1.00000000  1.00000000  1.00000000
  1                1.00000000  1.00000000  1.00000000
  2   GERMANIUM     4.10863352  4.02466417  4.01552804
  3                1.00000000  1.00000000  1.00000000
  4    SILICON     3.45268363  3.42530049  3.42206716
  5                1.00000000  1.00000000  1.00000000
  6   GERMANIUM     4.10863352  4.02466417  4.01552804
  7                1.00000000  1.00000000  1.00000000
  8    SILICON     3.45268363  3.42530049  3.42206716
  9                1.00000000  1.00000000  1.00000000
 10                1.00000000  1.00000000  1.00000000

HERMAL COEFFICIENT OF EXPANSION DATA:

urf      Glass            TCE
  0                0.00000000
  1                0.00000000
  2   GERMANIUM     5.69999981
  3                0.00000000
  4    SILICON     2.61999989
  5                0.00000000
  6   GERMANIUM     5.69999981
  7                0.00000000
  8    SILICON     2.61999989
  9                0.00000000
 10                0.00000000

/# DATA:

/# calculations consider vignetting factors and ignore surface apertures.

           Wavelength:        2.000000             4.000000             5.000000
                Field        Tan       Sag        Tan       Sag        Tan       Sag
1           1.7500 deg:    5.1446    5.1361     5.1440    5.1362     5.1449    5.1371
2           0.0000 deg:    5.1338    5.1338     5.1342    5.1342     5.1352    5.1352
           -1.7500 deg:    5.1446    5.1361     5.1440    5.1362     5.1449    5.1371
            1.2500 deg:    5.1389    5.1349     5.1388    5.1351     5.1397    5.1361
5          -1.2500 deg:    5.1389    5.1349     5.1388    5.1351     5.1397    5.1361
6           0.7000 deg:    5.1353    5.1342     5.1355    5.1345     5.1365    5.1354
           -0.7000 deg:    5.1353    5.1342     5.1355    5.1345     5.1365    5.1354

OBAL VERTEX COORDINATES AND DIRECTIONS:

urf      X coord         Y coord          Z coord    X direc    Y direc    Z direc
1       0.000000        0.000000         0.000000   0.000000   0.000000   1.000000
2       0.000000        0.000000       504.841047   0.000000   0.000000   1.000000
3       0.000000        0.000000       508.841047   0.000000   0.000000   1.000000
4       0.000000        0.000000       512.841047   0.000000   0.000000   1.000000
5       0.000000        0.000000       517.841047   0.000000   0.000000   1.000000
6       0.000000        0.000000       714.903029   0.000000   0.000000   1.000000
```

```
 7      0.000000      0.000000    718.903029  0.000000  0.000000  1.000000
 8      0.000000      0.000000    728.903029  0.000000  0.000000  1.000000
 9      0.000000      0.000000    733.903029  0.000000  0.000000  1.000000
10      0.000000      0.000000   1090.902767  0.000000  0.000000  1.000000

LEMENT VOLUME DATA:

Values are only accurate for plane and spherical surfaces.
Element volumes are computed by assuming edges are squared up
o the larger of the front and back radial aperture.

                                   Volume cc    Density g/cc        Mass g
Element surf   2 to   3            67.373483        5.327000    358.898551
Element surf   4 to   5            54.562077        2.329000    127.075078
lement surf    6 to   7            38.180777        5.327000    203.389005
lement surf    8 to   9            39.817293        2.329000     92.734475
Total Mass:                                                     782.097108

CARDINAL POINTS:

bject space positions are measured with respect to surface 1.
Image space positions are measured with respect to the image surface.
The index in both the object space and image space is considered.

                              Object Space          Image Space
 = 2.000000
Principal Planes   :           543.564588          -543.974954
Nodal Planes       :           543.564588          -543.974954
ocal Planes        :            -0.460714             0.050348
nti-Nodal Planes   :          -544.486017           544.075650

W = 4.000000 (Primary)
Principal Planes   :           543.357922          -544.199755
odal Planes        :           543.357922          -544.199755
ocal Planes        :            -0.841833            -0.000000
Anti-Nodal Planes  :          -545.041588           544.199755

 = 5.000000
rincipal Planes    :           543.330302          -544.226016
odal Planes        :           543.330302          -544.226016
Focal Planes       :            -0.984429             0.088715
Anti-Nodal Planes  :          -545.299161           544.403447
```

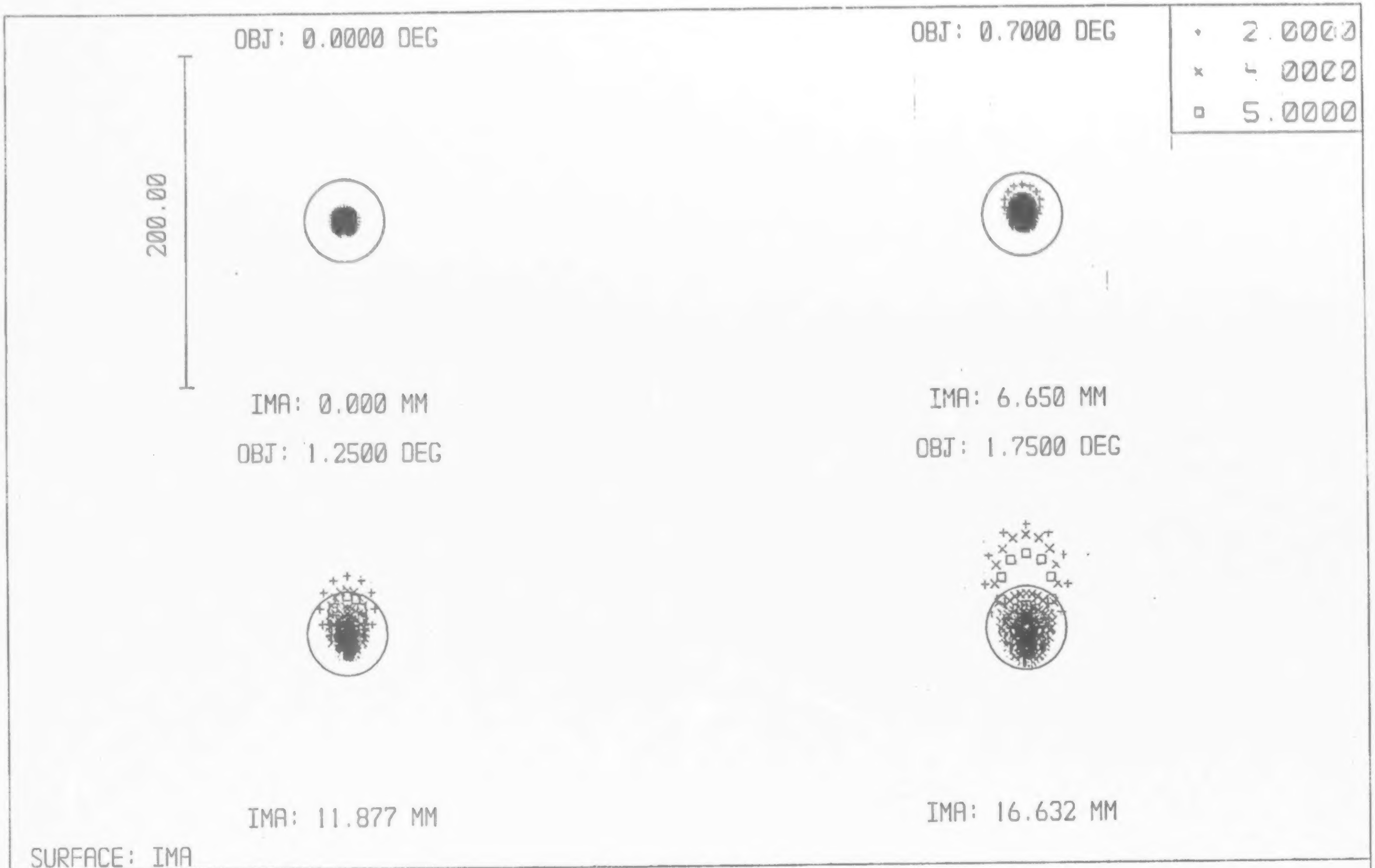

SPOT DIAGRAM

```
OBJ 2-5 MICROMETERS
MON DEC 1 12:26:19 1997  UNITS ARE MICRONS.
FIELD      :          1        2        3        4
RMS RADIUS :      3.918    5.853   10.555   18.345
GEO RADIUS :      7.906   18.366   34.983   62.739
AIRY DISK  :    25.05              REFERENCE  : CENTROID
```

NATIONAL OPTICS INSTITUTE

H:\IR_PROJECTOR\PRE_DESIGN\SEARCH_OCT18\NEWDMD\OBJ_NOV7.ZMX

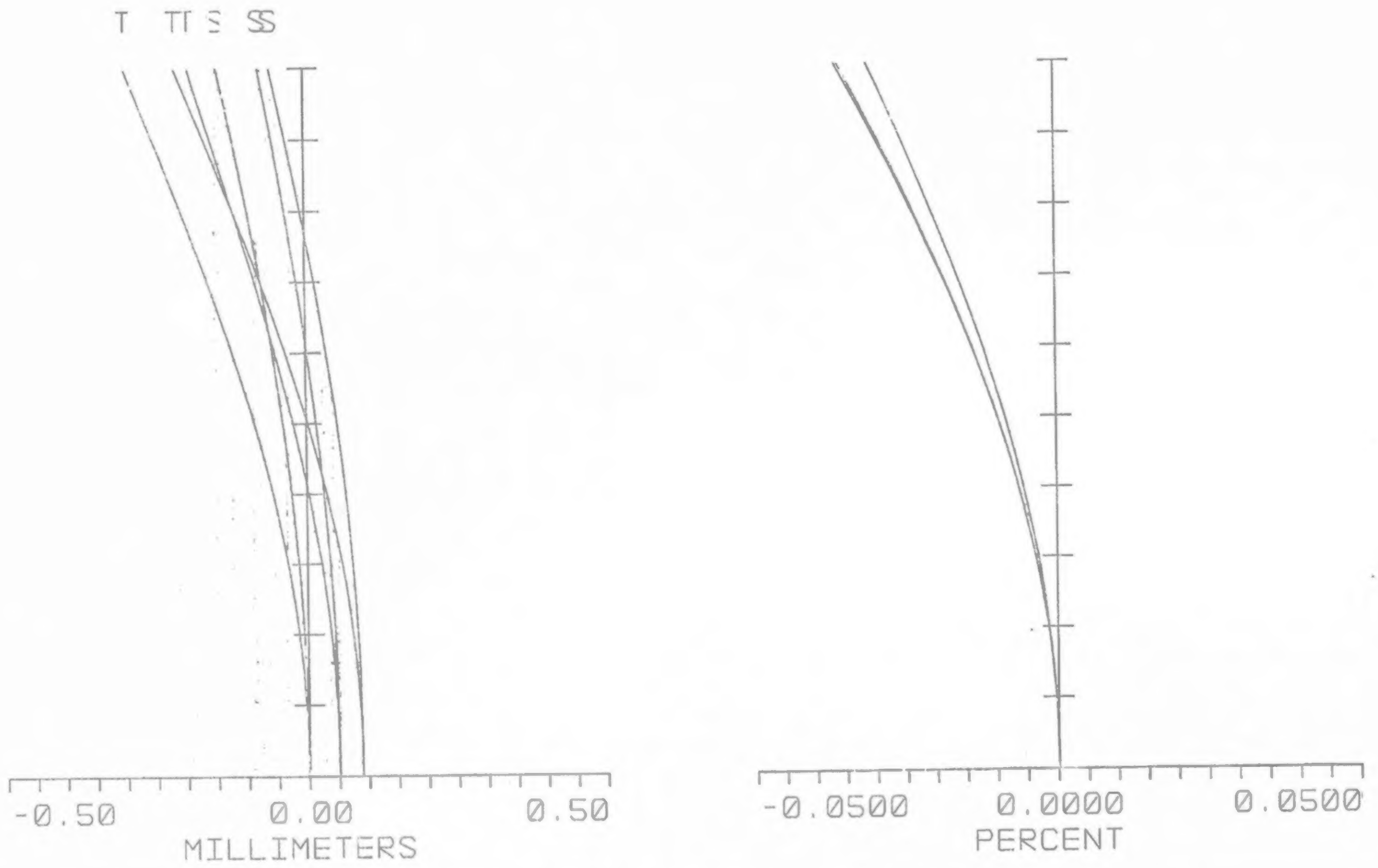

FIELD CURVATURE / DISTORTION

OBJ 2-5 MICROMETERS
THU NOV 6 16:50:4 1997
MAXIMUM FIELD IS 1.750 DEGREES
WAVELENGTHS: 2.000 4.000 5.000

NATIONAL OPTICS INSTITUTE
SR. OPTICAL DESIGNER: DR. EUGENE CURATU

H:\IR_PROJECTOR\PRE_DESIGN\SEARCH_OCT18\NEWDMD\OBJ_NOV7.ZMX

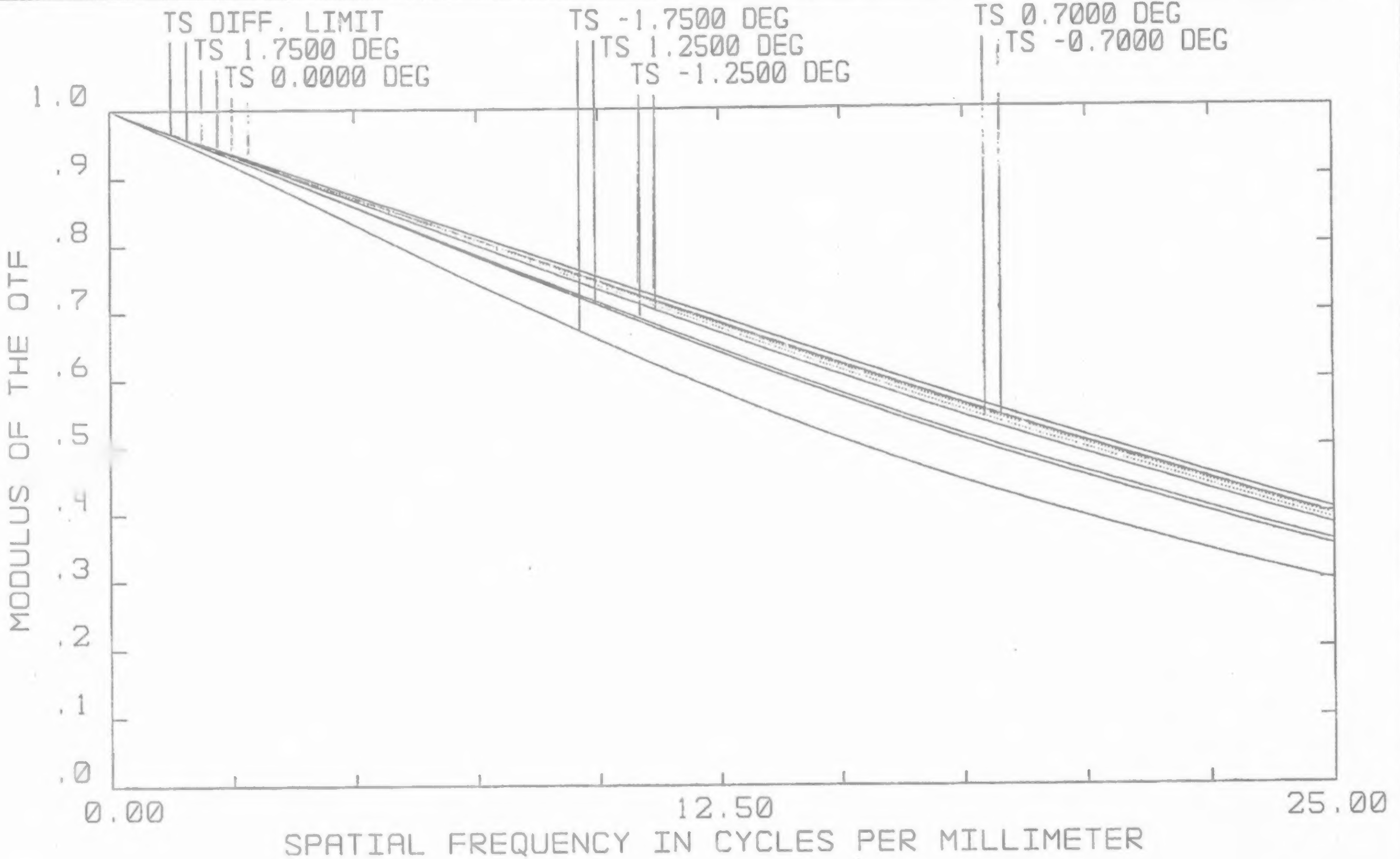

POLYCHROMATIC DIFFRACTION MODULATION TRANSFER FUNCTION

OBJ 2-5 MICROMETERS
THU NOV 6 16:48:58 1997
DATA FOR 2.0000 TO 5.0000 MICRONS.

NATIONAL OPTICS INSTITUTE
SR. OPTICAL DESIGNER: DR. EUGENE CURATU

H:\IR_PROJECTOR\PRE_DESIGN\SEARCH_OCT18\NEWDMD\OBJ_NOV7.ZMX

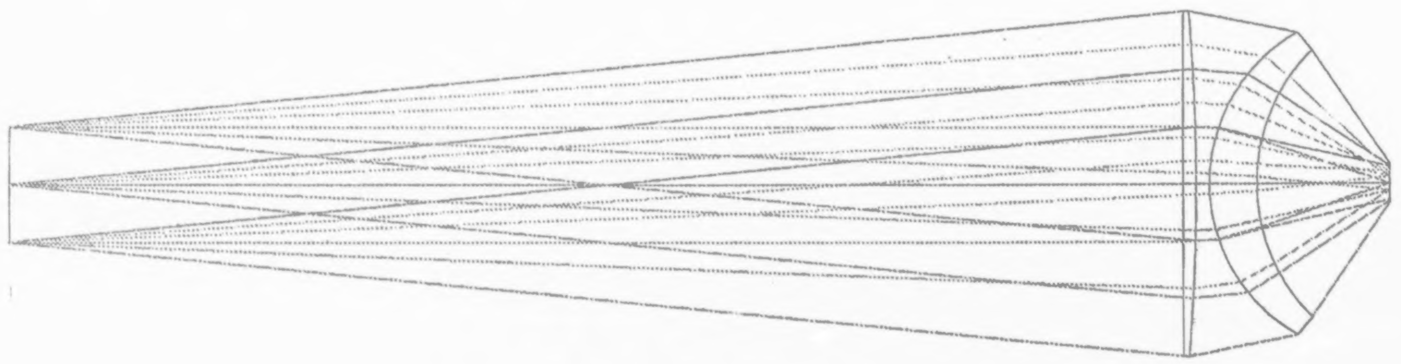

3D LAYOUT

COLLECTOR
THU NOV 6 14:49:23 1997
SCALE: 0.5000

40.00 MILLIMETERS

NATIONAL OPTICS INSTITUTE
SR. OPTICAL DESIGNER: DR. EUGENE CURATU

H:\IR_PROJECTOR\PRE_DESIGN\SEARCH_OCT10\NEWOMD\ILL_JUNK_OCT20.ZMX

```
ystem/Prescription Data

ile : H:\IR_projector\pre_design\search_oct18\newDMD\ill_junk_oct20.zmx
Title: Collector
ate : THU NOV 6 14:49:25 1997

ENERAL LENS DATA:

Surfaces          :                  6
top               :                  1
ystem Aperture    : Entrance Pupil Diameter = 33.25
ay aiming         : Off
Apodization       :Uniform, factor =   0.00000E+000
Eff. Focal Len.   :          52.01675 (in air)
ff. Focal Len.    :          52.01675 (in image space)
otal Track        :          411.1861
mage Space F/#    :          1.564414
Para. Wrkng F/#   :          1.564414
orking F/#        :          1.587382
bj. Space N.A.    :       1.6625e-009
top Radius        :            16.625
Parax. Ima. Hgt.  :              4.87
Parax. Mag.       :                 0
ntr. Pup. Dia.    :             33.25
ntr. Pup. Pos.    :                 0
xit Pupil Dia.    :          5.929052
Exit Pupil Pos.   :           9.27549
Field Type        : Image height in Millimeters
aximum Field      :              4.87
rimary Wave       :                 4
ens Units         :   Millimeters
Angular Mag.      :         -5.607979

ields             : 7
ield Type: Image height in Millimeters
        X-Value         Y-Value         Weight
 1      0.000000        4.870000        0.700000
        0.000000        0.000000        1.000000
        0.000000       -4.870000        0.700000
        0.000000        3.460000        0.800000
 5      0.000000        0.000000        0.800000
 6      0.000000        2.000000        0.900000
        0.000000       -2.000000        0.900000

ignetting Factors
#       VDX       VDY       VCX       VCY
   0.000000  0.000000  0.000000  0.000000
   0.000000  0.000000  0.000000  0.000000
   0.000000  0.000000  0.000000  0.000000
   0.000000  0.000000  0.000000  0.000000
5  0.000000  0.000000  0.000000  0.000000
   0.000000  0.000000  0.000000  0.000000
   0.000000  0.000000  0.000000  0.000000

avelengths        : 3
nits: Microns
          Value         Weight
        2.500000        0.500000
        4.000000        1.000000
 3      5.000000        0.500000

RFACE DATA SUMMARY:

rf       Type            Comment          Radius      Thickness          Glass        Diameter          Conic
 OBJ STANDARD                           Infinity       Infinity                               0              0
 STO STANDARD                           Infinity       349.8004                           33.25              0
   2 STANDARD                           Infinity              4      GERMANIUM          98.7492              0
   3 STANDARD                           -540.716              4                        98.82988              0
   4 STANDARD                           49.04656             14        SILICON         86.65796              0
   5 STANDARD                           52.90358       39.38575                        76.65195              0
 MA STANDARD                           -826.6244                                       11.57303              0

RFACE DATA DETAIL:

urface OBJ       : STANDARD
rface STO        : STANDARD
rface   2        : STANDARD
rface   3        : STANDARD
urface  4        : STANDARD
urface  5        : STANDARD
rface IMA        : STANDARD

GE THICKNESS DATA:

urf          Edge
TO      349.200356
```

```
  2       1.741001
  3      55.309261
  4      10.484473
  5      23.839044
IMA      -0.020254

LVE AND VARIABLE DATA:

hickness of    1        : Variable
rvature of     3        : Variable
rvature of     4        : Variable
rvature of     5        : Variable
hickness of    5        : Solve, marginal ray height = 0.00000
urvature of    6        : Variable

DEX OF REFRACTION DATA:

urf     Glass       2.500000    4.000000    5.000000
  0               1.00000000  1.00000000  1.00000000
  1               1.00000000  1.00000000  1.00000000
  2  GERMANIUM     4.06609110  4.02466417  4.01552804
  3               1.00000000  1.00000000  1.00000000
  4   SILICON     3.43943711  3.42530049  3.42206716
  5               1.00000000  1.00000000  1.00000000
  6               1.00000000  1.00000000  1.00000000

HERMAL COEFFICIENT OF EXPANSION DATA:

rf      Glass             TCE
  0               0.00000000
  1               0.00000000
  2  GERMANIUM     5.69999981
  3               0.00000000
  4   SILICON     2.61999989
  5               0.00000000
  6               0.00000000

# DATA:

# calculations consider vignetting factors and ignore surface apertures.

           Wavelength:       2.500000           4.000000           5.000000
                 Field      Tan      Sag      Tan      Sag      Tan      Sag
            4.8700 mm:   1.3789   1.5979   1.3804   1.6067   1.3807   1.6088
            0.0000 mm:   1.5739   1.5739   1.5874   1.5874   1.5905   1.5905
 3         -4.8700 mm:   1.3789   1.5979   1.3804   1.6067   1.3807   1.6088
 4          3.4600 mm:   1.4818   1.5842   1.4897   1.5955   1.4915   1.5980
            0.0000 mm:   1.5739   1.5739   1.5874   1.5874   1.5905   1.5905
            2.0000 mm:   1.5442   1.5770   1.5559   1.5897   1.5585   1.5926
           -2.0000 mm:   1.5442   1.5770   1.5559   1.5897   1.5585   1.5926

OBAL VERTEX COORDINATES AND DIRECTIONS:

rf       X coord        Y coord         Z coord   X direc   Y direc   Z direc
 1      0.000000       0.000000        0.000000  0.000000  0.000000  1.000000
 2      0.000000       0.000000      349.800356  0.000000  0.000000  1.000000
 3      0.000000       0.000000      353.800356  0.000000  0.000000  1.000000
 4      0.000000       0.000000      357.800356  0.000000  0.000000  1.000000
 5      0.000000       0.000000      371.800356  0.000000  0.000000  1.000000
 6      0.000000       0.000000      411.186110  0.000000  0.000000  1.000000

EMENT VOLUME DATA:

lues are only accurate for plane and spherical surfaces.
lement volumes are computed by assuming edges are squared up
o the larger of the front and back radial aperture.

                               Volume cc   Density g/cc        Mass g
ement surf    2 to   3        22.012212       5.327000    117.259056
lement surf   4 to   5        71.669968       2.329000    166.919356
tal Mass:                                                 284.178412

RDINAL POINTS:

bject space positions are measured with respect to surface 1.
age space positions are measured with respect to the image surface.
e index in both the object space and image space is considered.

                           Object Space          Image Space
 = 2.500000
incipal Planes  :           343.782506           -51.942228
dal Planes      :           343.782506           -51.942228
cal Planes      :           292.241848            -0.401570
nti-Nodal Planes :          240.701190            51.139088

= 4.000000 (Primary)
```

```
rincipal Planes  :           343.725579          -52.016749
odal Planes      :           343.725579          -52.016749
Focal Planes     :           291.708830           -0.000000
Anti-Nodal Planes :          239.692081           52.016749

 = 5.000000
rincipal Planes  :           343.712615          -52.033718
Nodal Planes     :           343.712615          -52.033718
Focal Planes     :           291.587683            0.091214
Anti-Nodal Planes :          239.462750           52.216147
```

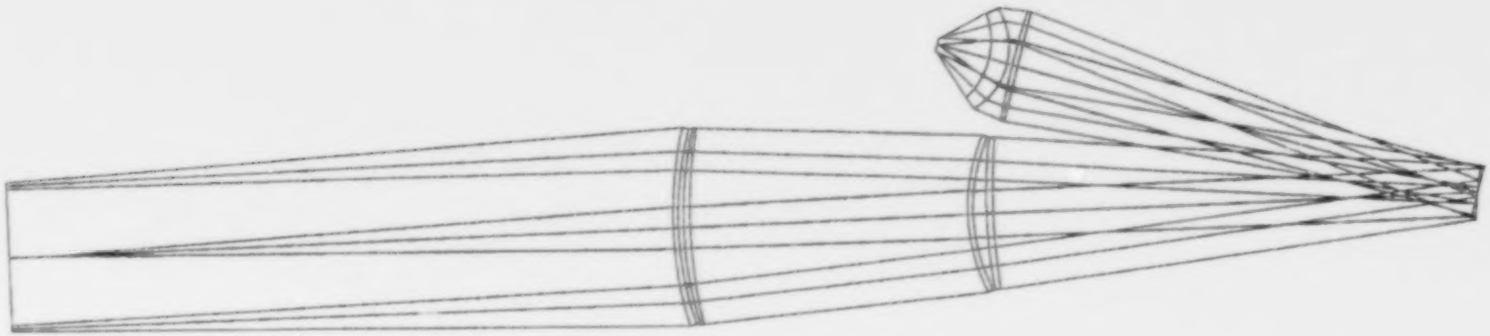

3D LAYOUT

IR_PRO_544MM_DMD23.5MM / 8.5DEG
THU NOV 6 15:9:49 1997
SCALE: 0.2000

100.00 MILLIMETERS

ON: +8.5 DEG.

NATIONAL OPTICS INSTITUTE
SR. OPTICAL DESIGNER: DR. EUCENE CURATU

H:\IR_PROJECTOR\PRE_DESIGN\SEARCH_OCT18\NEWDMD\SIMUL_PUP_OCT28.ZMX

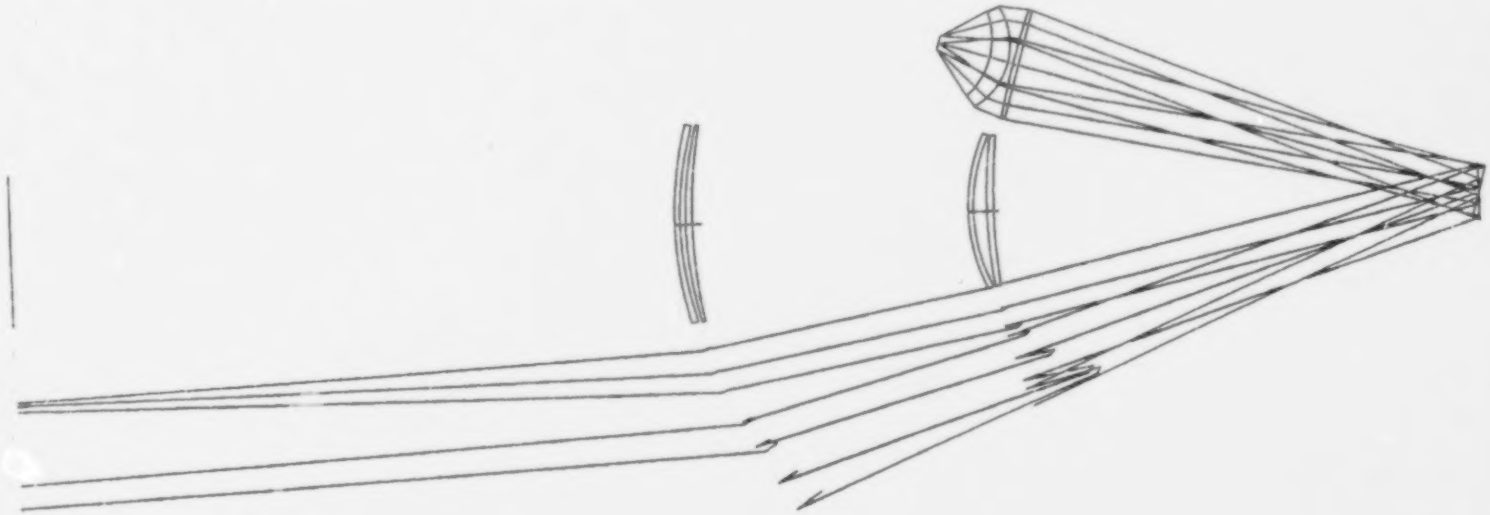

3D LAYOUT

IR_PRO_544MM_DMD23.5MM / 8.5DEG
THU NOV 6 15:11:18 1997
SCALE: 0.2000

100.00 MILLIMETERS

OFF: 0 DEG.

NATIONAL OPTICS INSTITUTE
SR. OPTICAL DESIGNER: DR. EUGENE CURATU

H:\IR_PROJECTOR\PRE_DESIGN\SEARCH_OCT18\NEWDMD\SIMUL_PUP_OCT20.ZMX

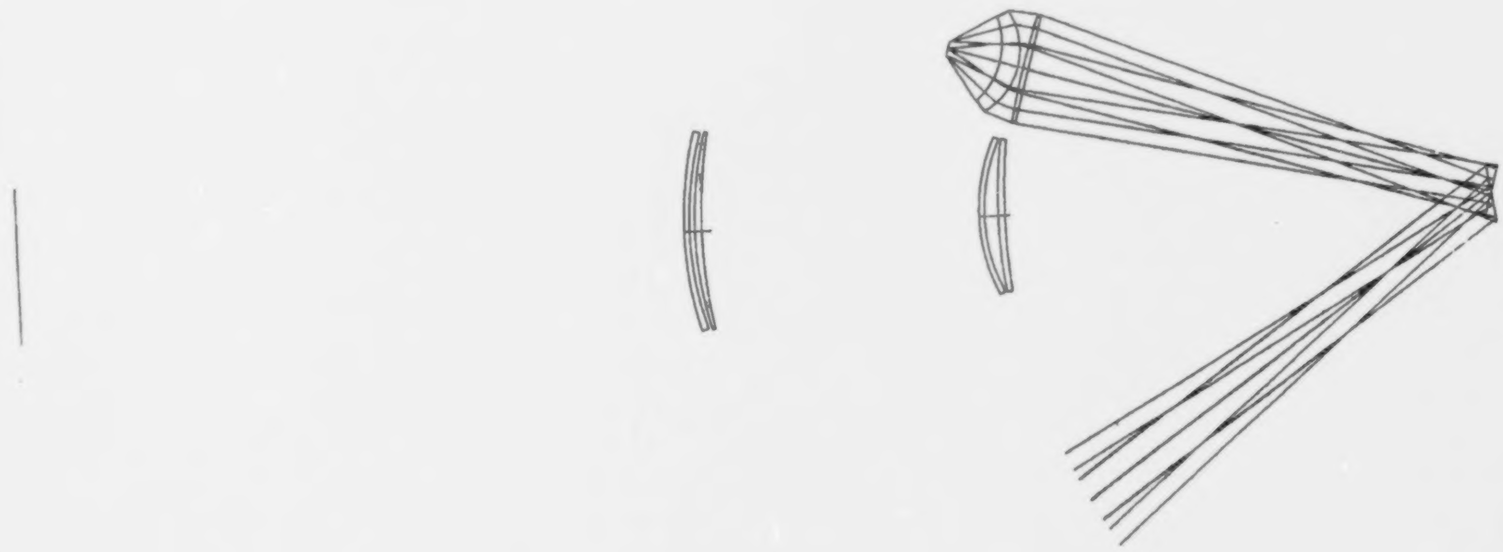

3D LAYOUT

IR_PRO_544MM_DMD23.5MM / 8.5DEG
THU NOV 6 15:10:47 1997
SCALE: 0.2000

100.00 MILLIMETERS

ON: -8.5 DEG.

NATIONAL OPTICS INSTITUTE
SR. OPTICAL DESIGNER: DR. EUGENE CURATU

H:\IR_PROJECTOR\PRE_DESIGN\SEARCH_OCT18\NEWDMD\SIMUL_PUP_OCT20.ZMX

APPENDIX III
MIRROR_1

Reflective Optics – 5° – (Mirror_1)

Item	Characteristics
Spectral range	0.2..12 µm
Configuration	Thermal source in the focal plane of Collimator No Beam Splitter Bistable operating mode (ON-OFF) Telecentric illumination Source imaged at the UUT entrance aperture Vignetting No diffuser in optical layout
ENP	106 mm
Field angle (2σ)	5°
DMD (array diagonal)	22.5 mm
Deflection angle (α)	±7°
Objective focal length (f_{PRO})	258 mm
Angle subtended by a reflected beam from each pixel	28°
Collimator focal length (f_{COL})	50 mm
Source diameter	20.54 mm

In the following pages we give the layout, prescription data, spot diagram, distortion, and MTF graphics of the reflective projection objective, followed by three layouts showing the bistable operating mode of this configuration.

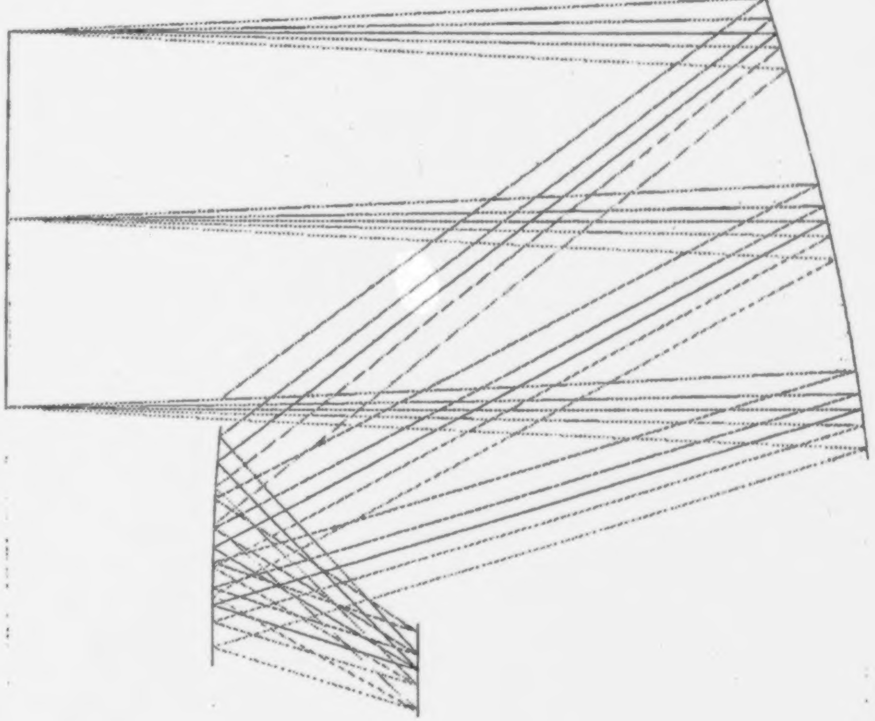

3D LAYOUT

MIRROR_PROJECTOR
FRI NOV 7 11:45:0 1997
SCALE: 0.5000

40.00 MILLIMETERS

NATIONAL OPTICS INSTITUTE
SR. OPTICAL DESIGNER: DR. EUGENE CURATU

H:\IR_PROJECTOR\PRE_DESIGN\NEW_ESS\PARA_PLAN1.ZMX

```
ystem/Prescription Data

ile : H:\IR_projector\pre_design\new_ess\para_plan1.zmx
itle: mirror_projector
ate : FRI NOV 7 14:6:21 1997

ENERAL LENS DATA:

Surfaces        :                    5
Stop            :                    1
ystem Aperture  : Entrance Pupil Diameter = 106
ay aiming       : Off
Apodization     :Uniform, factor =   0.00000E+000
Eff. Focal Len. :                  258 (in air)
ff. Focal Len.  :                  258 (in image space)
otal Track      :                  258
mage Space F/#  :             2.433962
Para. Wrkng F/# :             2.433962
Working F/#     :             2.221206
bj. Space N.A.  :             5.3e-009
top Radius      :                   53
arax. Ima. Hgt.:             11.26452
Parax. Mag.     :                    0
Entr. Pup. Dia. :                  106
ntr. Pup. Pos.  :                    0
xit Pupil Dia.  :        6.656464e+015
Exit Pupil Pos. :       -1.620158e+016
Field Type      : Angle in degrees
aximum Field    :                  2.5
rimary Wave     :                  0.2
ens Units       :   Millimeters
Angular Mag.    :      1.621053e-014

ields          : 5
ield Type: Angle in degrees
        X-Value          Y-Value          Weight
 1      0.000000         0.000000        1.000000
 2      0.000000        -1.000000        1.000000
 3      0.000000         1.000000        1.000000
 4      0.000000        -2.500000        1.000000
 5      0.000000         2.500000        1.000000

ignetting Factors
        VDX       VDY       VCX       VCY
   0.000000  0.000000  0.000000  0.000000
 2 0.000000  0.000000  0.000000  0.000000
 3 0.000000  0.000000  0.000000  0.000000
   0.000000  0.000000  0.000000  0.000000
   0.000000  0.000000  0.000000  0.000000

Wavelengths     : 3
nits: Microns
          Value         Weight
 1      0.200000       1.000000
 2      4.000000       1.000000
 3     12.000000       1.000000

URFACE DATA SUMMARY:

Surf    Type              Comment           Radius       Thickness         Glass       Diameter          Conic
 OBJ STANDARD                             Infinity        Infinity                            0              0
 STO STANDARD                             Infinity             258                          106              0
   2 COORDBRK                                    -               0             -              -              -
   3 EVENASPH                                 -516            -197        MIRROR       379.5738     -0.8056721
   4 EVENASPH                             Infinity              61        MIRROR       155.1051              0
 IMA STANDARD                             Infinity                                     25.90128              0

URFACE DATA DETAIL:

Surface OBJ      : STANDARD
Surface STO      : STANDARD
urface   2       : COORDBRK
 Decenter X      :                0
 Decenter Y      :             -127
 Tilt About X    :                0
 Tilt About Y    :                0
 Tilt About Z    :                0
 Order           : Decenter then tilt
Surface   3      : EVENASPH
 Coeff on r  2   :                0
 Coeff on r  4   :   6.4619899e-010
 Coeff on r  6   :   1.9261882e-014
 Coeff on r  8   :  -5.7734037e-019
 Coeff on r 10   :     8.66358e-024
 Coeff on r 12   :                0
 Coeff on r 14   :                0
Coeff on r 16   :             0
Aperture        : Circular Aperture
Minimum Radius  :          0
Maximum Radius  :         67
Y- Decenter     :             127
urface   4      : EVENASPH
Coeff on r  2   :                 0
Coeff on r  4   :   1.8896668e-007
Coeff on r  6   :  -3.4953222e-011
Coeff on r  8   :    4.548105e-015
Coeff on r 10   :  -2.5942449e-019
Coeff on r 12   :                 0
Coeff on r 14   :                 0
Coeff on r 16   :                 0
Aperture        : Circular Aperture
Minimum Radius  :          0
Maximum Radius  :         34
Y- Decenter     :             35
Surface IMA     : STANDARD

DGE THICKNESS DATA:

Surf         X-Edge          Y-Edge
 STO     258.000000      258.000000
   2       0.000000        0.000000
   3   -9624.102860    -9624.102860
   4      57.859367       57.859367
 IMA       0.000000        0.000000

OLVE AND VARIABLE DATA:

Semi Diameter    1        : Fixed
Conic of     3            : Variable
arameter   2 Surf    3  : Variable
arameter   3 Surf    3  : Variable
arameter   4 Surf    3  : Variable
Parameter  5 Surf    3  : Variable
hickness of     4         : Solve, marginal ray height = 0.00000
arameter   2 Surf    4  : Variable
arameter   3 Surf    4  : Variable
Parameter  4 Surf    4  : Variable
Parameter  5 Surf    4  : Variable

NDEX OF REFRACTION DATA:

Surf      Glass       0.200000    4.000000   12.000000
  0                 1.00000000  1.00000000  1.00000000
  1                 1.00000000  1.00000000  1.00000000
  2 <CRD BRK>       1.00000000  1.00000000  1.00000000
  3    MIRROR       1.00000000  1.00000000  1.00000000
  4    MIRROR       1.00000000  1.00000000  1.00000000
  5                 1.00000000  1.00000000  1.00000000

HERMAL COEFFICIENT OF EXPANSION DATA:

Surf      Glass             TCE
  0                 0.00000000
  1                 0.00000000
  2 <CRD BRK>       0.00000000
  3    MIRROR       0.00000000
  4    MIRROR       0.00000000
  5                 0.00000000

/# DATA:

F/# calculations consider vignetting factors and ignore surface apertures.

         Wavelength:        0.200000              4.000000              12.000000
              Field      Tan        Sag        Tan        Sag        Tan        Sag
 1  0.0000, 0.0000 deg:   2.0713     2.4179     2.0713     2.4179     2.0713     2.4179
 2 0.0000, -1.0000 deg:   2.1702     2.4626     2.1702     2.4626     2.1702     2.4626
 3  0.0000, 1.0000 deg:   1.9794     2.3746     1.9794     2.3746     1.9794     2.3746
 4 0.0000, -2.5000 deg:   2.3246     2.5284     2.3246     2.5284     2.3246     2.5284
 5  0.0000, 2.5000 deg:   1.9184     2.3132     1.9184     2.3132     1.9184     2.3132

LOBAL VERTEX COORDINATES AND DIRECTIONS:

urf       X coord        Y coord        Z coord    X direc    Y direc    Z direc
  1      0.000000       0.000000       0.000000   0.000000   0.000000   1.000000
  2      0.000000    -127.000000     258.000000   0.000000   0.000000   1.000000
  3      0.000000    -127.000000     258.000000   0.000000   0.000000   1.000000
  4      0.000000    -127.000000      61.000000   0.000000   0.000000   1.000000
  5      0.000000    -127.000000     122.000000   0.000000   0.000000   1.000000

ELEMENT VOLUME DATA:
```

```
alues are only accurate for plane and spherical surfaces.
lement volumes are computed by assuming edges are squared up
o the larger of the front and back radial aperture.

                        Volume cc    Density g/cc          Mass g
otal Mass:                                               0.000000

ARDINAL POINTS:

bject space positions are measured with respect to surface 1.
mage space positions are measured with respect to the image surface.
he index in both the object space and image space is considered.

                        Object Space        Image Space
 = 0.200000 (Primary)
rincipal Planes   :      258.000000         -258.000000
odal Planes       :      258.000000         -258.000000
ocal Planes       :       -0.000000           -0.000000
nti-Nodal Planes  :     -258.000000          258.000000

 = 4.000000
rincipal Planes   :      258.000000         -258.000000
odal Planes       :      258.000000         -258.000000
ocal Planes       :       -0.000000           -0.000000
nti-Nodal Planes  :     -258.000000          258.000000

 = 12.000000
rincipal Planes   :      258.000000         -258.000000
odal Planes       :      258.000000         -258.000000
ocal Planes       :       -0.000000           -0.000000
nti-Nodal Planes  :     -258.000000          258.000000
```

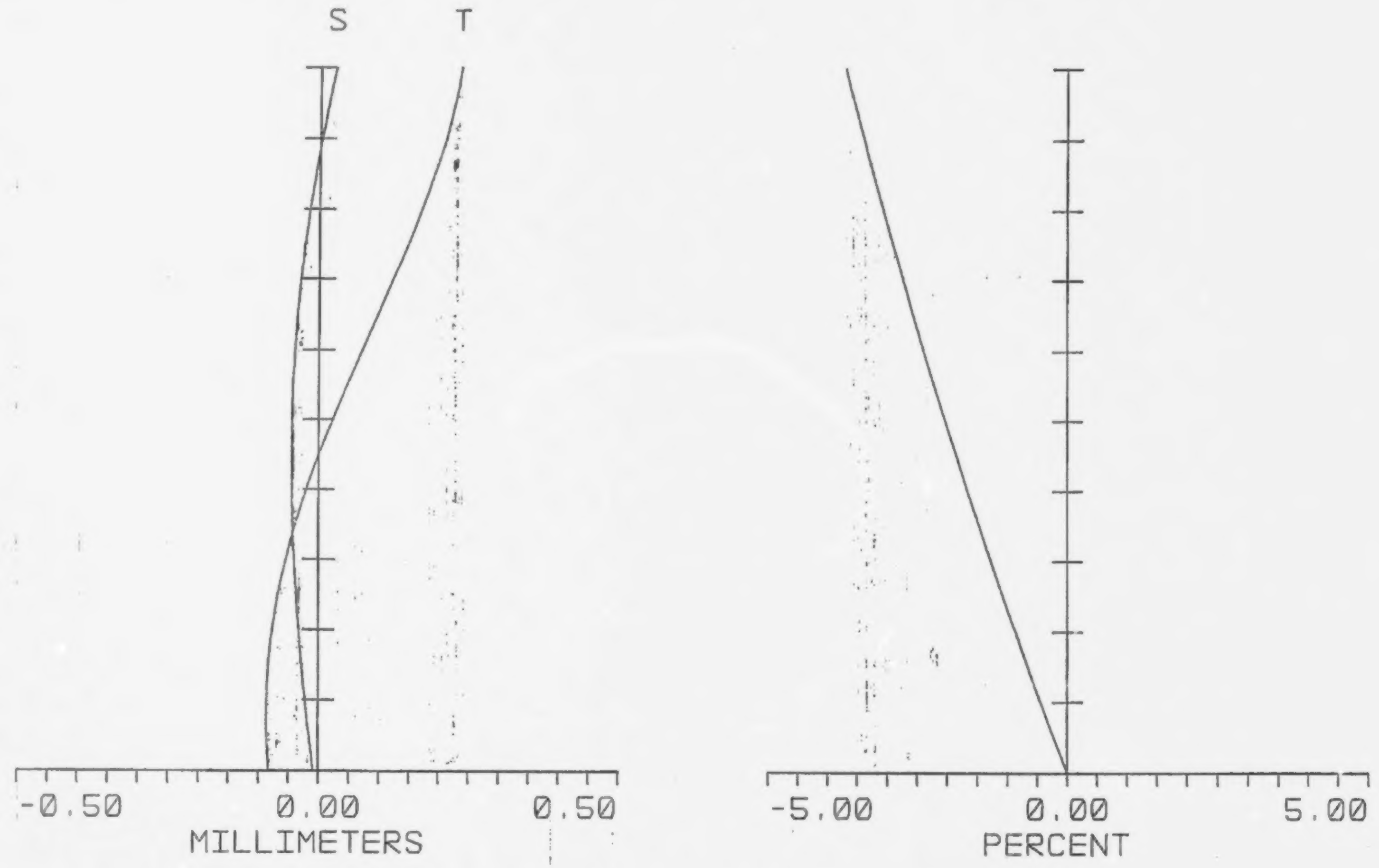

FIELD CURVATURE / DISTORTION

MIRROR_PROJECTOR
FRI NOV 7 11:46:43 1997
MAXIMUM FIELD IS 2.500 DEGREES
WAVELENGTHS: 4.000

NATIONAL OPTICS INSTITUTE
SR. OPTICAL DESIGNER: DR. EUGENE CURATU

H:\IR_PROJECTOR\PRE_DESIGN\NEW_ESS\PARA_PLAN1.ZMX

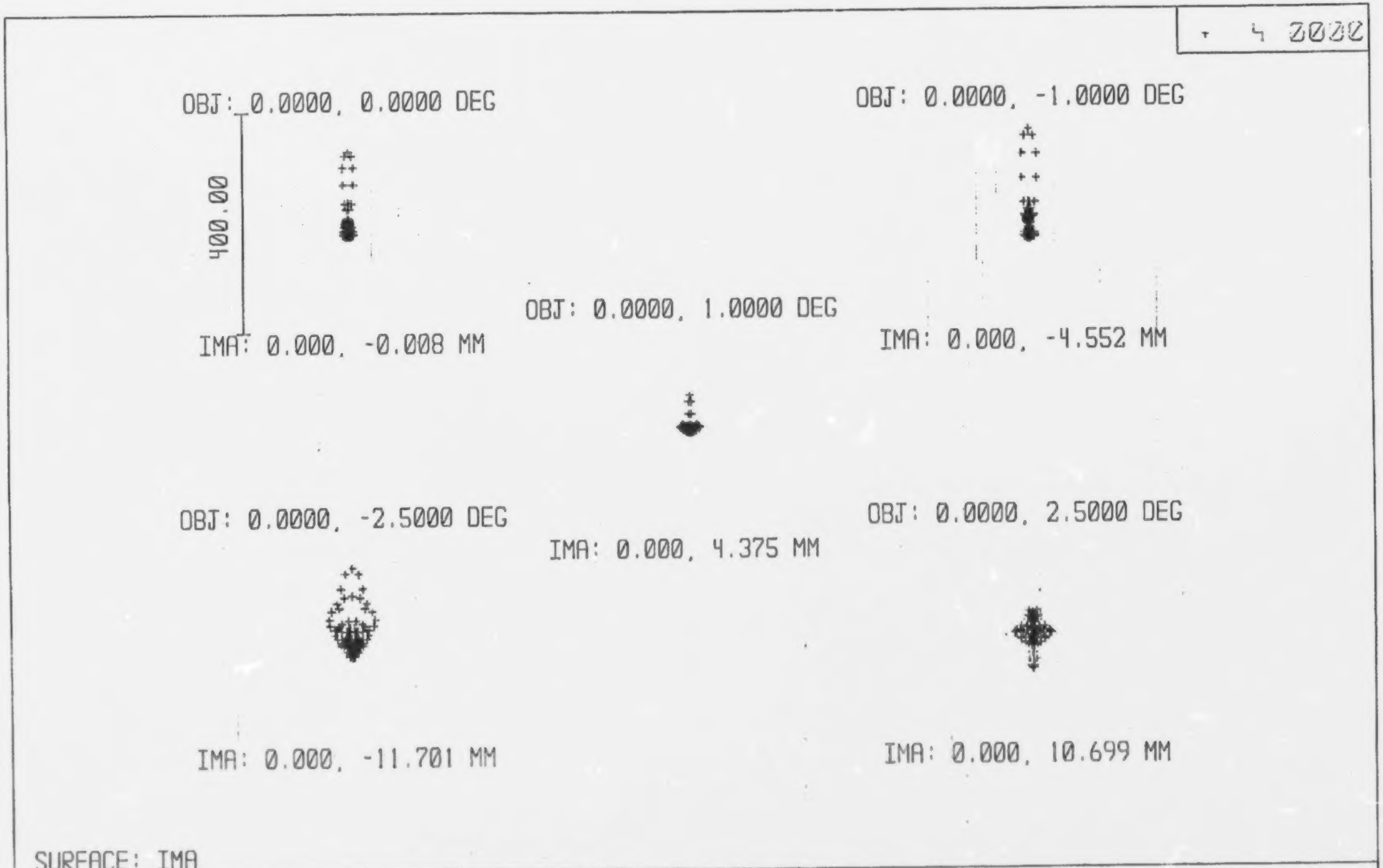

SPOT DIAGRAM

```
MIRROR_PROJECTOR
FRI NOV 7 11:46:14 1997  UNITS ARE MICRONS.
FIELD       :       1         2         3         4         5
RMS RADIUS  :    28.605    34.126    12.219    36.117    28.076
GEO RADIUS  :   129.486   162.285    60.398   126.126    65.355
AIRY DISK   :    10.84                   REFERENCE  : CENTROID
```

NATIONAL OPTICS INSTITUTE

SR. OPTICAL DESIGNER: DR. EUGENE CURATU

H:\IR_PROJECTOR\PRE_DESIGN\NEW_ESS\PARA_PLAN1.ZMX

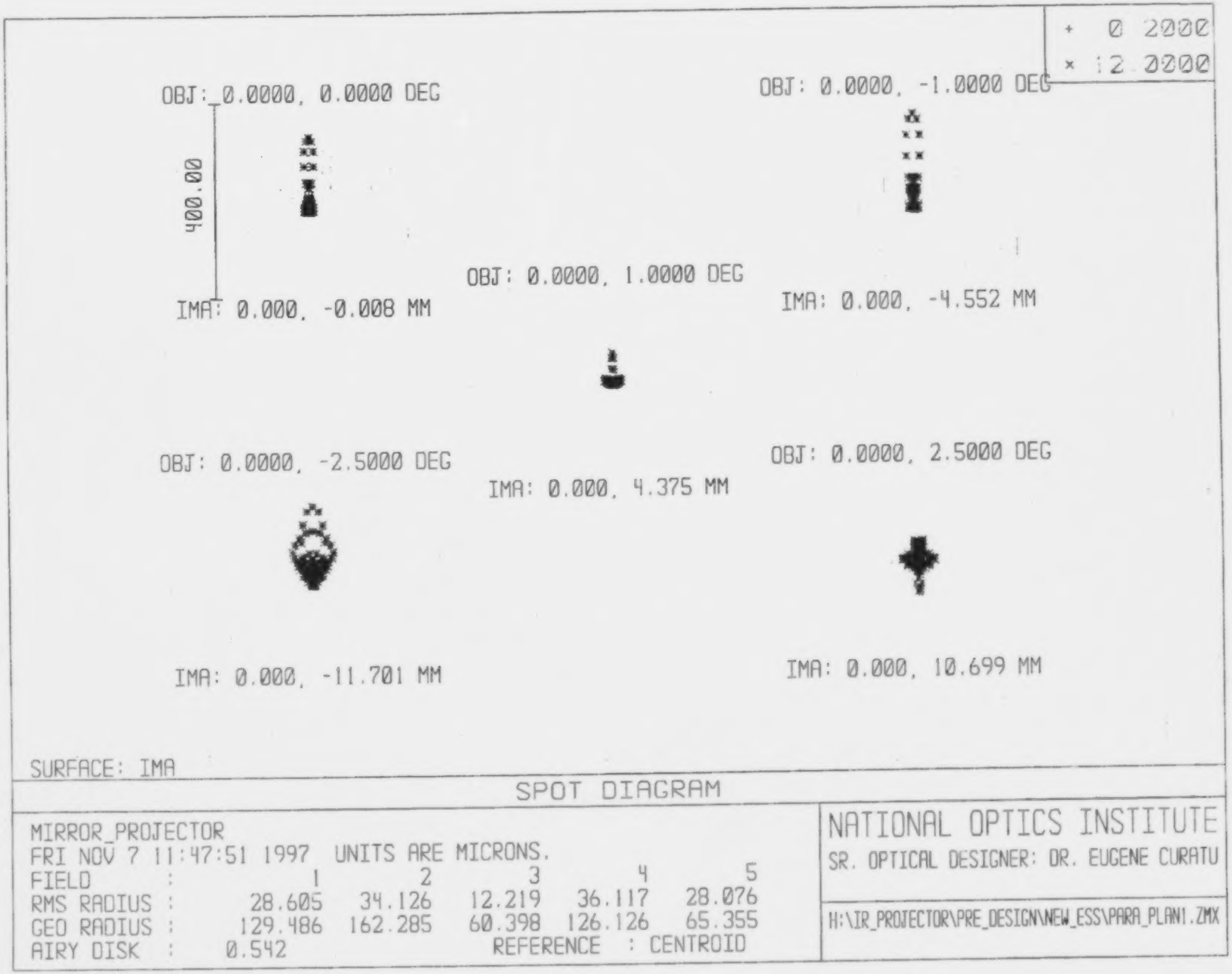

SPOT DIAGRAM

```
MIRROR_PROJECTOR
FRI NOV 7 11:47:51 1997  UNITS ARE MICRONS.
FIELD       :         1        2        3        4        5
RMS RADIUS  :    28.605   34.126   12.219   36.117   28.076
GEO RADIUS  :   129.486  162.285   60.398  126.126   65.355
AIRY DISK   :     0.542                REFERENCE  : CENTROID
```

NATIONAL OPTICS INSTITUTE
SR. OPTICAL DESIGNER: DR. EUGENE CURATU

H:\IR_PROJECTOR\PRE_DESIGN\NEW_ESS\PARA_PLAN1.ZMX

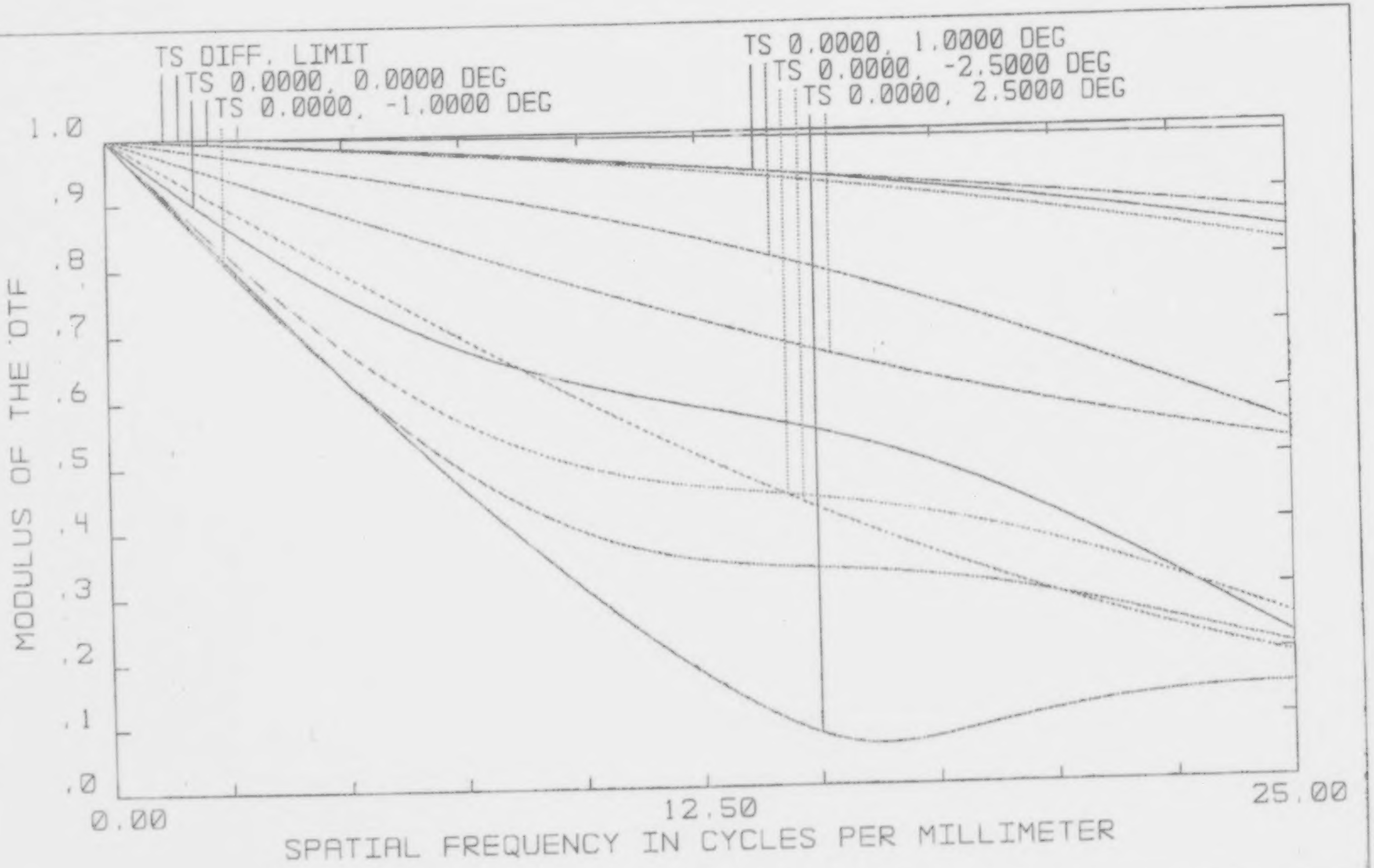

POLYCHROMATIC DIFFRACTION MODULATION TRANSFER FUNCTION

MIRROR_PROJECTOR
FRI NOV 7 14:4:27 1997
DATA FOR 0.2000 TO 0.2000 MICRONS.

NATIONAL OPTICS INSTITUTE
SR. OPTICAL DESIGNER: DR. EUGENE CURATU

H:\IR_PROJECTOR\PRE_DESIGN\NEW_ESS\PARA_PLAN1.ZMX

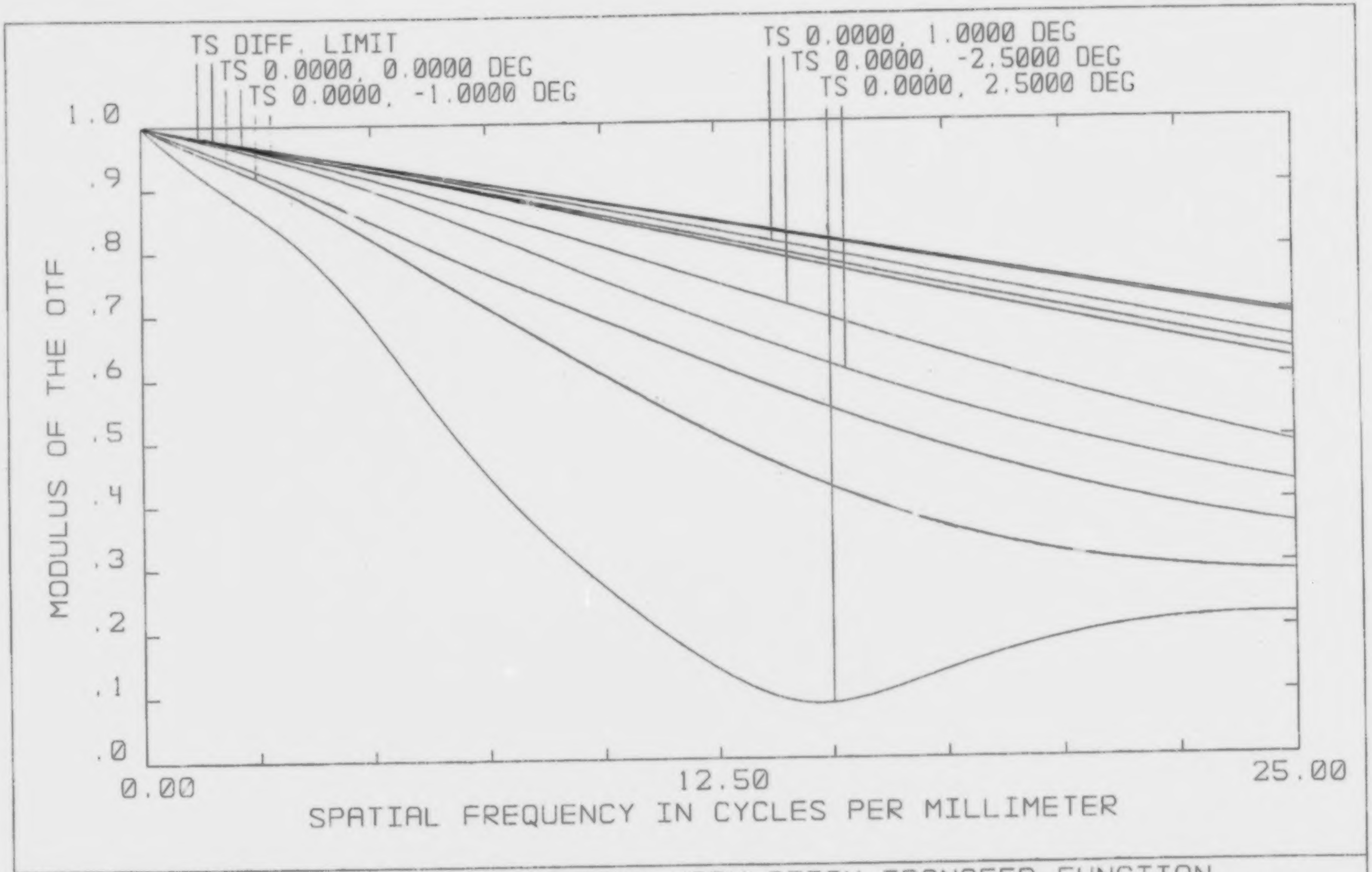

POLYCHROMATIC DIFFRACTION MODULATION TRANSFER FUNCTION

MIRROR_PROJECTOR
FRI NOV 7 11:45:28 1997
DATA FOR 4.0000 TO 4.0000 MICRONS.

NATIONAL OPTICS INSTITUTE
SR. OPTICAL DESIGNER: DR. EUGENE CURATU

H:\IR_PROJECTOR\PRE_DESIGN\NEW_ESS\PARA_PLAN1.ZMX

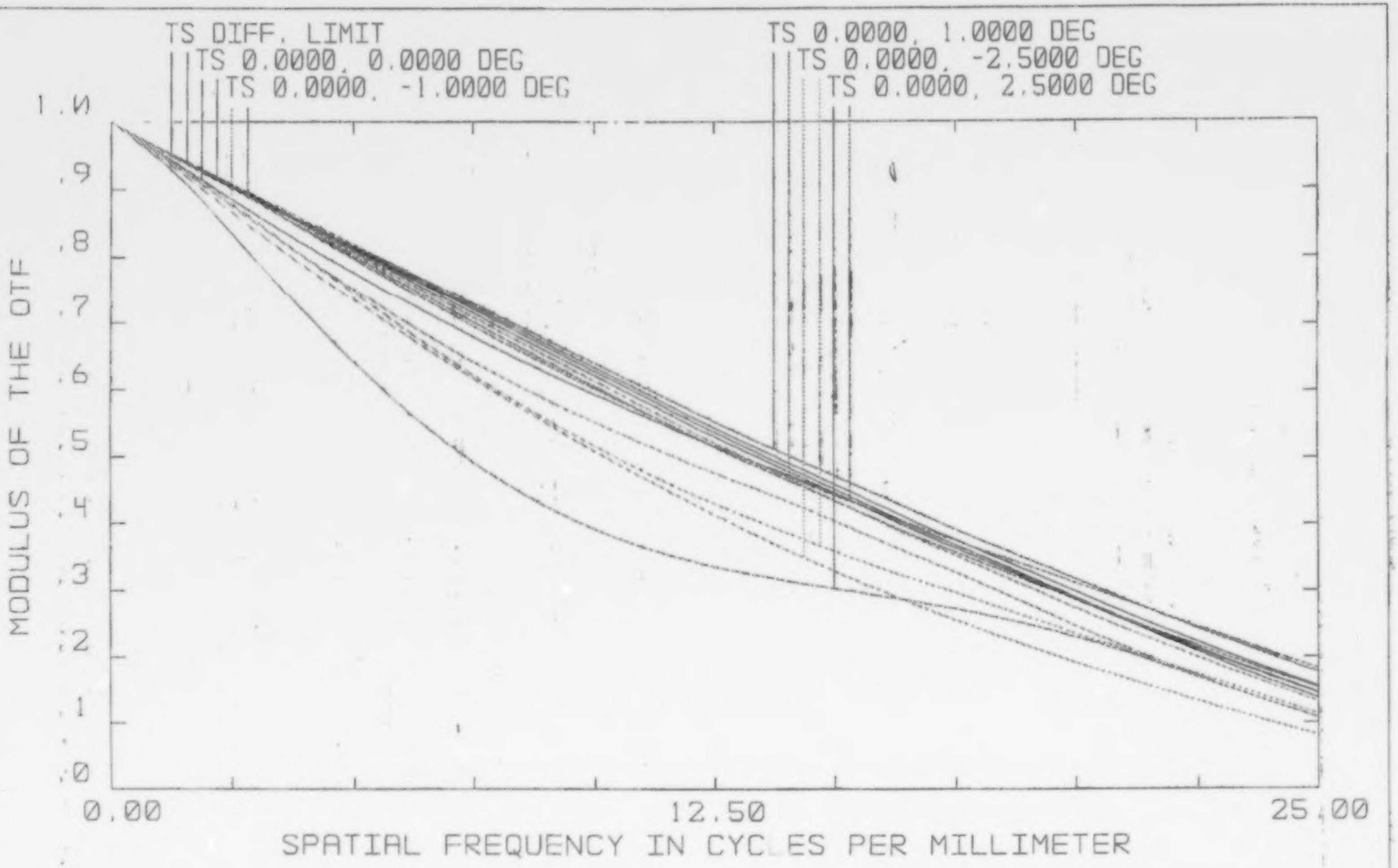

POLYCHROMATIC DIFFRACTION MODULATION TRANSFER FUNCTION

MIRROR_PROJECTOR
FRI NOV 7 13:59:25 1997
DATA FOR 12.0000 TO 12.0000 MICRONS.

NATIONAL OPTICS INSTITUTE
SR. OPTICAL DESIGNER: DR. EUGENE CURATU

H:\IR_PROJECTOR\PRE_DESIGN\NEW_ESS\PARA_PLAN1.ZMX

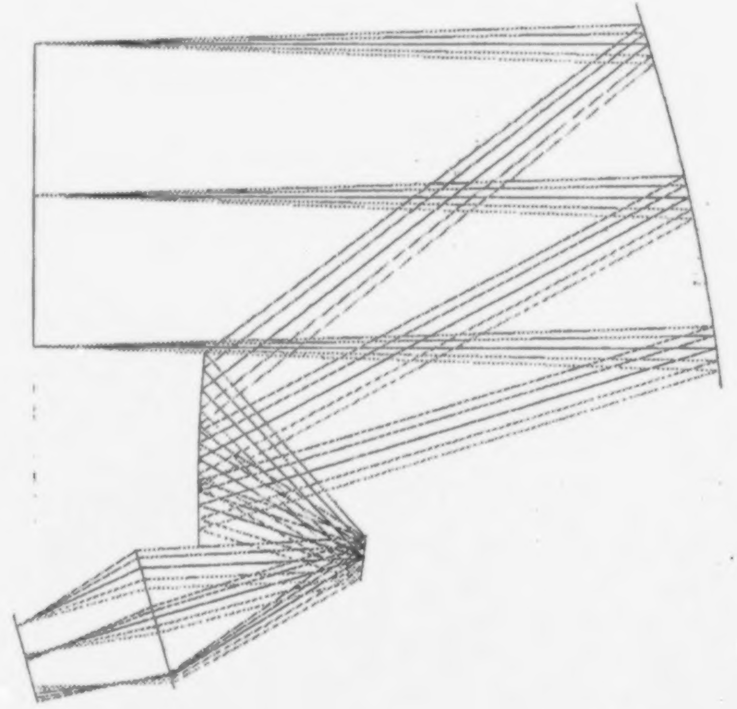

3D LAYOUT

MIRROR_PROJECTOR 3.5 DEG.
MON DEC 1 13:57:34 1997
SCALE: 0.4000

50.00 MILLIMETERS

NATIONAL OPTICS INSTITUTE

H:\IR_PROJECTOR\PRE_DESIGN\NEW_ESS\JUNK_MIRR2_ILL.ZMX

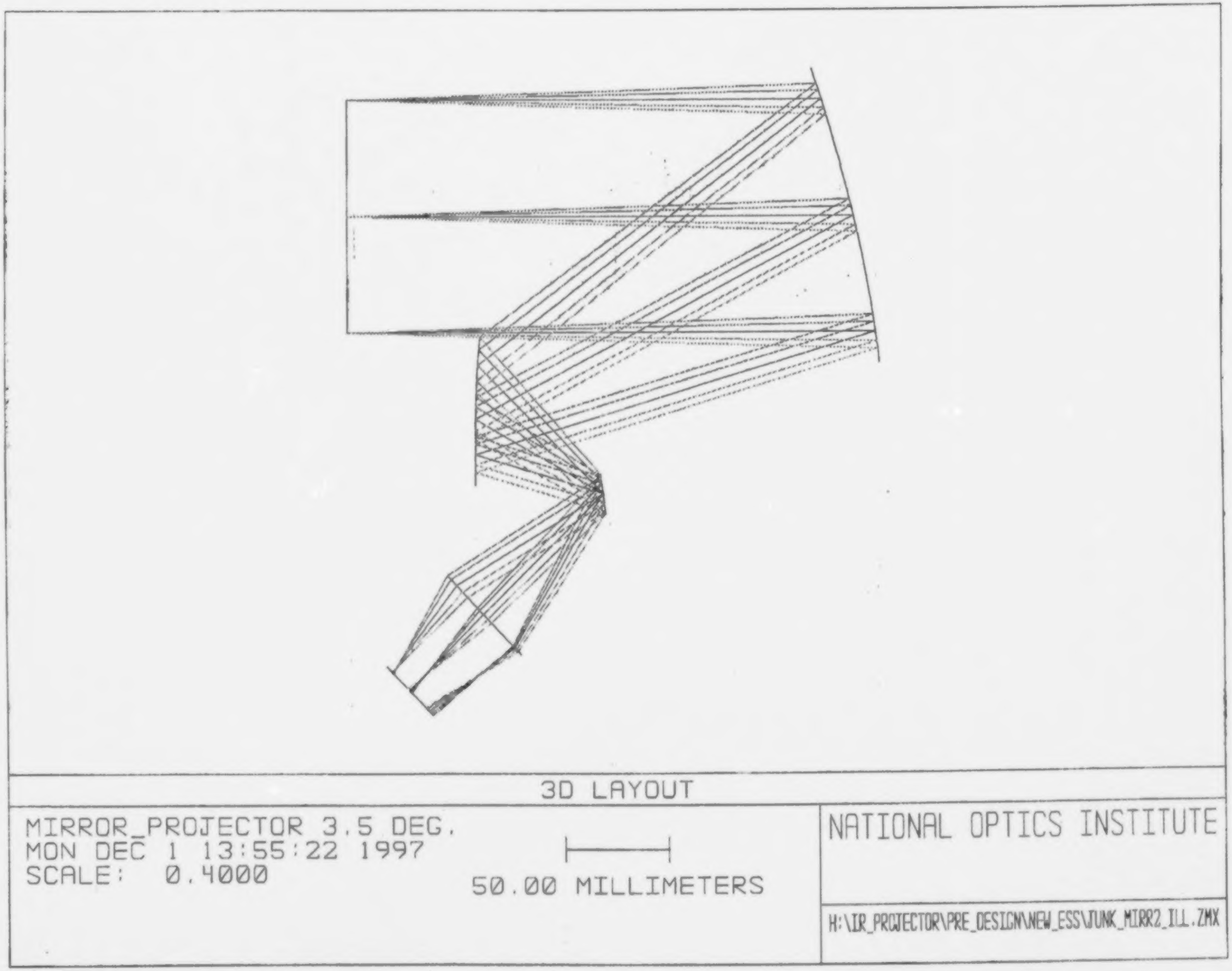
3D LAYOUT
MIRROR_PROJECTOR 3.5 DEG.
MON DEC 1 13:55:22 1997
SCALE: 0.4000
50.00 MILLIMETERS
NATIONAL OPTICS INSTITUTE
H:\IR_PROJECTOR\PRE_DESIGN\NEW_ESS\JUNK_MIRR2_ILL.ZMX

APPENDIX IV
MIRROR_2

Reflective Optics – 3.5° – (Mirror_2)

Item	Characteristics
Spectral range	0.2..12 μm
Configuration	Thermal source in the focal plane of Collimator No Beam Splitter (BS) Tristable operating mode (ON-OFF-ON) Telecentric illumination Source imaged at the UUT entrance aperture No vignetting No diffuser in optical layout
ENP	106 mm
Field angle (2σ)	3.5°
DMD (array diagonal)	33.25 mm
Deflection angle (α)	±8.5°
Objective focal length (f_{PRO})	544.2 mm
Angle subtended by a reflected beam from each pixel	13°
Collimator focal length (f_{COL})	50 mm
Source diameter	9.74 mm

In the following pages we give the layout, prescription data, spot diagram, distortion, and MTF graphics of the reflective projection objective, followed by three layouts showing the tristable operating mode of this configuration.

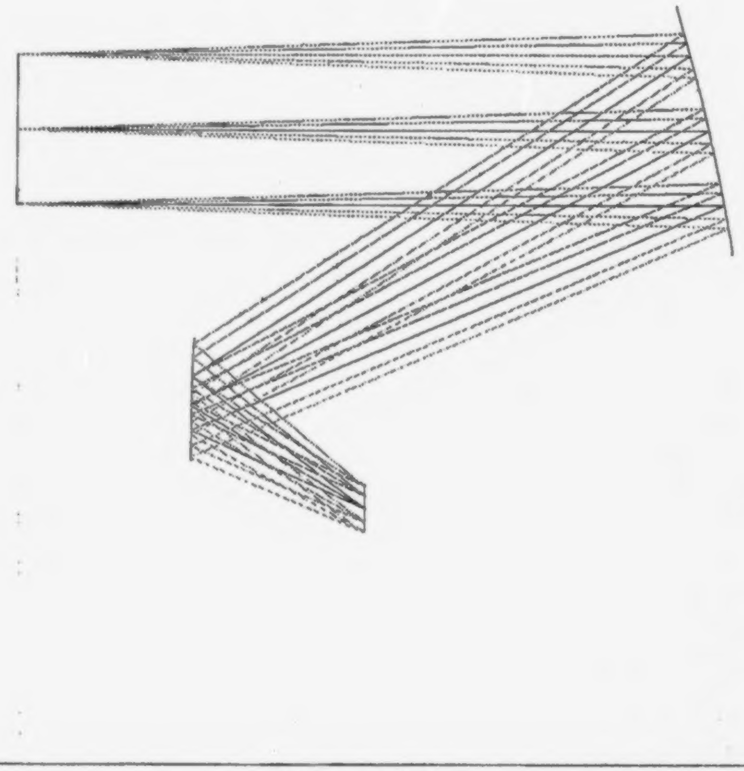

3D LAYOUT

MIRROR_PROJECTOR 3.5 DEG.
FRI NOV 7 13:36:57 1997
SCALE: 0.2000

100.00 MILLIMETERS

NATIONAL OPTICS INSTITUTE
SR. OPTICAL DESIGNER: DR. EUGENE CURATU

H:\IR_PROJECTOR\PRE_DESIGN\NEW_ESS\MIRROR544.ZMX

```
ystem/Prescription Data

ile : H:\IR_projector\pre_design\new_ess\mirror544.zmx
Title: mirror_projector 3.5 deg.
Date : FRI NOV 7 13:37:48 1997

ENERAL LENS DATA:

Surfaces         :                    5
top              :                    1
ystem Aperture   : Entrance Pupil Diameter = 106
ay aiming        : Off
Apodization      :Uniform, factor =    0.00000E+000
Eff. Focal Len.  :           544.1994 (in air)
ff. Focal Len.   :           544.1994 (in image space)
otal Track       :           544.1994
mage Space F/#   :           5.133957
Para. Wrkng F/#  :           5.133957
orking F/#       :           4.739202
bj. Space N.A.   :           5.3e-009
top Radius       :                 53
arax. Ima. Hgt.  :            16.6268
arax. Mag.       :                  0
ntr. Pup. Dia.   :                106
ntr. Pup. Pos.   :                  0
xit Pupil Dia.   :     2.588625e+016
Exit Pupil Pos.  :     1.328989e+017
ield Type        : Angle in degrees
aximum Field     :               1.75
rimary Wave      :                0.2
ens Units        :    Millimeters
ngular Mag.      :   -4.201569e-015

ields            : 5
ield Type: Angle in degrees
         X-Value        Y-Value          Weight
 1       0.000000        0.000000        1.000000
 2       0.000000       -1.000000        1.000000
 3       0.000000        1.000000        1.000000
 4       0.000000       -1.750000        1.000000
 5       0.000000        1.750000        1.000000

ignetting Factors
        VDX       VDY       VCX       VCY
   0.000000  0.000000  0.000000  0.000000
   0.000000  0.000000  0.000000  0.000000
   0.000000  0.000000  0.000000  0.000000
   0.000000  0.000000  0.000000  0.000000
   0.000000  0.000000  0.000000  0.000000

avelengths       : 8
nits: Microns
           Value          Weight
 1       0.200000        1.000000
 2       0.550000        1.000000
 3       0.800000        1.000000
 4       1.500000        1.000000
 5       2.000000        1.000000
 6       4.000000        1.000000
 7       8.000000        1.000000
 8      12.000000        1.000000

RFACE DATA SUMMARY:

urf     Type              Comment          Radius       Thickness          Glass         Diameter          Conic
OBJ STANDARD                             Infinity        Infinity                               0              0
TO STANDARD                              Infinity        544.1994                             106              0
  2 COORDBRK                                    -               0              -                -              -
  3 EVENASPH                            -1088.399       -415.5321         MIRROR         671.9062   -0.[illegible]3648
  4 EVENASPH                             Infinity        128.6673         MIRROR         232.8515              0
IMA STANDARD                             Infinity                                        34.24164              0

RFACE DATA DETAIL:

urface OBJ       : STANDARD
urface STO       : STANDARD
urface  2        : COORDBRK
Decenter X       :               0
Decenter Y       :       -267.8811
Tilt About X     :               0
Tilt About Y     :               0
Tilt About Z     :               0
rder             : Decenter then tilt
urface  3        : EVENASPH
Coeff on r  2    :               0
Coeff on r  4    :   7.225154e-011
Coeff on r  6  :   3.4506251e-016
Coeff on r  8  :  -2.3681158e-021
Coeff on r 10  :   9.3929737e-027
Coeff on r 12  :                0
Coeff on r 14  :                0
Coeff on r 16  :                0
Aperture       : Circular Aperture
Minimum Radius :             0
Maximum Radius :            87
Y- Decenter    :        267.88101
urface   4     : EVENASPH
Coeff on r  2  :                0
Coeff on r  4  :   1.9740088e-008
Coeff on r  6  :  -8.7332989e-013
Coeff on r  8  :   3.0375995e-017
Coeff on r 10  :  -5.0319517e-022
Coeff on r 12  :                0
Coeff on r 14  :                0
Coeff on r 16  :                0
Aperture       : Circular Aperture
Minimum Radius :             0
Maximum Radius :            43
Y- Decenter    :               77
urface IMA     : STANDARD

DGE THICKNESS DATA:

Surf          X-Edge          Y-Edge
STO       544.199400      544.199400
  2         0.000000        0.000000
  3     -5655.361786    -5655.361786
  4       126.420181      126.420181
 IMA        0.000000        0.000000

OLVE AND VARIABLE DATA:

Semi Diameter   1       : Fixed
onic of    3            : Variable
arameter   2 Surf   3   : Variable
arameter   3 Surf   3   : Variable
Parameter  4 Surf   3   : Variable
Parameter  5 Surf   3   : Variable
hickness of    4        : Solve, marginal ray height = 0.00000
arameter   2 Surf   4   : Variable
arameter   3 Surf   4   : Variable
Parameter  4 Surf   4   : Variable
Parameter  5 Surf   4   : Variable

NDEX OF REFRACTION DATA:

Surf      Glass         0.200000    0.550000    0.800000    1.500000    2.000000
  0                   1.00000000  1.00000000  1.00000000  1.00000000  1.00000000
  1                   1.00000000  1.00000000  1.00000000  1.00000000  1.00000000
  2 <CRD BRK>         1.00000000  1.00000000  1.00000000  1.00000000  1.00000000
  3     MIRROR        1.00000000  1.00000000  1.00000000  1.00000000  1.00000000
  4     MIRROR        1.00000000  1.00000000  1.00000000  1.00000000  1.00000000
  5                   1.00000000  1.00000000  1.00000000  1.00000000  1.00000000

Surf      Glass         4.000000    8.000000   12.000000
  0                   1.00000000  1.00000000  1.00000000
  1                   1.00000000  1.00000000  1.00000000
  2 <CRD BRK>         1.00000000  1.00000000  1.00000000
  3     MIRROR        1.00000000  1.00000000  1.00000000
  4     MIRROR        1.00000000  1.00000000  1.00000000
  5                   1.00000000  1.00000000  1.00000000

HERMAL COEFFICIENT OF EXPANSION DATA:

Surf      Glass             TCE
  0                   0.00000000
  1                   0.00000000
  2 <CRD BRK>         0.00000000
  3     MIRROR        0.00000000
  4     MIRROR        0.00000000
  5                   0.00000000

/# DATA:

F/# calculations consider vignetting factors and ignore surface apertures.

             Wavelength:         0.200000              0.550000              0.800000
                   Field       Tan       Sag         Tan       Sag         Tan       Sag
 1   0.0000, 0.0000 deg:    4.4343    5.1207      4.4343    5.1207      4.4343    5.1207
 2  0.0000, -1.0000 deg:    4.6441    5.2158      4.6441    5.2158      4.6441    5.2158
 3   0.0000, 1.0000 deg:    4.2434    5.0270      4.2434    5.0270      4.2434    5.0270
```

```
4  0.0000, -1.7500 deg:    4.8122     5.2859    4.8122    5.2859    4.8122    5.2859
5  0.0000,  1.7500 deg:    4.1139     4.9586    4.1139    4.9586    4.1139    4.9586

        Wavelength:          1.500000            2.000000            4.000000
#            Field         Tan        Sag       Tan       Sag       Tan       Sag
1  0.0000,  0.0000 deg:    4.4343     5.1207    4.4343    5.1207    4.4343    5.1207
2  0.0000, -1.0000 deg:    4.6441     5.2158    4.6441    5.2158    4.6441    5.2158
3  0.0000,  1.0000 deg:    4.2434     5.0270    4.2434    5.0270    4.2434    5.0270
4  0.0000, -1.7500 deg:    4.8122     5.2859    4.8122    5.2859    4.8122    5.2859
5  0.0000,  1.7500 deg:    4.1139     4.9586    4.1139    4.9586    4.1139    4.9586

        Wavelength:          8.000000            12.000000
#            Field         Tan        Sag       Tan       Sag
1  0.0000,  0.0000 deg:    4.4343     5.1207    4.4343    5.1207
2  0.0000, -1.0000 deg:    4.6441     5.2158    4.6441    5.2158
3  0.0000,  1.0000 deg:    4.2434     5.0270    4.2434    5.0270
4  0.0000, -1.7500 deg:    4.8122     5.2859    4.8122    5.2859
5  0.0000,  1.7500 deg:    4.1139     4.9586    4.1139    4.9586

LOBAL VERTEX COORDINATES AND DIRECTIONS:

urf       X coord       Y coord       Z coord   X direc   Y direc   Z direc
 1       0.000000      0.000000      0.000000  0.000000  0.000000  1.000000
 2       0.000000   -267.881100    544.199400  0.000000  0.000000  1.000000
 3       0.000000   -267.881100    544.199400  0.000000  0.000000  1.000000
 4       0.000000   -267.881100    128.667300  0.000000  0.000000  1.000000
 5       0.000000   -267.881100    257.334600  0.000000  0.000000  1.000000

LEMENT VOLUME DATA:

alues are only accurate for plane and spherical surfaces.
Element volumes are computed by assuming edges are squared up
o the larger of the front and back radial aperture.

                               Volume cc   Density g/cc        Mass g
otal Mass:                                                   0.000000

ARDINAL POINTS:

bject space positions are measured with respect to surface 1.
mage space positions are measured with respect to the image surface.
he index in both the object space and image space is considered.

                             Object Space         Image Space
= 0.200000 (Primary)
rincipal Planes  :            544.199400          -544.199400
odal Planes      :            544.199400          -544.199400
ocal Planes      :              0.000000            0.000000
nti-Nodal Planes :           -544.199400           544.199400

= 0.550000
rincipal Planes  :            544.199400          -544.199400
odal Planes      :            544.199400          -544.199400
ocal Planes      :              0.000000            0.000000
nti-Nodal Planes :           -544.199400           544.199400

= 0.800000
rincipal Planes  :            544.199400          -544.199400
odal Planes      :            544.199400          -544.199400
ocal Planes      :              0.000000            0.000000
nti-Nodal Planes :           -544.199400           544.199400

= 1.500000
rincipal Planes  :            544.199400          -544.199400
odal Planes      :            544.199400          -544.199400
ocal Planes      :              0.000000            0.000000
ti-Nodal Planes  :           -544.199400           544.199400

= 2.000000
rincipal Planes  :            544.199400          -544.199400
odal Planes      :            544.199400          -544.199400
cal Planes       :              0.000000            0.000000
ti-Nodal Planes  :           -544.199400           544.199400

= 4.000000
incipal Planes   :            544.199400          -544.199400
dal Planes       :            544.199400          -544.199400
cal Planes       :              0.000000            0.000000
ti-Nodal Planes  :           -544.199400           544.199400

= 8.000000
incipal Planes   :            544.199400          -544.199400
dal Planes       :            544.199400          -544.199400
cal Planes       :              0.000000            0.000000
ti-Nodal Planes  :           -544.199400           544.199400
```

```
 = 12.000000
Principal Planes   :         544.199400         -544.199400
Nodal Planes       :         544.199400         -544.199400
Focal Planes       :           0.000000           0.000000
Anti-Nodal Planes  :        -544.199400          544.199400
```

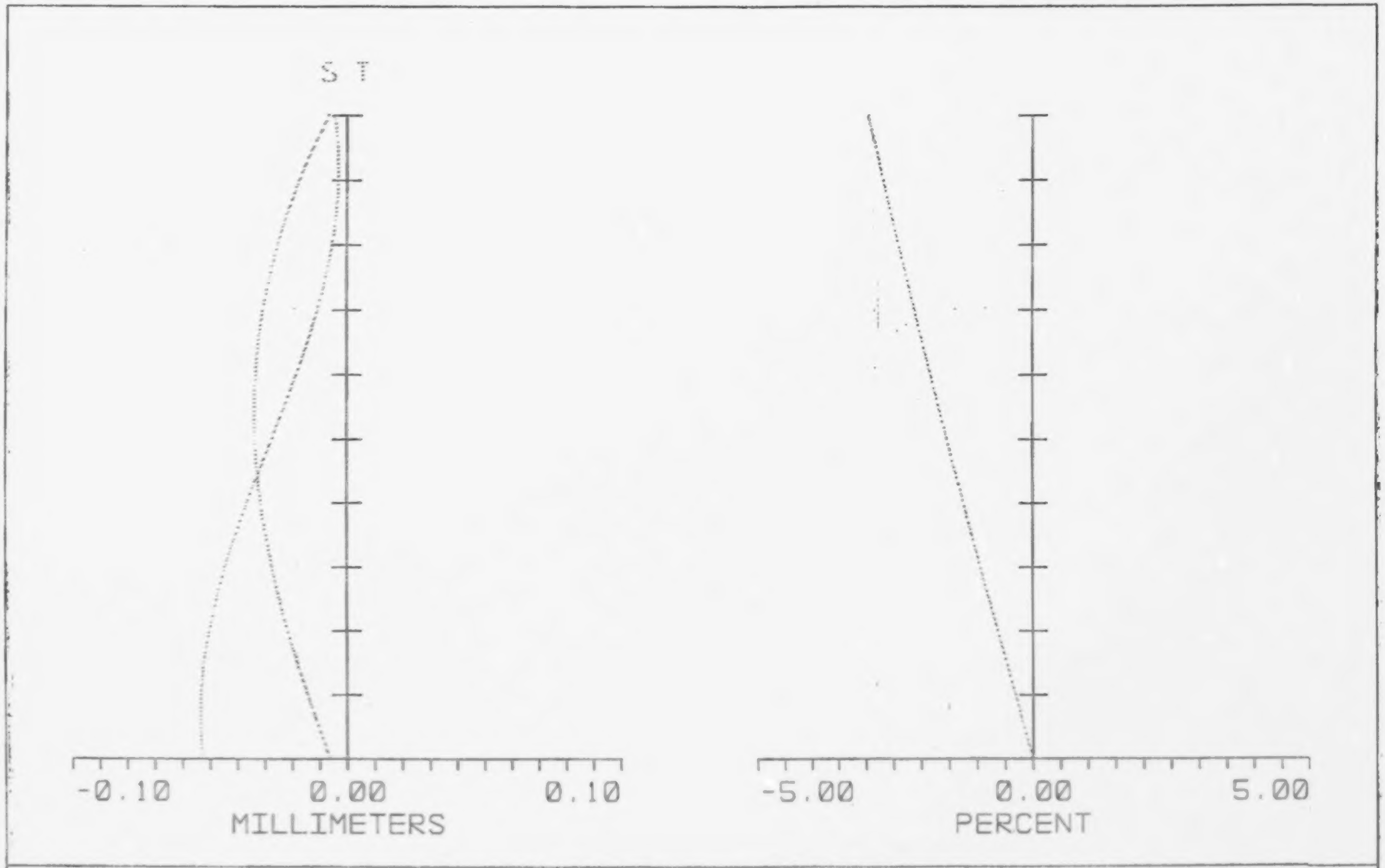

FIELD CURVATURE / DISTORTION

MIRROR_PROJECTOR 3.5 DEG.
FRI NOV 7 13:38:0 1997
MAXIMUM FIELD IS 1.750 DEGREES
WAVELENGTHS: 0.200 0.550 0.800 1.500 2.000 4.000 8.000 12.00

NATIONAL OPTICS INSTITUTE
SR. OPTICAL DESIGNER: DR. EUGENE CURATU
H:\IR_PROJECTOR\PRE_DESIGN\NEW_ESS\MIRROR544.ZMX

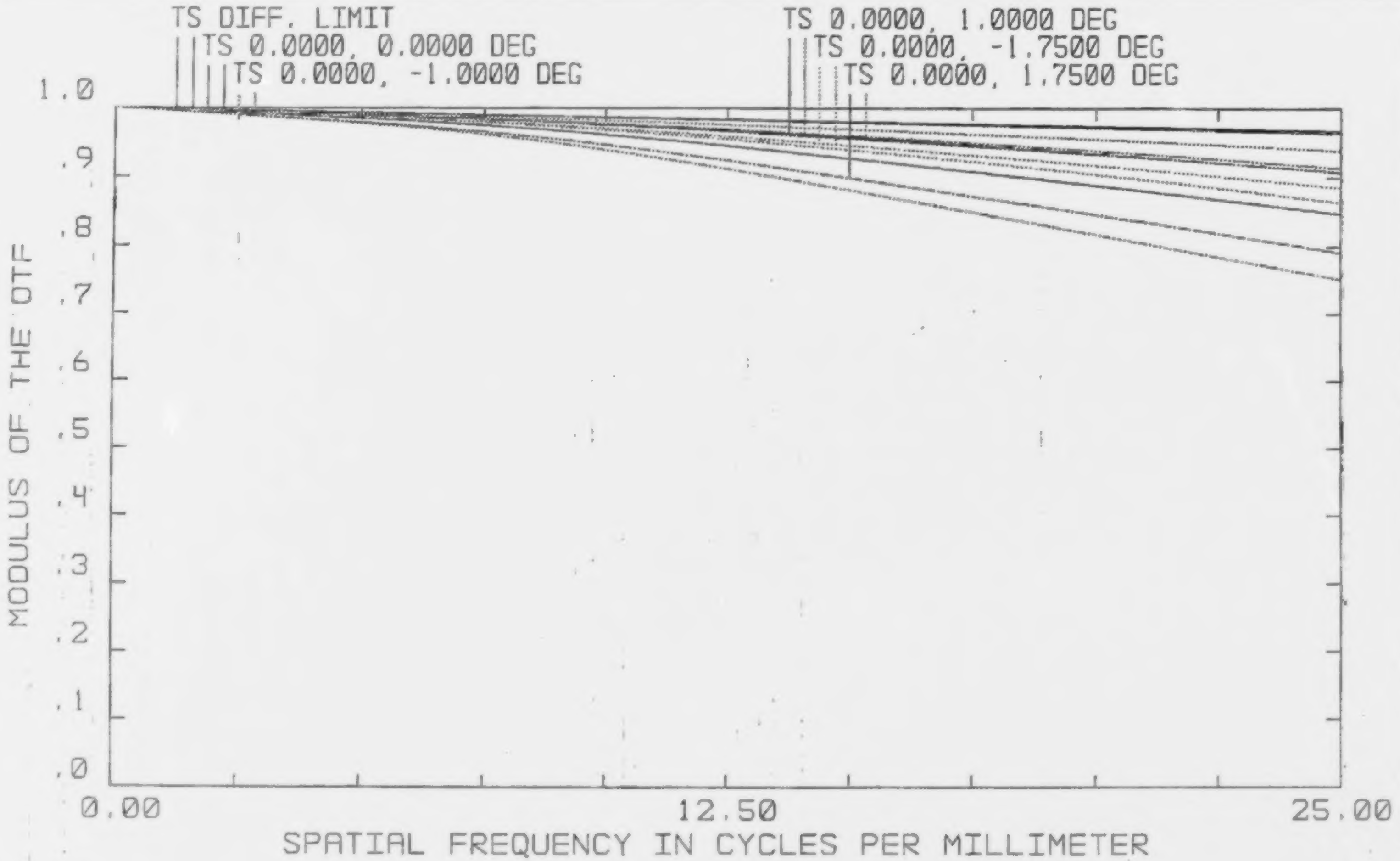

POLYCHROMATIC DIFFRACTION MODULATION TRANSFER FUNCTION

MIRROR_PROJECTOR 3.5 DEG.
FRI NOV 7 14:8:36 1997
DATA FOR 0.2000 TO 0.2000 MICRONS.

NATIONAL OPTICS INSTITUTE
SR. OPTICAL DESIGNER: DR. EUGENE CURATU

H:\IR_PROJECTOR\PRE_DESIGN\NEW_ESS\MIRROR544.ZMX

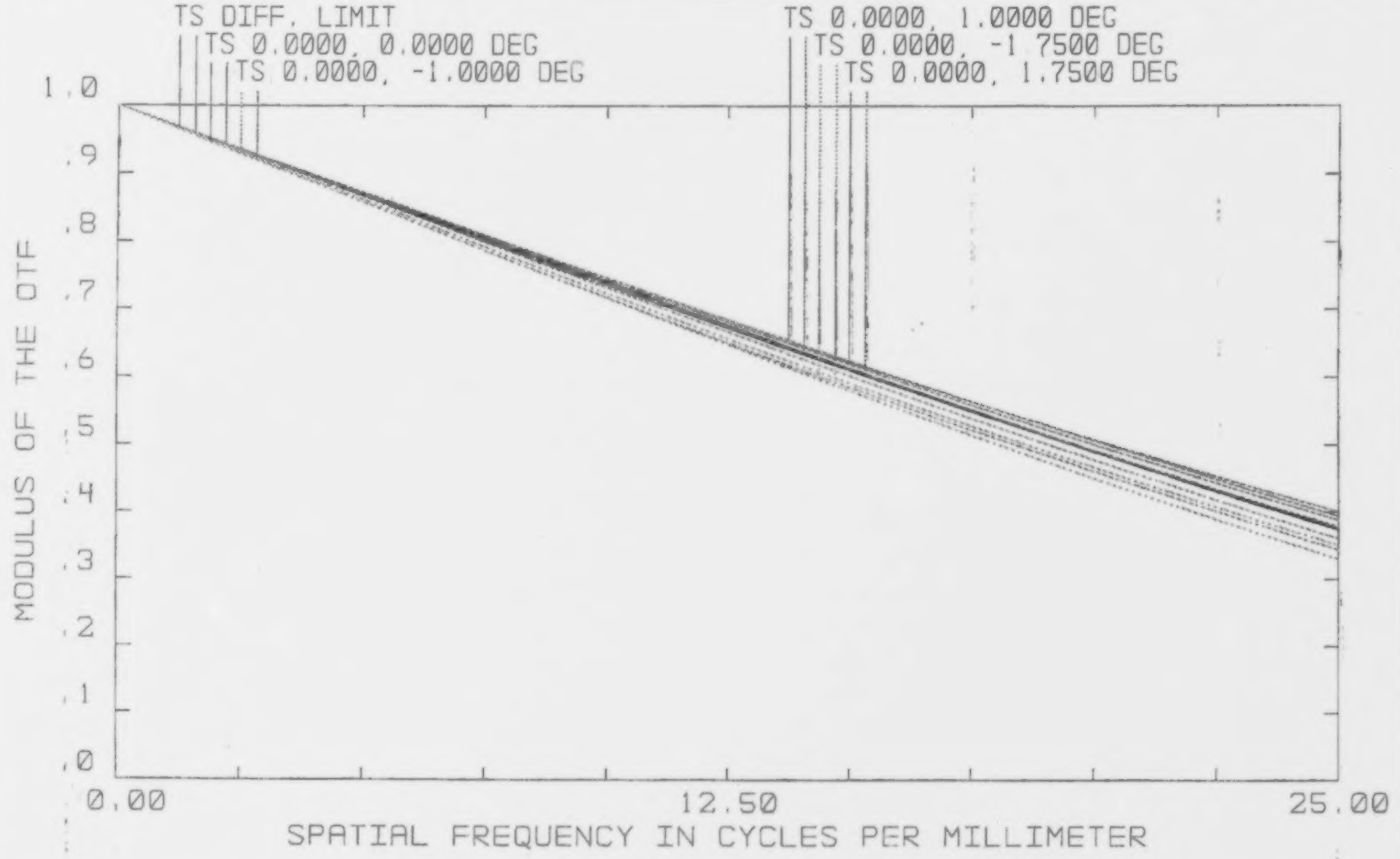

POLYCHROMATIC DIFFRACTION MODULATION TRANSFER FUNCTION

MIRROR_PROJECTOR 3.5 DEG.
FRI NOV 7 14:9:6 1997
DATA FOR 4.0000 TO 4.0000 MICRONS.

NATIONAL OPTICS INSTITUTE
SR. OPTICAL DESIGNER: DR. EUGENE CURATU

H:\IR_PROJECTOR\PRE_DESIGN\NEW_ESS\MIRROR544.ZMX

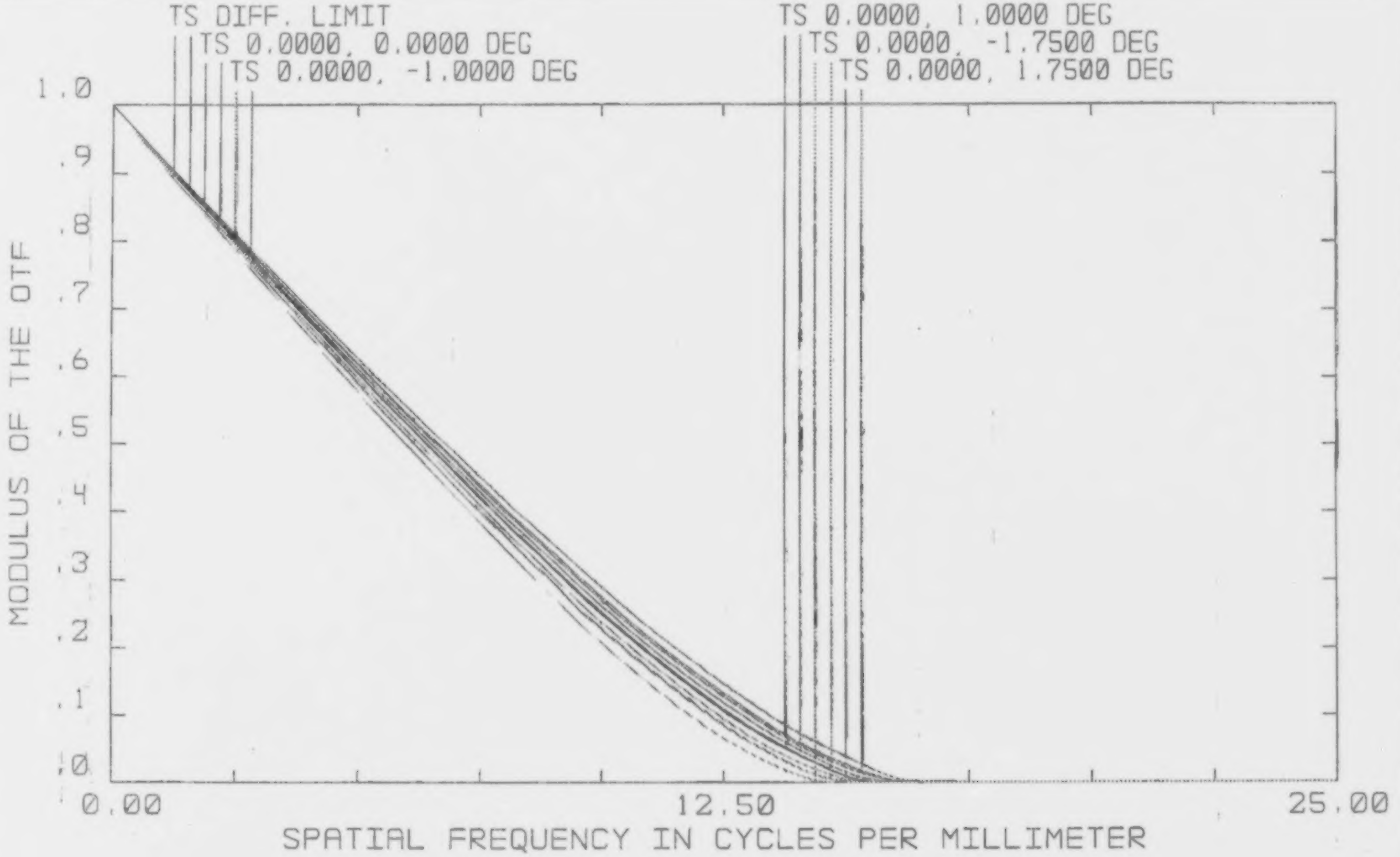

POLYCHROMATIC DIFFRACTION MODULATION TRANSFER FUNCTION

MIRROR_PROJECTOR 3.5 DEG.
FRI NOV 7 14:9:38 1997
DATA FOR 12.0000 TO 12.0000 MICRONS.

NATIONAL OPTICS INSTITUTE
SR. OPTICAL DESIGNER: DR. EUGENE CURATU

H:\IR_PROJECTOR\PRE_DESIGN\NEW_ESS\MIRROR544.ZMX

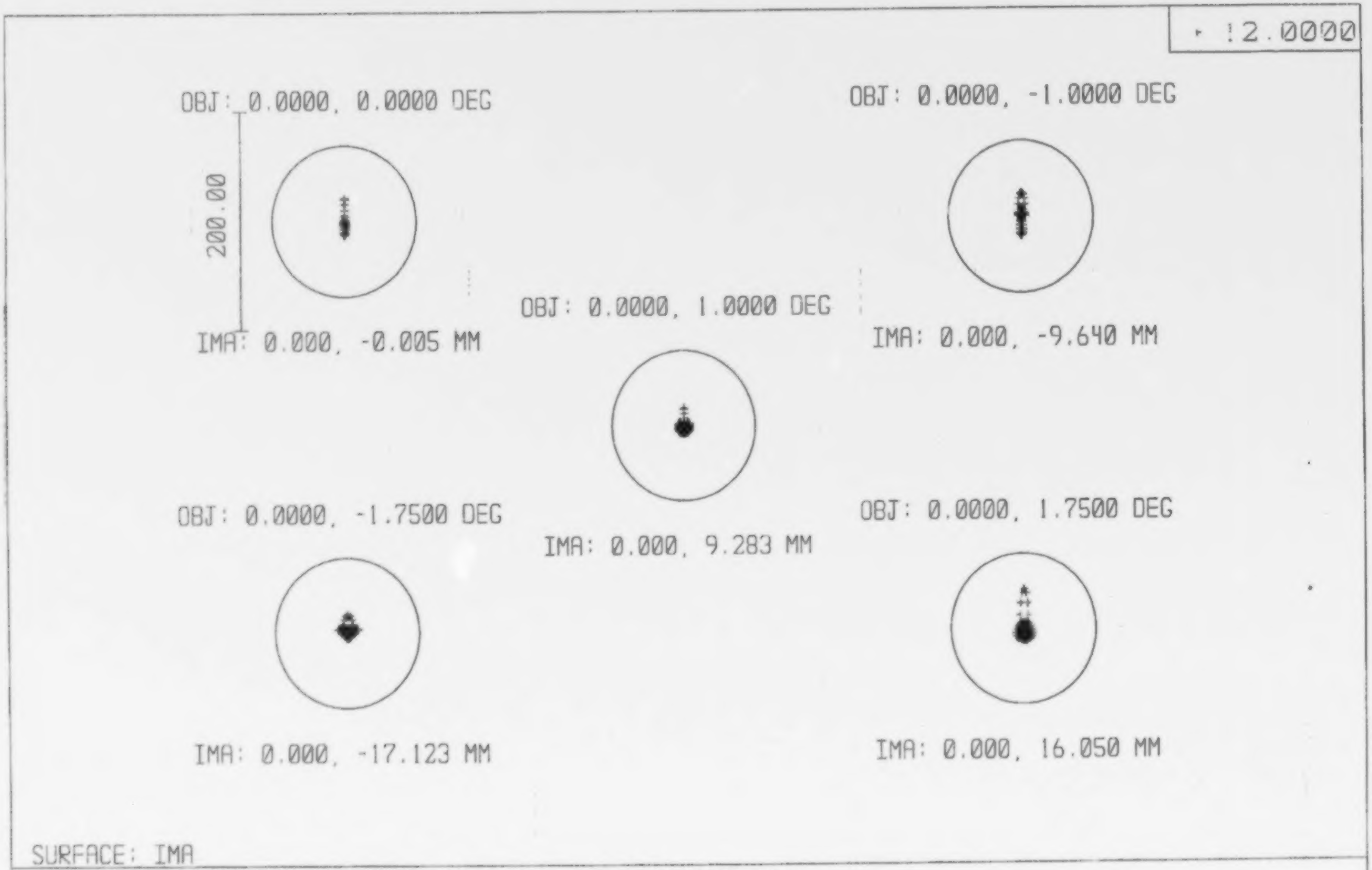

```
SPOT DIAGRAM
MIRROR_PROJECTOR 3.5 DEG.
FRI NOV 7 13:43:41 1997  UNITS ARE MICRONS.
FIELD       :        1        2        3        4        5
RMS RADIUS  :    5.306    6.739    4.474    5.379    7.784
GEO RADIUS  :   21.856   21.612   16.420   16.666   35.911
AIRY DISK   :    69.38            REFERENCE   : CENTROID
```

NATIONAL OPTICS INSTITUTE

SR. OPTICAL DESIGNER: DR. EUGENE CURATU

H:\IR_PROJECTOR\PRE_DESIGN\NEW_ESS\MIRROR544.ZMX

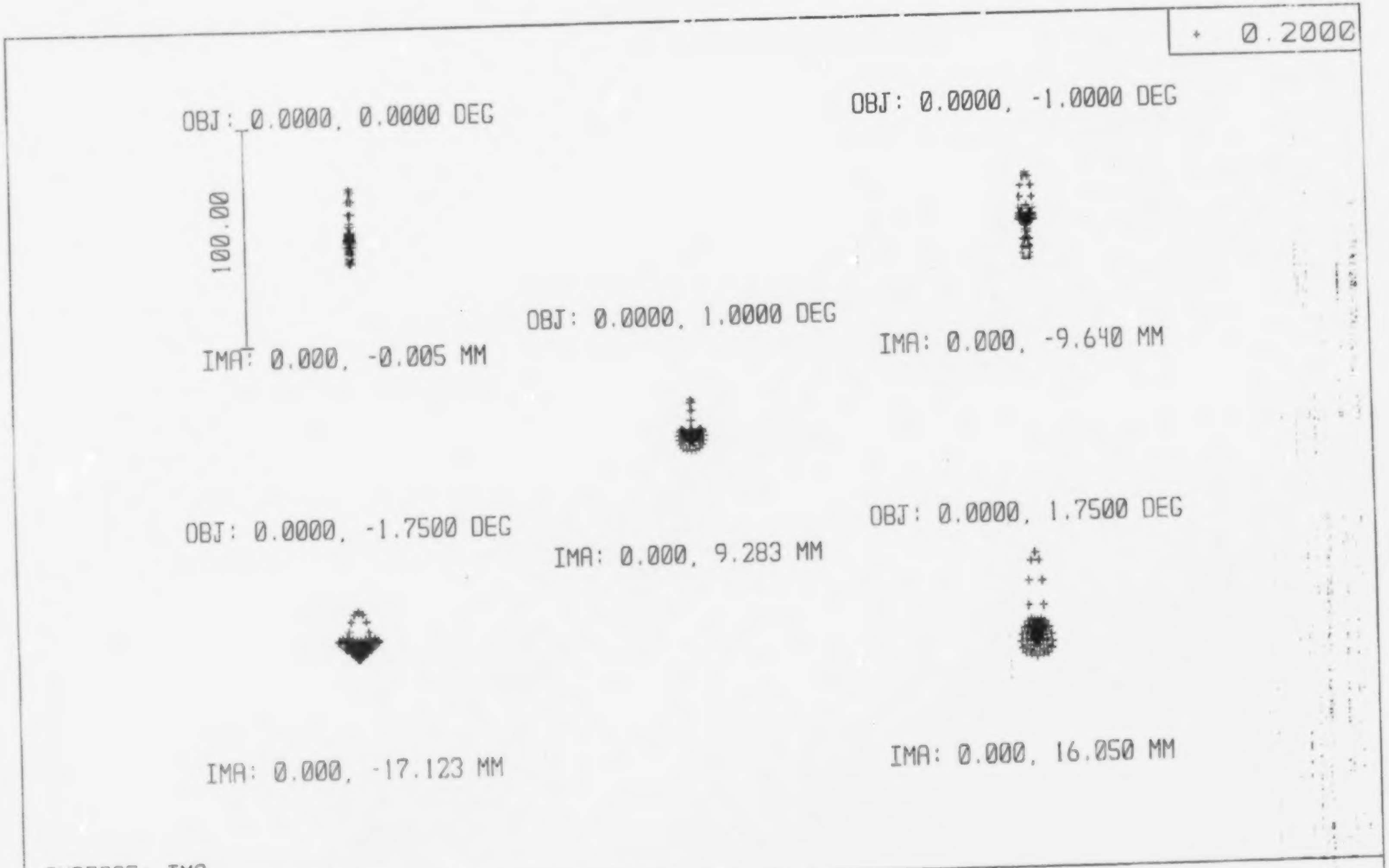

```
SURFACE: IMA
                              SPOT DIAGRAM
MIRROR_PROJECTOR 3.5 DEG.                :
FRI NOV 7 13:42:52 1997  UNITS ARE MICRONS.
FIELD       :          1        2        3        4        5
RMS RADIUS  :      5.306    6.739    4.474    5.379    7.784
GEO RADIUS  :     21.856   21.612   16.420   16.666   35.911
AIRY DISK   :      1.156             REFERENCE  : CENTROID
```

NATIONAL OPTICS INSTITUTE

SR. OPTICAL DESIGNER: DR. EUGENE CURATU

H:\IR_PROJECTOR\PRE_DESIGN\NEW_ESS\MIRROR544.ZMX

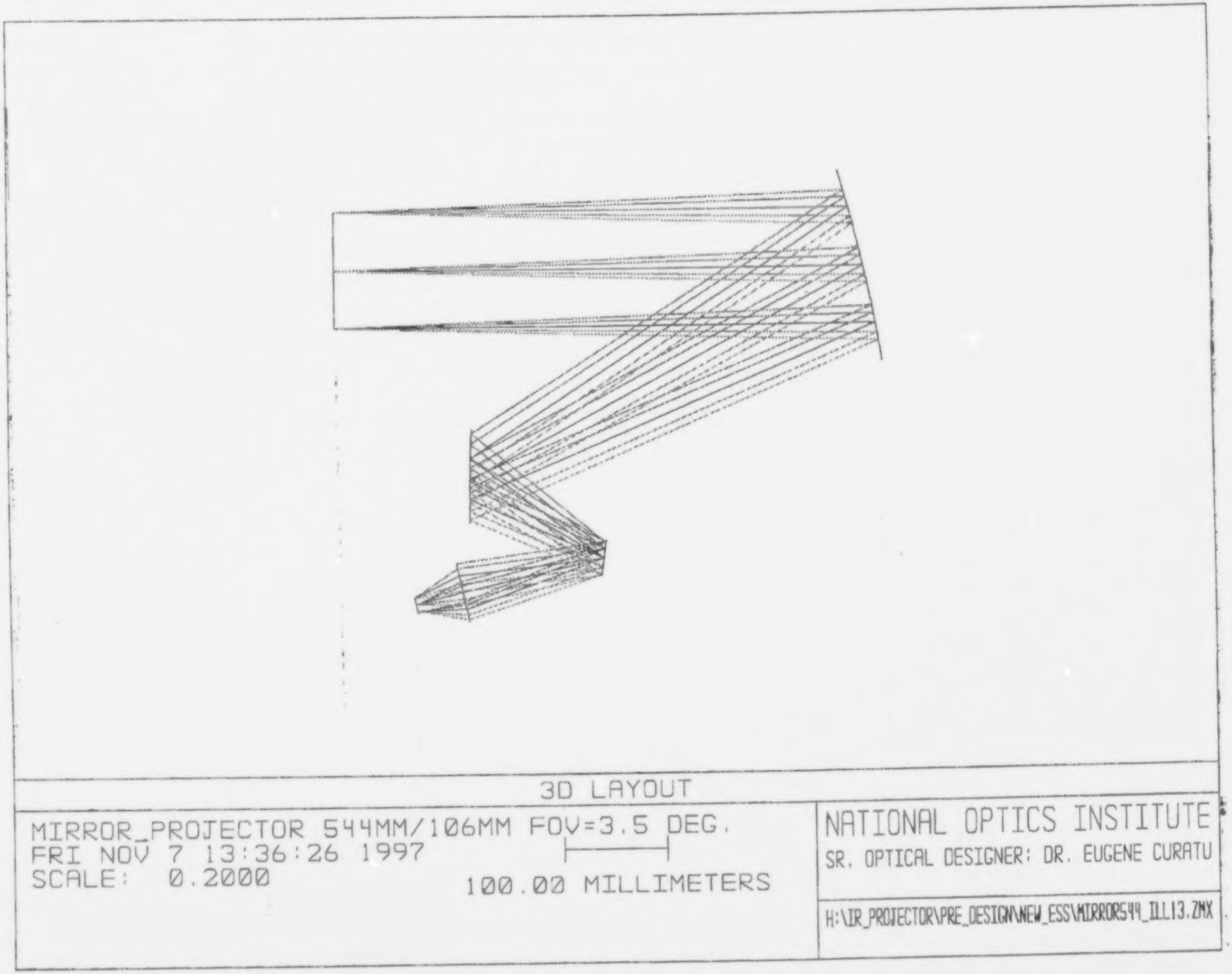
3D LAYOUT
MIRROR_PROJECTOR 544MM/106MM FOV=3.5 DEG.
FRI NOV 7 13:36:26 1997
SCALE: 0.2000
100.00 MILLIMETERS
NATIONAL OPTICS INSTITUTE
SR. OPTICAL DESIGNER: DR. EUGENE CURATU
H:\IR_PROJECTOR\PRE_DESIGN\NEW_ESS\MIRROR544_ILL13.ZMX

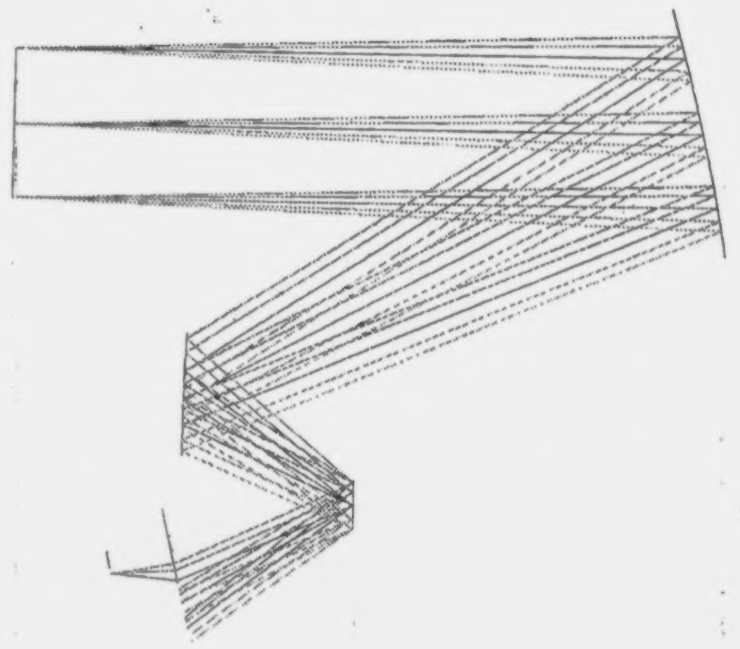

3D LAYOUT

MIRROR_PROJECTOR 544MM/106MM FOV=3.5 DEG.
WED NOV 12 14:29:47 1997
SCALE: 0.2000

100.00 MILLIMETERS

NATIONAL OPTICS INSTITUTE
SR. OPTICAL DESIGNER: DR. EUGENE CURATU

H:\IR_PROJECTOR\PRE_DESIGN\NEW_ESS\MIRROR544_ILL13.ZMX

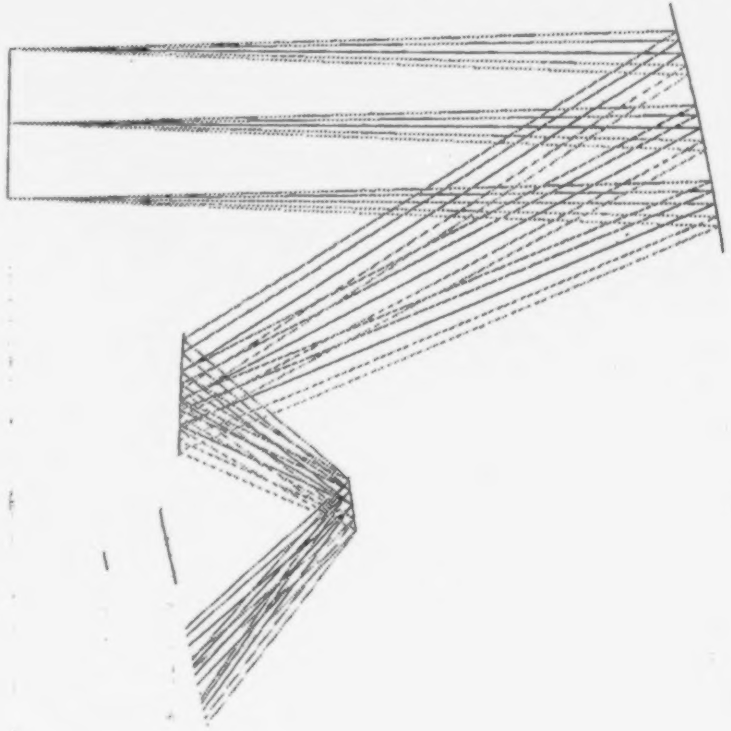

3D LAYOUT

MIRROR_PROJECTOR 544MM/106MM FOV=3.5 DEG.
WED NOV 12 14:30:4 1997
SCALE: 0.2000

100.00 MILLIMETERS

NATIONAL OPTICS INSTITUTE
SR. OPTICAL DESIGNER: DR. EUGENE CURATU

H:\IR_PROJECTOR\PRE_DESIGN\NEW_ESS\MIRROR544_ILL13.ZMX

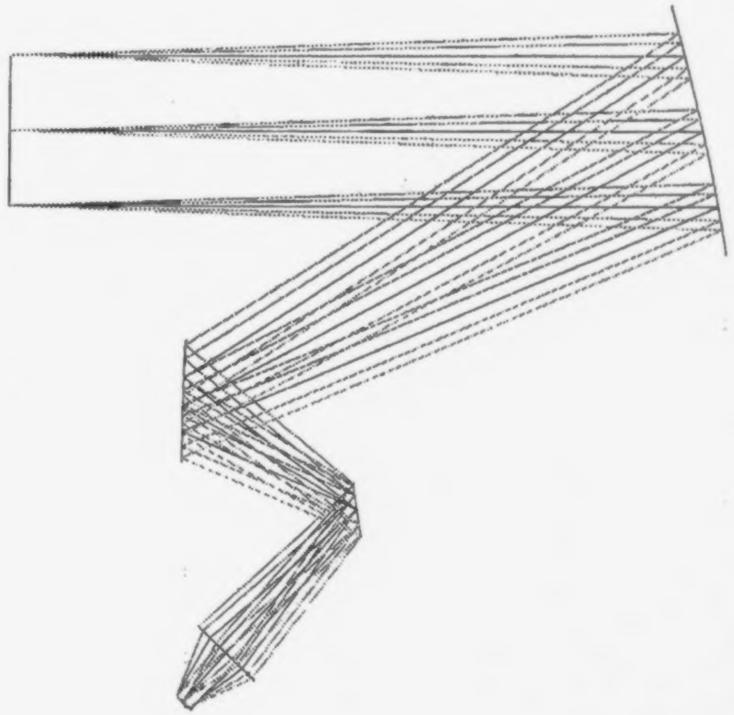

3D LAYOUT

MIRROR_PROJECTOR 544MM/106MM FOV=3.5 DEG.
FRI NOV 7 13:35:28 1997
SCALE: 0.2000

100.00 MILLIMETERS

NATIONAL OPTICS INSTITUTE
SR. OPTICAL DESIGNER: DR. EUGENE CURATU

H:\IR_PROJECTOR\PRE_DESIGN\NEW_ESS\MIRROR544_ILL47.ZMX

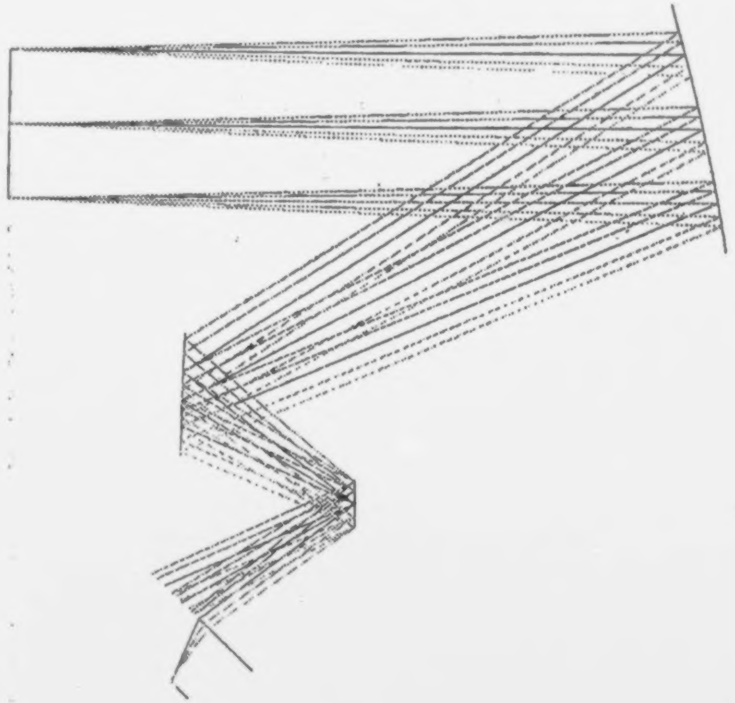

3D LAYOUT

MIRROR_PROJECTOR 544MM/106MM FOV=3.5 DEG.
WED NOV 12 14:28:54 1997
SCALE: 0.2000

100.00 MILLIMETERS

NATIONAL OPTICS INSTITUTE
SR. OPTICAL DESIGNER: DR. EUGENE CURATU

H:\IR_PROJECTOR\PRE_DESIGN\NEW_ESS\MIRROR544_ILL47.ZMX

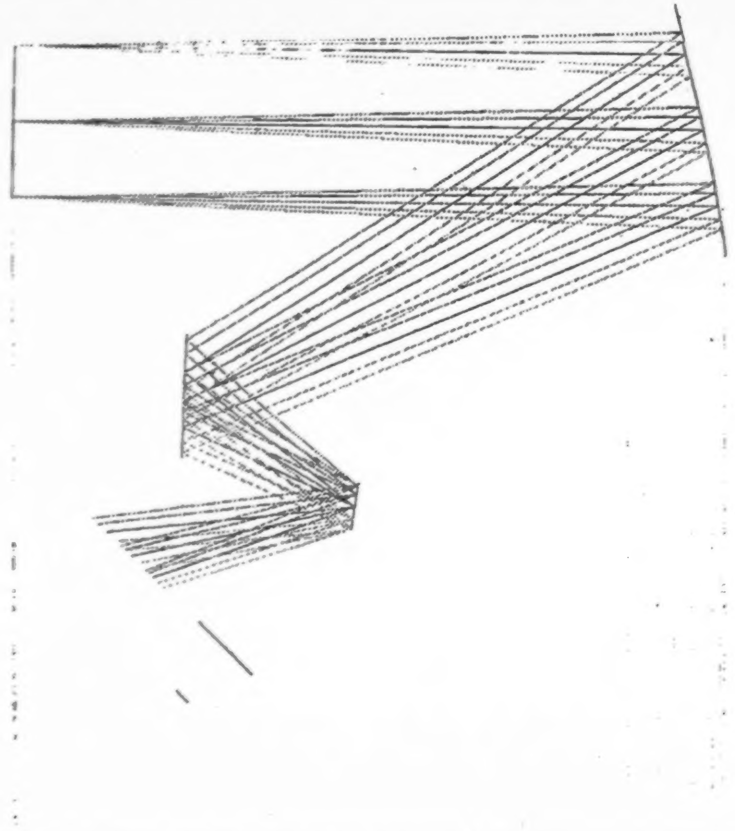

3D LAYOUT

MIRROR_PROJECTOR 544MM/106MM FOV=3.5 DEG.
WED NOV 12 14:28:42 1997
SCALE: 0.2000

100.00 MILLIMETERS

NATIONAL OPTICS INSTITUTE
SR. OPTICAL DESIGNER: DR. EUGENE CURATU

H:\IR_PROJECTOR\PRE_DESIGN\NEW_ESS\MIRROR544_ILL47.ZMX